7.2 Composition of hydrogels

Hydrogel composition was examined in order to verify the efficiency of blending process. On account of this, the presence of the blended component (PVP or PEG) was investigated through ATR-FTIR analysis, by examination of variations in their characteristic absorptions before and after extraction in water.

7.2.1 ATR-FTIR experimental conditions

Infrared analyses were performed using a Nexus 870 FT-IR spectrometer from Thermo Nicolet equipped with a Golden Gate diamond accessory for the ATR analysis. Data were collected with a liquid nitrogen cooled MCT detector with a sampling area of 150 μm^2. The spectra were obtained at room temperature and gathering 128 scans to get an acceptable signal-to-noise ratio. The optical resolution was 2 cm^{-1}. The spectral range was from 650 to 4000 cm^{-1}.

Previous to ATR-FTIR measurement hydrogel film samples were dried in a desiccator for at least 7 days to significantly reduce absorption bands related to water, which could hinder a correct interpretation of obtained IR-spectra.

7.3 Water content and free water

The investigation on water and free water content within hydrogels is of paramount importance to evaluate if a hydrogel has suitable characteristics for being used as a carrier for water-based cleaning systems.

The equilibrium water content (EWC), that provides information on networks hydrophilicity, can be obtained after gravimetric evaluation of the dry weight of the hydrogel W_d and the weight of the water-swollen hydrogel in equilibrium W_w, that

is, hydrogels weight after at least 7 days immersion in deionized water. EWC is then calculated according to the formula

$$EWC(\%) = (W_d/W_0)\times 100 \qquad \text{(Eq. 7.2)}$$

The calculation of the free water index (FWI) permits to estimate the quantity of water within hydrogels structure acting as bulk water, being thus available for the cleaning process. The general formula for the calculation of FWI is

$$FWI = \Delta H_{exp}/WC\times\Delta H_{theo} \qquad \text{(Eq. 7.3)}$$

where ΔH_{exp} (J/g) is the experimentally determined enthalpy of melting of water for the given sample, ΔH_{theo} is the theoretical value for the enthalpy of fusion of bulk water, while WC is the water content, that corresponds to EWC for fully swollen hydrogels.

7.3.1 DSC and DTG experimental conditions

Enthalpy of fusion of water, for the determination of the free water index (FWI), was calculated by integration of the peaks in thermograms obtained from differential scanning calorimetry (DSC). Equilibrium swelled hydrogel samples (5-10 mg for cast-drying method and 18-22 mg for freeze-thawing method hydrogels) were analyzed in Tzero™ aluminum hermetic pans using a Q1000 (TA Instruments) apparatus. Temperature range scan was from -60 to 25 °C with 0.5 °C/min rate. A modified procedure, which consists in a 0.1 °C/min rate in the range -15 to 5 °C, was used for samples with very low free water content, to achieve better separation of the peaks of fusion.

After DSC measurements hermetic pans were drilled to permit water evaporation and water content was determined by differential thermogravimetry (DTG), using a SDT Q600 (TA Instruments) apparatus. The temperature scan was from 20 to 450

°C with a heating rate of 10 °C/min.

FWI was calculated according to Eq. 7.3, by considering the theoretical value for the enthalpy of fusion bulk water being 333.61 J/g (Lide, 1998).

7.4 Crystallinity of hydrogels

The degree of crystallinity is defined as the fractional amount of crystallinity in semi-crystalline polymer sample (Alemán et al., 2007). The calculation of an absolute crystallinity value is a formidable task; nevertheless for most purposes absolute crystallinity is not needed and the calculation of a reproducible data, which compares, on an arbitrary basis, the crystallinity of different samples (of the same polymer), is often adequate. Such a relative evaluation is termed crystallinity index X_c (Fava, 1980). In the following sections the term degree of crystallinity and crystallinity index will be both referred to the relative value of crystallinity.

Calculation of crystallinity index is based on a two-phase model that assumes that the sample can be subdivided into a crystalline and an amorphous phase. Properties of the two phases are assumed to be identical with those of their ideal states, with no influence of the interphases.

The most commonly used techniques to determine the degree of crystallinity are: x-ray diffraction (XRD), differential scanning calorimetry (DSC), infrared spectroscopy (IR) and density measurements.

It is worth to point out that imperfections in crystals are not easily distinguished from the amorphous phase and that the various techniques may be affected to different extents by imperfections and interfacial effects. Hence, some disagreement among the results obtained by measuring the degree of crystallinity by means of different methods is frequently encountered (Alemán et al., 2007; Mo and Zhang, 1995).

Calorimetric methods permit determine the degree of crystallinity by measuring the

specific enthalpy of fusion of the sample. The degree of crystallinity is then calculated according to

$$X_{c,h} = \Delta H_{exp} / \Delta H_{100} \quad \text{(Eq. 7.4)}$$

where ΔH_{exp} is the experimental specific enthalpy of fusion of the sample and ΔH_{100} the specific enthalpy of fusion of the completely crystalline polymer over the same temperature range.

When using infra-red techniques for the determination of the degree of crystallinity, following formula provides crystallinity values (Meille et al., 2011)

$$X_{c,ir} = \frac{1}{a_c \rho l} log_{10}(I_0/I) \quad \text{(Eq. 7.5)}$$

where I_0 and I are, respectively, the incident and the transmitted intensities at the frequency of the absorption band due to the crystalline portion, a_c is the absorptivity of the crystalline material, and ρl is the thickness of the sample.
However, in the case of PVA, it is possible to evaluate the degree of crystallinity by analyzing the relationship between crystalline sensitive absorptions and bands that are not affected by crystallinity (Kenney and Willcockson, 1966; Lee et al., 2008; Mallapragada and Peppas, 1996; Mansur et al., 2008; Peppas, 1977). The degree of crystallinity can then be obtained by a relation of the form:

$$X_{c,ir} = A\ (a/b) + B \quad \text{(Eq. 7.6)}$$

where a and b are, respectively, the heights or integrated intensities of the crystalline and amorphous peaks, while A and B are constants that can be obtained using known values of the degrees of crystallinity (Kenney and Willcockson, 1966; Mallapragada and Peppas, 1996; Peppas, 1977).

The degree of crystallinity can be determined by XRD experiments through the procedure developed by Hermans and Weidinger. This simple procedure does not require special corrections and is proved to be consistent with more elaborate procedures, thus it is considered one of the most appropriate and adaptable for routine work (Hermans and Weidinger, 1961; Weidinger and Hermans, 1961).

According to this method, after a scan over a preselected range to include the crystalline diffraction peaks and the underlying amorphous peaks, an arbitrary but precise method is defined to resolve crystalline and amorphous peaks and the background.

Based on the assumptions that (i) the total scattering from the sample is divided between the crystalline peaks deriving from crystallites and the amorphous peaks of the remaining amorphous regions; (ii) the total scattering of the sample is that included in the resolved crystalline and amorphous regions; (iii) relative areas of crystalline and amorphous regions are respectively proportional to the number of electrons (and consequently to the mass) in the crystalline and amorphous regions; the crystallinity index $X_{c,x}$ can be calculated from the resolved peak areas according to

$$X_{c,x} = I_c/(I_c + KI_a) \qquad \text{(Eq. 7.7)}$$

where I_c and I_a are, respectively, the integrated intensities scattered by the crystalline and the amorphous phases. The constant K is a calibration constant that can be set to unit for measurements with comparative purpose (Fava and Marton, 1980), otherwise, for absolute crystallinity determination, K needs to be determined by absolute methods.

The degree of crystallinity can also be determined through density measurements according to the formula

$$X_{c,d} = \frac{\rho_c}{\rho}\frac{\rho-\rho_a}{\rho_c-\rho_a} \qquad \text{(Eq. 7.8)}$$

where ρ, ρ_c and ρ_a are, respectively, the densities of the sample, of the completely crystalline polymer, and of the completely amorphous polymer. However, this method for crystallinity determination was not used, due to difficulty of preparation of completely amorphous/crystalline samples.

7.4.1 Cristallinity by differential scanning calorimery: experimental conditions

Values for the enthalpy of fusion of the samples were obtained from temperature scan from 20 to 400 °C with a heating rate of 10 °C/min using the SDT Q600 (TA Instruments) apparatus, that provides the signal for weight corrected heat flow (J/g). The specific enthalpy of fusion of completely crystalline PVA is reported to be 161 J/g (Wunderlich, 2005) .

7.4.2 Crystallinity by ATR-FTIR analysis: experimental conditions

Infrared analyses were performed using a Nexus 870 FT-IR spectrometer from Thermo Nicolet equipped with a Golden Gate diamond accessory for the ATR analysis. Data were collected with a liquid nitrogen cooled MCT detector with a sampling area of 150 μm^2. The spectra were obtained at room temperature and gathering 128 scans to get an acceptable signal-to-noise ratio. The optical resolution was 2 cm^{-1}. The spectral range was from 650 to 4000 cm^{-1}.

To obtain integrated peak intensities at 1141 and 850 cm^{-1} a multi-peak fitting of ATR-FTIR spectra was performed using MagicPlotPro® application. After linear baseline subtraction, peaks were fitted using a given number of Lorentzian-type curves, first using the auto-locate function in the fitting range 790-1160 cm^{-1}. Best fitting results were then attained by manual adjustment of the curves.

7.4.3 Crystallinity by XRD: experimental conditions

Wide-angle X-ray powder diffraction profiles were collected at room temperature, with a XRD Bruker New D8 Da Vinci diffractometer using Cu Kα radiation (λ=1.5418 Å) and scans at 0.02 deg(*2θ*)/s in the *2θ* range 10-60°. XRD measurement was performed on wet (fully swollen hydrogels) and dry (hydrogels after being placed for at least 7 days in a dessicator) samples.

The integrated intensities of the crystalline reflections at *2θ*=19.4° and *2θ* =20° and of the amorphous halo were determined through multi-peak fitting using MagicPlotPro® application. Best fitting was obtained using Gaussian-peak type fit for the amorphous halo and Lorentzian-peak type fit for the crystalline reflections. Fit range was from *2θ*=10 to *2θ* = 60°.

7.5 Morphology and structure

7.5.1 SEM analysis: experimental conditions

For the investigation on meso- and macroporosity, previous to SEM analysis, hydrogels were subject to a freeze-drying process, to obtain xerogels whose porous structure is as close as possible to that of swollen hydrogels. Images were acquired with a FEG-SEM ΣIGMA (Carl Zeiss, Germany) using an acceleration potential of 1 kV and a working distance of 1.4 mm. For analysis a gold-metallization of xerogels was performed with an Agar Scientific Auto Sputter Coater.

7.6 Structure at the nanoscale

7.6.1 SAXS analysis: experimental conditions

SAXS measurements were carried out with a HECUS S3-MICRO camera (Kratky-type) equipped with a position-sensitive detector (OED 50M) containing 1024 channels of width 54 μm. Cu Kα radiation of wavelength λ = 1.542 Å was provided by an ultrabrilliant point microfocus X-ray source (GENIX-Fox 3D, Xenocs, Grenoble), operating at a maximum power of 50 W (50 kV and 1 mA). The sample-to-detector distance was 269 mm. The volume between the sample and the detector was kept under vacuum during the measurements to minimize scattering from the air. The Kratky camera was calibrated in the small angle region using silver behenate (d = 58.38 Å)(Blanton et al., 1995). Scattering curves were obtained in the q-range between 0.01 and 0.54 Å−1, assuming that q is the scattering vector, $q = 4\pi/\lambda \sin\theta$, and 2θ the scattering angle. Gel samples were placed into a 1 mm demountable cell having Nalophan films as windows. The temperature was set to 25 °C and was controlled by a Peltier element, with an accuracy of 0.1 °C. All scattering curves were corrected for the empty cell contribution considering the relative transmission factor.

References

Alemán, J.V., Chadwick, A.V., He, J., Hess, M., Horie, K., Jones, R.G., Kratochvíl, P., Meisel, I., Mita, I., Moad, G., Penczek, S., Stepto, R.F.T., 2007. Definitions of terms relating to the structure and processing of sols, gels, networks, and inorganic-organic hybrid materials (IUPAC Recommendations 2007). Pure Appl. Chem. 79.

Blanton, T.N., Huang, T.C., Toraya, H., Hubbard, C.R., Robie, S.B., Louër, D., Göbel, H.E., Will, G., Gilles, R., Raftery, T., 1995. JCPDS—International Centre for Diffraction Data round robin study of silver behenate. A possible low-angle X-ray diffraction calibration standard. Powder Diffr. 10, 91–95.

Fava, R.A., 1980. Crystal Structure and Morphology. Academic Press.

Fava, R.A., Marton, L. (Eds.), 1980. Polymers: Crystal Structure and Morphology Pt. B. Academic Press Inc, New York.

Hermans, P.H., Weidinger, A., 1961. On the determination of the crystalline fraction of polyethylenes from X-ray diffraction. Makromol. Chem. 44, 24–36.

Kenney, J.F., Willcockson, G.W., 1966. Structure–Property relationships of poly(vinyl alcohol). III. Relationships between stereo-regularity, crystallinity, and water resistance in poly(vinyl alcohol). J. Polym. Sci. [A1] 4, 679–698.

Lee, J., Jin Lee, K., Jang, J., 2008. Effect of silica nanofillers on isothermal crystallization of poly(vinyl alcohol): In-situ ATR-FTIR study. Polym. Test. 27, 360–367.

Lide, D.R., 1998. CRC Handbook of Chemistry and Physics, 79th ed. CRC Press, Boca Raton, FL.

Mallapragada, S.K., Peppas, N.A., 1996. Dissolution mechanism of semicrystalline poly(vinyl alcohol) in water. J. Polym. Sci. Part B Polym. Phys. 34, 1339–1346.

Mansur, H.S., Sadahira, C.M., Souza, A.N., Mansur, A.A.P., 2008. FTIR spectroscopy characterization of poly (vinyl alcohol) hydrogel with different hydrolysis degree and chemically crosslinked with glutaraldehyde. Mater. Sci. Eng. C, Proceedings of the Symposium on Nanostructured Biological Materials, V Meeting of the Brazilian Materials Research Society (SBPMat) 28, 539–548.

Meille, S.V., Allegra, G., Geil, P.H., He, J., Hess, M., Jin, J.-I., Kratochvíl, P., Mormann, W., Stepto, R., 2011. Definitions of terms relating to crystalline polymers (IUPAC Recommendations 2011). Pure Appl. Chem. 83.

Mo, Z., Zhang, H., 1995. The Degree of Crystallinity in Polymers by Wide-Angle X-Ray Diffraction (Waxd). J. Macromol. Sci. Part C Polym. Rev. 35, 555–580.

Peppas, N.A., 1977. Infrared spectroscopy of semicrystalline poly(vinyl alcohol) networks. Makromol. Chem. 178, 595–601.

Weidinger, A., Hermans, P.H., 1961. On the determination of the crystalline fraction of isotactic

polypropylene from x-ray diffraction. Makromol. Chem. 50, 98–115.

Wunderlich, B., 2005. Thermal Analysis of Polymeric Materials. Springer Science & Business Media.

Chapter 8 – Results and discussion

This chapter presents the discussion of the experimental results obtained after investigation on hydrogels obtained through the two synthesis methods described in Chapter 7. Since the systems obtained through the two different pathways present different characteristics, and to facilitate the comprehension of the obtained results, the chapter is divided in two main sections. Section 8.1 illustrates the results related to investigations on cast-drying method hydrogels while section 8.2 describes the hydrogel systems obtained through repeated freezing and thawing.

8.1 Characterization of hydrogels obtained through cast-drying method

8.1.1 List of the prepared materials and general observations

Table 8.1 displays a list of the prepared polymer aqueous solutions subject to cast-drying process. Solutions prepared with low-molecular weight PVP (i.e. $M_w \approx$ 40.000) or low hydrolysis degree PVA (i.e. HD=87-89%) are marked by an asterisk.

After being casted into a Petri dish and completely dried, hard and glassy transparent xerogels are obtained. Complete rehydration with deionized water is achieved after about 20 minutes: as a result, thin, transparent and highly elastic hydrogels are obtained, that are able to perfectly adhere on the surface they are put in contact with (see Fig. 8.1).

After cooling, the *PVA/PEG (3:1)* solution separate into two phases, an opaque and dense polymer-rich and a transparent polymer-poor phase. The two phases were separated and only the polymer-rich phase was casted into the petri dish. After

drying and rehydration, no significant swelling was observed. For this reason, no further characterization was performed on the PVA/PEG blend obtained through cast-drying method.

Sample	PVA % (w/w)	PVP % (w/w)	Tot. polymer concentration	Annotations
PVP*12%	0	12	12%	*PVP Mw ≈ $4x10^4$
PVA*12%	12	0	12%	*PVA 87-89% HD
PVA 12%	12	0	12%	PVA 98-99% HD
PVA 9%	9	0	9%	PVA 98-99% HD
PVA/PVP*(3:1)	9	3	12%	*PVP Mw ≈ $4x10^4$
PVA/PVP*(1:1)	6	6	12%	*PVP Mw ≈ $4x10^4$
PVA/PVP*(1:3)	3	9	12%	*PVP Mw ≈ $4x10^4$
PVA/PVP(3:1)	9	3	12%	PVP Mw ≈$1,3x10^6$
PVA/PVP(1:1)	6	6	12%	PVP Mw ≈$1,3x10^6$
PVA/PVP(2:1)	9	4.5	13,5%	PVP Mw ≈$1,3x10^6$
PVA/PEG (3:1)	9	3	12%	PEG Mw ≈ $3,5x10^4$

Table 8.1: List of prepared polymer solutions for cast-drying method.

Fig. 8.1: Sample PVA/PVP(3:1) after rehydration of the xerogel obtained by casting and dehydration of the original solution.

Some solution did not gelate, that is, polymer dissolved completely after rehydration in deionized water. Table 8.2 lists formulations for which gelification is not achieved. Lacking gel formation for these three formulations is correlated to the impossibility of the three-dimensional PVA network formation responsible for hydrogels stability. In particular, missed gel formation for sample *PVP*12%* indicates that PVP does not participate to network formation and is in fact only incorporated within the formed PVA structure. The fact that no gel was obtained from sample *PVA/PVP*(1:3)*, prepared with only 3% w/w PVA, indicates that a minimum PVA concentration is needed to form a stable network. Stable hydrogels were obtained from solutions prepared with at least 4.5% w/w PVA. Also formulation *PVA*12%*, prepared using PVA with HD=87-89%, completely dissolves after rehydration. This confirms that formation of a stable and insoluble network is related to formation of crosslinks arising form crystallites. As stated in Chapter 5, PVA with low HD is not able to crystallize and the hydrogen bonds existing between polymer chains are destroyed by the presence of water.

Name	PVA % (w/w)	PVP % (w/w)	Annotations	Reason
PVA*12%	12	0	*PVA 87-89% HD	HD too low
PVA/PVP*(1:3)	3	9	*PVP Mw ≈ $4x10^4$	%PVA too low
PVP*12%	0	12	*PVP Mw ≈ $4x10^4$	PVP still soluble

Table 8.2: Formulations for which no gel formation through cast-drying method was observed.

All other formulations swell but not dissolve in water at room temperature, even if stored in water for months. Nevertheless, since crosslinks made up by crystallites are physical cross-links, the obtained hydrogels are thermoreversible, that is, they completely dissolve when water is heated over 80°C.

8.1.2 Gel fraction G%

Hydrogel synthesis through cast-drying of neat or blended PVA solutions leads to formation of a polymer network which is insoluble in water at room temperature. Evaluation of the insoluble fraction of the gel provides information about the efficiency of network formation, i.e. the efficiency of crosslinking through crystallites formation between PVA chains, and of embedding the water-soluble PVP chains.

Left column in Table 8.3 provides obtained gel fraction values for different formulations. Since PVA is the component responsible for the network formation, higher gel fractions are observed for higher PVA contents. Gel fractions lower than 50% were obtained for formulations *PVA/PVP*(1:1)* and *PVA/PVP (1:1)*.

Gel fractions obtained for formulations characterized by the same PVA/PVP ratio, result in lower values for hydrogels prepared with low molecular weight PVP (*PVA/PVP*(3:1)* and *PVA/PVP*(1:1)*), indicating that probably the shorter chains (PVP $M_w \approx 40.000$) are less efficiently entangled within the forming PVA network than the chains of PVP $M_w \approx 1.300.000$.

Sample	Gel Content (G%)	
	not annealed	annealed
PVA 12%	81.7 ±1.6	97.1 ±0.1
PVA/PVP*(3:1)	62.8 ±2.4	77.4 ±1.1
PVA/PVP*(1:1)	38.1 ±2.5	58.6 ±1.4
PVA/PVP (3:1)	73.8 ±3.1	91.9 ±0.8
PVA/PVP (2:1)	73.8 ±2.3	88.6 ±3.2
PVA/PVP (1:1)	46.9 ±2.5	74.6 ±3.3

Table 8.3: Gel fractions for different hydrogel formulations after extraction in deionized water. Right column indicates G% values for annealed samples, left column for not annealed.

To enhance gel fractions, and thus avoid waste of material, same formulations were subject to a thermal treatment, as described in section 6.1.1. Annealing process

consists in a thermal treatment above the glass transition temperature of PVA and is usually carried out to enhance the mechanical strength of PVA based hydrogels (Peppas and Merrill, 1976; Peppas and Tennenhouse, 2004). Increasing the temperature above the T_g should permit the macromolecular chains to have more mobility and, thus, to reorganize through new formation or growth of previously formed crystallites. Chosen annealing conditions (4 hours at 120°C) are severe in respect to conditions described in literature, were the annealing temperatures usually range from 90 to 120°C and annealing times are lower, usually less than 1 hour (Peppas and Merrill, 1976; Peppas and Tennenhouse, 2004). These overboard conditions were expressively chosen to enhance the effect of the treatment and thus to permit an easier evaluation of its impact on hydrogel properties.

Results of gel fraction for the different formulations subject to annealing are listed in Table 8.3 (left column). As for not annealed samples, gel fraction decreases for increasing PVP content, but G% is generally higher for annealed samples where values over 90% are reached.

Figure 8.2 illustrates the effect on gel fraction of PVP concentration and of annealing process.

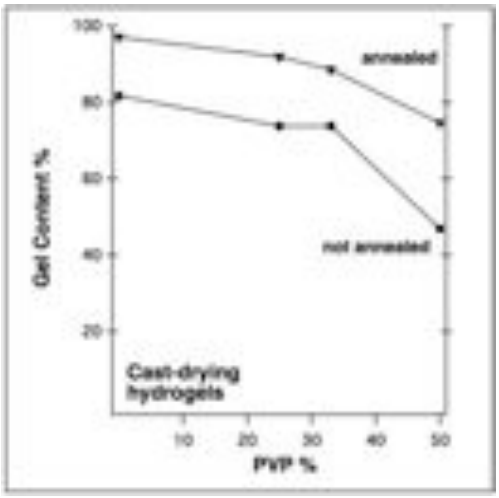

Fig. 8.2: Effect of PVP content and annealing process on gel fraction G%.

8.1.3 Composition of hydrogels

Investigation on hydrogels composition, performed through ATR-FTIR analysis, was carried out to verify how efficiently the second component is embedded into the PVA network. For this purpose, infrared spectra of previously dried hydrogel films were collected before and after extraction of soluble components. The obtained spectra were examined by evaluating the intensities of the characteristic absorption bands of PVP in samples prepared by blending low and high molecular weight PVP with PVA. Obtained spectra, presented in Figure 8.2, were compared to that of a pure PVA film.

PVP has characteristic absorptions at 1648, 1492 and 1288 cm^{-1}. The absorption band at 1648 cm^{-1} is the most intense and is related to both, C=O and C-N stretching vibrations; while bands at 1492 and 1288 cm^{-1} are correlated to C-N bond vibrational modes (Borodko et al., 2006).

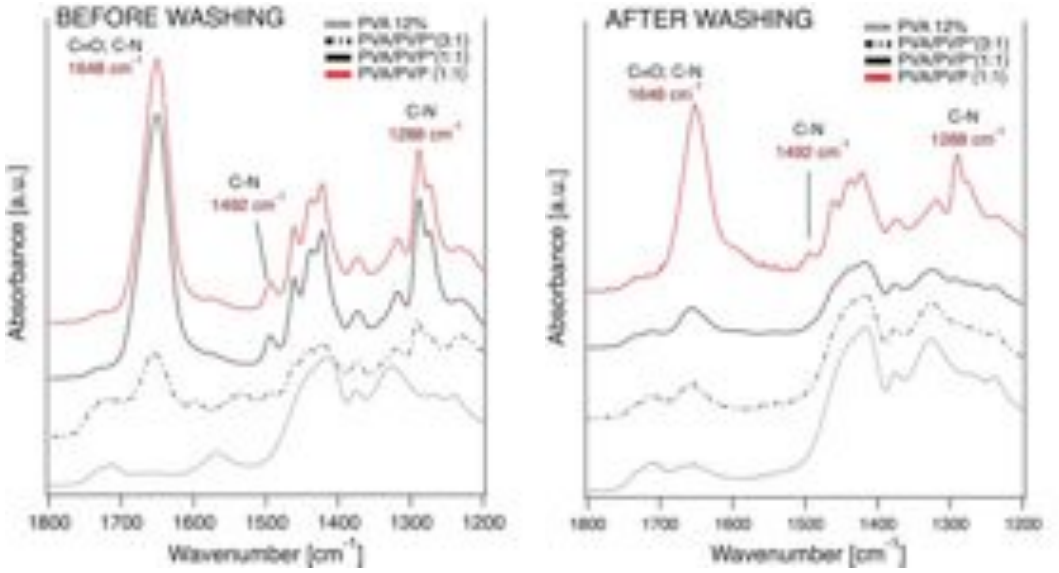

Fig. 8.3: ATR-FTIR spectra of dried hydrogel films of pure PVA (dotted line, bottom) and PVA blended with low (dotted and solid line, center) and high (red line) molecular weight PVP.

Except for the non-blended sample PVA 12%, these three characteristic absorptions are present in all the collected spectra before extraction in water of soluble

components. After extraction, the sole sample presenting PVP absorption bands is that prepared with high molecular weight PVP (red line in Fig. 8.3). In fact, after storage in deionized water, hydrogels prepared with low molecular weight PVP can be considered as pure PVA hydrogels.
This result is consistent with the observations obtained through the analysis of the gel fraction, where higher weight loss after extraction was observed for samples prepared with low molecular weight PVP, indicating that this component remains soluble after synthesis.

8.1.4 Water content and free water

The investigation on equilibrium and free water content within hydrogels is of paramount importance to evaluate if a hydrogel has suitable characteristics for being used as a carrier for water-based cleaning systems. In fact, to be efficient, the cleaning system must be able to interact with the surface on which it is put in contact through the hydrogel. It is thus necessary that the interactions between the polymeric network and the liquid phase are adequate to grant an efficient confining, but loose enough to permit the water-phase to act as free water.

Unlike for water-soluble polymers, where the total amount of added water may be extended from zero to infinity (corresponding to an infinite dilution), the water that can be absorbed by a crosslinked hydrogel is limited: once the equilibrium water content (EWC) is reached, no further water can be absorbed by the hydrogel (Li et al., 2005). Within a water-swollen polymer it is generally accepted that the states of water should be divided into three main categories: *free water*, characterized by thermal phase transitions similar to that of bulk water; *freezable bound water*, whose phase transitions are shifted in respect to bulk water; and *non-freezing water*, which is the bound water for which no detectable phase transitions over the range of temperatures normally associated to bulk water are observed. PVA has been shown

to contain all these separate states of water (Cha et al., 1993).

This differentiate behavior of water depends on the degree of chemical or physical association between the water and the polymer phase and temperature shifts in phase transitions of freezable-bound water are related to interactions with the polymer chains and/or capillary effects (Burghoff and Pusch, 1979). The effect is a depression of the freezing point of bound water, for which the main contribution is due to the low energy of water molecules near the surface of a hydrophilic polymer. In fact, in the vicinity of a polar or dipolar region of a macromolecule, water molecules assume a non-random average orientation and have thus a lower potential energy than in bulk state. If hydrogen bonding occurs, this energy may be further lowered. The non-random average orientation makes the specific entropy of this vicinal water lower than that of bulk water, but greater than that of ice, resulting in depression of the melting point (Wolfe et al., 2002).

Differential scanning calorimetry (DSC) and differential thermogravimetry (DTG) has been extensively used to determine the relative contents of the different water states in PVA hydrogels obtained through different synthesis methods (Cha et al., 1993; Hodge et al., 1996; Li et al., 2005).

Water content values and free water index for the hydrogel systems studied in the present work, and reported in Table 8.4, permit to evaluate the influence of PVP content on the state of water contained in the water-swollen hydrogels.

Sample	EWC (%)	FWI
PVA 12%	74.4	0.07
PVA 9%	70.9	0.04
PVA/PVP*(3:1)	70.3	0.07
PVA/PVP*(1:1)	82.9	0.87
PVA/PVP (3:1)	76.3	0.79
PVA/PVP (2:1)	82.5	0.89
PVA/PVP (1:1)	92.8	0.94

Table 8.4: Equilibrium water content (EWC) and free water index (FWI) for different cast-drying hydrogel formulations.

Water content values for fully swollen hydrogels (EWC) are greater than 70% for all the studied systems, although a noticeable increase is observed for formulations with higher PVP content. For same formulations, hydrogels prepared with high molecular weight PVP display higher water contents. This behavior may be related to the fact that after swelling in water the low molecular weight PVP is completely removed due to its non-efficient combination within the PVA network, as verified through the ATR-FTIR analysis.

Major effects than on EWC, owing to presence of PVP within the gel structure, are recorded in the FWI values. Only hydrogel formulations containing PVP also after swelling in water, that is the formulations prepared with high molecular weight PVP, present FWI that are consistent with their possible use as carriers for water-based cleaning systems. The only exception is given by the sample PVA/PVP*(1:1) for which a high FWI is recorded, even its PVP content after extraction approaches zero. This behavior may be related to the fact that the great quantity of PVP washed out during the swelling process leads to formation of a porosity characterized by greater dimensions, thus reducing the capillarity effects and permitting the water to behave as free water.

Figure 8.3 (A) shows typical DSC thermograms for three hydrogel formulation prepared with pure PVA (solid line) or by blending PVA with high molecular weight PVP (dotted lines). The observed thermal transition is related to the melting of water contained within hydrogels. Pure PVA hydrogel sample shows a multi-peak profile with small narrow peak at a temperature greater than 0°, which is related to the melting of free water, while the broader peak displays the typical temperature shift that characterizes phase transitions for freezable bound-water.

The peak related to sample PVA/PVP 3:1, containing 25% PVP in its original formulation, shows a clear one-peak profile, indicating that almost all water is behaving as free water, although a shoulder towards lower temperatures of melting is still visible. Further increase in PVP content, as for sample PVA/PVP 2:1, leads definitely to a one-peak profile characteristic for the melting of free water. This

indicates that the presence of PVP induces a neat change in the state of water within PVA hydrogels obtained through cast-drying method.

The trend of EWC and FWI produced by the addition of PVP into hydrogels structure is summarized in Figure 8.3 (B).

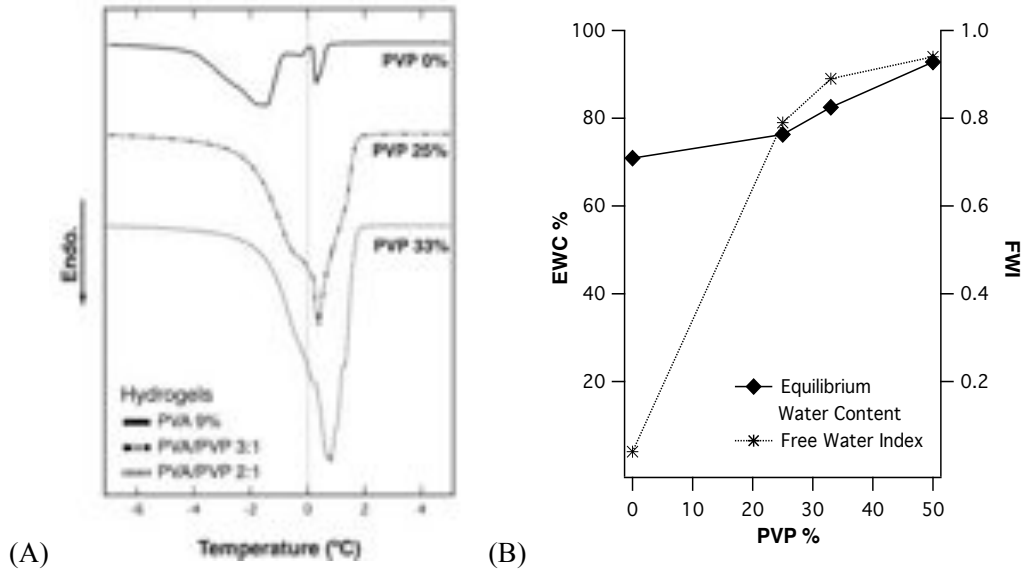

Fig. 8.3: (A) DSC thermograms of pure PVA and blended PVA/PVP hydrogels, endothermic peaks are related to the melting of water, zero-line highlights the phase transition temperature of pure bulk water and thermograms are normalized to sample weight; (B) EWC and FWI increase promoted by the presence of PVP.

8.1.5 Effect of annealing on water and free water content

Annealing process permits to enhance gel fraction and thus to reduce waste of material during hydrogel synthesis, as ascertained in section 8.1.2. Figure 8.4 shows DSC thermograms of sample PVA/PVP 3:1 before and after annealing.

Integration of the thermograms yields the enthalpy of fusion of the water contained within the hydrogels. Without annealing, a single broad transition is observed at a temperature over 0ºC, indicating that a great quantity of the water contained into the hydrogel behaves as bulk water. After annealing, peak area is noticeably lower, that is, the gel contains less water. Furthermore, two different peaks are observed,

denoting the presence of at least two different types of freezable water (free and freezable bound water). The first sharp peak is related to free water, since the peak temperature is +0.3°C, the broader peak, with maximum heat absorption at -0.8°C is related to bound water.

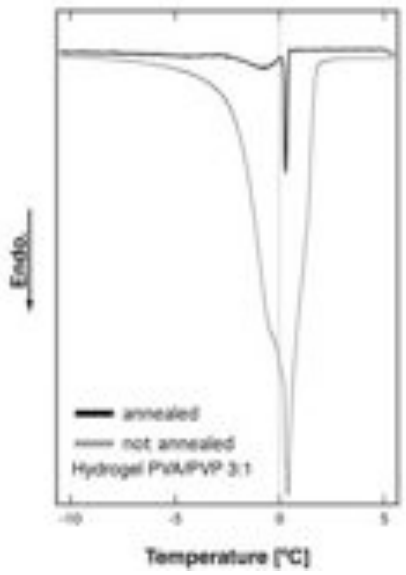

Fig. 8.4: DSC thermograms of *PVA/PVP (3:1)* hydrogels without any heat treatment (not annealed) and after annealing (4h at 120ºC), thermograms are normalized to sample weight.

Sample	EWC (%)		FWI	
	not ann.	**ann.**	**not ann.**	**ann.**
PVA 9%	70.9	**54.7**	0.04	**0.08**
PVA/PVP (3:1)	76.3	**65.3**	0.79	**0.1**

Table 8.5: Equilibrium water content (EWC) and free water index (FWI) for annealed and not annealed hydrogels samples.

Table 8.5 summarizes equilibrium water content and free water index for sample PVA 9% and PVA/PVP 3:1 before and after annealing. The annealing process decreases water content of approximately 10% and has an even stronger impact on free water, whose content is reduced to about zero making annealed samples not suitable for cleaning purposes. However, it is important to remind that the applied

annealing conditions were outstanding (high temperature and long exposure). A more in-depth study of the effect of annealing under milder conditions could probably permit to enhance gel fraction with less effect on free water content.

8.1.6 Crystallinity of hydrogels

The size and amount of crystalline aggregates in PVA hydrogels play an important role on their performances in applications; they determine properties such as dimensional stability, the toughness, and strength to external stresses. A too high crystallinity determines less elasticity and ability to adhere to rough surfaces, while a too low crystallinity degree makes gels poorly coherent and lower their general mechanical stability.

Analysis of hydrogels crystallinity was performed by means of three different techniques to permit a comparative study and, thus, validation of obtained results. In particular, evaluation of the crystallinity degree was performed through differential scanning calorimetry (DSC), infrared analysis (ATR-FTIR) and x-ray diffraction (XRD) experiments, to evaluate the effect of composition variations and annealing process on neat PVA and blended PVA/PVP hydrogels.

8.1.6.1 Determination of crystallinity through DSC

Crystallinity of hydrogels was determined by integration of the melting peak between 200-250°C, as reported in literature (Mallapragada and Peppas, 1996; Peppas and Merrill, 1976; Peppas and Tennenhouse, 2004), and then calculated according to Eq. 7.4 (see section 7.4, Chapter 7).

Table 8.6 shows calculated crystallinity values (X_c) for annealed and not annealed samples obtained for neat PVA or blended systems; the melt peak temperatures and melt onset temperatures are also reported.

As expected, X_c data from DSC reveal higher crystallinity degrees for neat PVA samples than for blended PVA/PVP hydrogels, indicating that the presence of PVP interferes with PVA crystallization process. Surprisingly, no significant difference in crystallinity is observed for the annealed samples in respect to the not annealed. Considering that swelling behavior in PVA hydrogels is usually related to crosslinking density and, thus, to crystallinity, by an inverse proportionality (Peppas and Tennenhouse, 2004), DSC data seem to contradict EWC data discussed in previous sections. The considerable reduction in water content observed for the annealed samples is obviously not related to an increase in crystallinity, so one may suppose that the applied annealing conditions had greater impact on the amorphous rather than on the crystalline fraction. Decrease in water content may be related to a collapse of the amorphous regions, through a process close to vitrification, responsible for the fact that these regions can not be penetrated by water.

	Melt Onset Temp. (°C)	Melt Peak Temp. (°C)	Enthalpy (J/g)	X_c (%)	
				not ann.	**annealed**
PVA 9%	210.5 ±0.1	222.4 ±0.9	63.4 ±0.3	**39.4 ±0.2**	**-**
PVA 9%	208.4 ±0.9	222.3 ±0.3	62.0 ±1.9	**-**	**38.5 ±1.2**
PVA/PVP(3:1)	207.4 ±0.7	220.6 ±0.4	42.7 ±1.2	**26.5 ±0.7**	**-**
PVA/PVP(3:1)	204.3 ±0.9	219.3 ±0.4	40.6 ±0.4	**-**	**25.2 ±0.3**

Tab. 8.6: Crystallinity values obtained through DSC analysis on samples *PVA 9%* and blended *PVA/PVP (3:1)* with and without annealing treatment.

Moreover, together with the decrease in enthalpy of fusion, a sensible decrease in melting temperatures for blended systems in respect to those obtained from pure PVA is observed. The presence of PVP, with its hydrophilic groups interacting with the PVA chains may hinder the crystallization process by reducing the dimensions of the crystalline regions and acting as a diluent, which reflects in a decrease of melting temperature. Similar effects have been observed for the addition of plasticizers, such as glycerin, into PVA-base hydrogel systems (Jang and Lee, 2003).

8.1.6.2 Determination of crystallinity through ATR-FTIR

Evaluation of crystallinity of hydrogel samples obtained through cast-drying method, using ATR-FTIR analysis, was performed through multi-peak fitting of the spectra in order to evaluate the integrated intensities of the absorption bands at 1141 and 850 cm^{-1}. Notably, the intensity of absorption band at 1141 cm^{-1}, is related to crystalline C-O stretching vibration and depends on the crystallinity degree of the sample (Kenney and Willcockson, 1966; Lee et al., 2008; Mallapragada and Peppas, 1996; Mansur et al., 2008; Peppas, 1977). To evaluate the crystallinity degree, the intensity at 1141 cm^{-1} can be related to the intensity of peaks that are not affected by crystallization process and can thus be used as internal standards. According to Lee and to Mallapragada (Lee et al., 2008; Mallapragada and Peppas, 1996), in our case the peak related to CH_2 rocking mode of PVA at 850 cm^{-1} was chosen, since no significant bands from PVP are present in this wavelength interval.

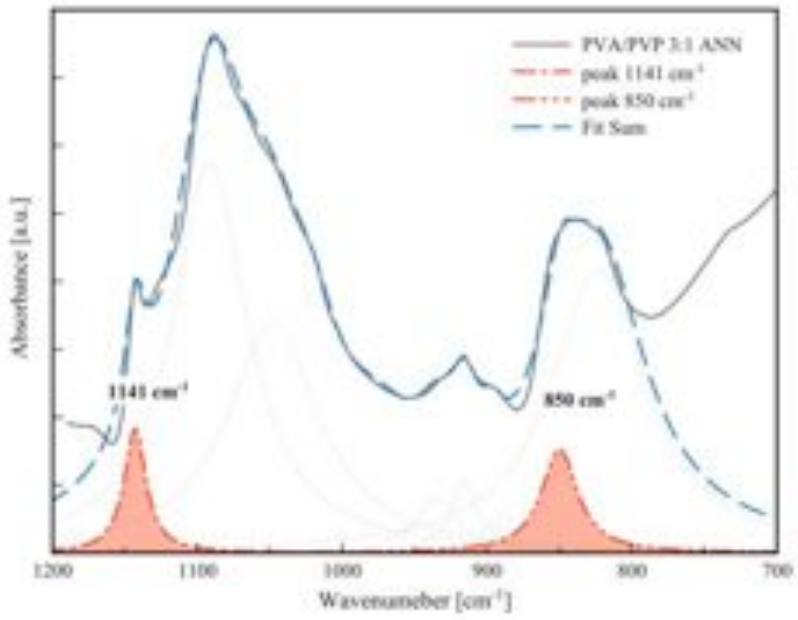

Fig. 8.5: ATR-FTIR spectra of the annealed sample *PVA/PVP (3:1)*. Blue line represents the fit sum of the multi-peak fitting performed with MagicPlotPro®. Areas of the crystalline peak at 1141 cm^{-1} and of the amorphous peak at 850 cm^{-1} are highlighted in red.

The calculation of the percent crystallinity degree requires, as reported in section 7.4 of Chapter 7, extrapolation of two constants that can be obtained from known values of crystallinity. In this section we report only the ratio between the integrated intensity of the peaks at 1141 cm^{-1}, I_{1141}, and 850 cm^{-1}, I_{850}. Since (I_{1141}/I_{850}) is correlated to crystallinity degree by a direct proportionality, obtained values can be considered a relative index for the crystallinity degree.

Analysis was performed on neat PVA and on blended systems with or without being subject to annealing treatment. Fig. 8.5 represents an example of the obtained ATR-FTIR spectra, while Tab. 8.7 summarizes calculated areas from multi-peak fitting for the crystalline and amorphous peak, and the ratio (I_{1141}/I_{850}).

Obtained values are in accordance with results for crystallinity obtained through DSC analysis described in previous section. Crystallinity seems to be strongly affected by the presence of PVP, which lowers considerably the crystallinity degree, while no significant effect on crystallinity is recorded for the annealed samples.

	Peak area 1141 cm^{-1}	Peak area 850 cm^{-1}	$\mathbf{I_{1141}/I_{850}}$
PVA 9% not ann.	3.04	4.90	**0.62**
PVA 9% ann.	2.36	3.92	**0.60**
PVA/PVP (3:1) not ann.	2.63	5.89	**0.45**
PVA/PVP (3:1) ann.	2.10	4.91	**0.43**

Tab. 8.7: Crystalline (1141 cm^{-1}) and amorphous (850 cm^{-1}) peak areas for the analyzed samples. I_{1141}/I_{850} represents a qualitative index, proportional to crystallinity of the samples.

8.1.6.3 Determination of crystallinity through XRD

X-ray diffraction patterns of neat PVA and blended hydrogel systems were examined in order to determine their degree of crystallinity according to Eq. 7.7, Chapter 7.

X-ray studies on PVA crystal structure were first reported by Mooney and Bunn (Bunn, 1948; Mooney, 1941) that established a monoclinic unit cell for PVA crystals with a=7.82 Å; b=2.52 Å (chain axis); c=5.51 Å and β=91.42°.

Diffraction maximum at d≈4.55 Å observed in previous studies (Watase and Nishinari, 1985) is identified as the superposition of the equatorial reflections of the $10\bar{1}$ and 101 planes. Specifically, the two reflections are found with a strong maximum at 2θ= 19.4° for the $10\bar{1}$ (d=4.68 Å) an da shoulder at 2θ=20° for the 101 (d=4.43 Å) (Ricciardi et al., 2004).

Evaluation of crystallinity by means of x-ray diffraction was performed on fully swollen hydrogels due to difficulty to prepare suitable dried samples for the powder diffraction sample holder. However, since "wet crystallinity" is very low due to high water content of the hydrogels, a diffraction profile of a dried sample was collected from a dried gel to confirm exact peak position.

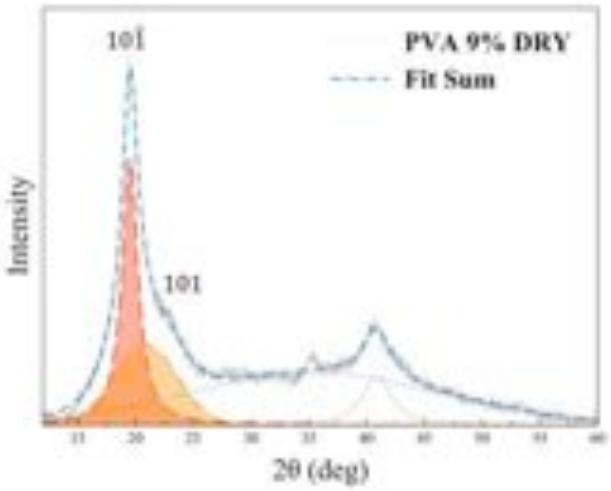

Fig. 8.6: X-ray powder diffraction profile of "dried" *PVA 9%* sample. The $10\bar{1}$ and 101 reflections, at 2θ=19.4° and 2θ=20° respectively, are indicated.

Fig. 8.6 shows the diffraction profile of dried *PVA 9%* sample, confirming the maximum at 2θ=19.4° and the shoulder at 2θ=20°; these peak positions were used to fit the diffraction profiles of the "wet" samples.

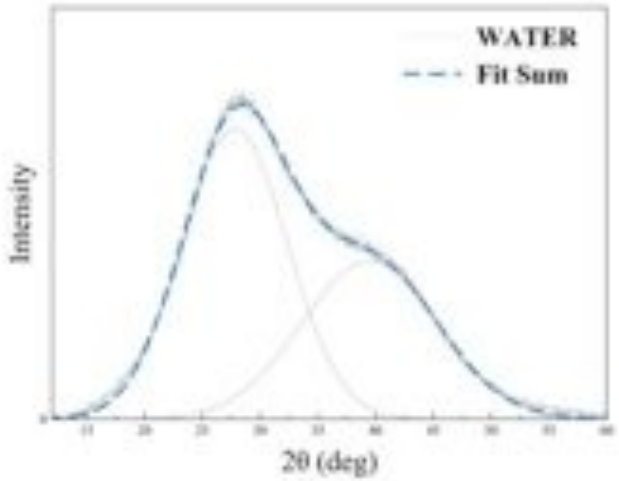

Fig.8.7: X-ray diffraction profile of pure liquid water.

Since water is the major component of the hydrogels, for comparison the x-ray diffraction pattern of pure liquid water was also collected as reported in figure 8.7.
Fig. 8.8 shows a typical diffraction profile from "wet" hydrogel samples: as in the diffraction of pure water, the hydrogels exhibit two halos in the range around 2θ=29° and 2θ=41° as well as a weak peak in the 2θ range 18-21°, related to the presence of crystalline aggregates.

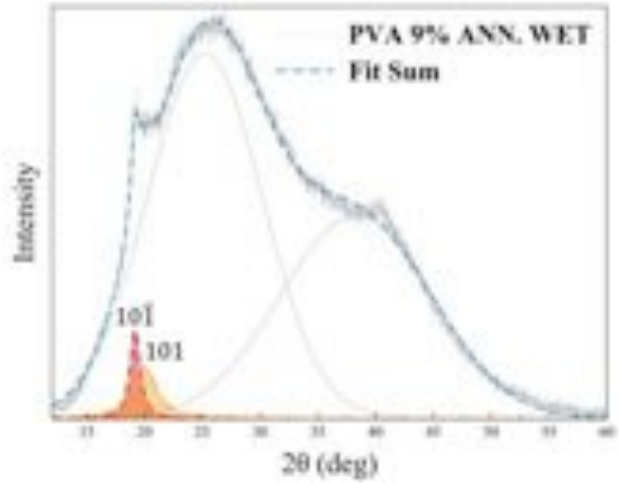

Fig. 8.8: X-ray powder diffraction profile of "wet" *PVA 9%* sample subject to annealing. The $10\bar{1}$ and 101 reflections, at 2θ=19.4° and 2θ=20° respectively, are indicated.

The crystallinity values obtained according to Eq. 7.7 are listed in Table 8.8 with indication of the crystalline and total peak areas obtained through multi-peak fitting with MagicPlotPro®. We remind that crystallinity values obtained using Eq. 7.7 are not absolute values, but suitable for comparative purposes. Obtained values are in accordance with results obtained from DSC and ATR-FTIR measurements, displaying higher crystallinity for neat PVA samples in respect to blended hydrogel systems. Values for annealed samples are similar to those of not annealed samples, confirming that under the performed annealing conditions no increase in crystallinity was attained. Moreover, percent crystallinity of the *PVA 9%* "dried" sample is of the same magnitude of the results obtained through calorimetric crystallinity determination.

	Area$_{cryst}$ (a.u.)	**Area$_{tot}$** (a.u.)	**$A_{cryst.}/A_{tot}$**
PVA 9% dry	8344	19593	**0.426**
PVA 9% not ann.	614	15484	**0.039**
PVA 9% ann.	2910	69990	**0.041**
PVA/PVP (3:1) not ann.	1594	48175	**0.033**
PVA/PVP (3:1) ann.	1273	37377	**0.034**

Tab. 8.8: Crystalline and total areas calculated from x-ray diffraction pattern of "wet" and "dried" hydrogel samples. The $A_{cryst.}/A_{tot}$ ratio gives a relative measure of crystallinity for comparative purposes.

8.1.7 Morphology and structure: SEM analysis

SEM images of different hydrogel formulations were collected on previously freeze-dried samples to study their morphology and porous structure.

Sample *PVA12%* (Fig. 8.9), exhibit a rather smooth, homogeneous and quite compact surface; porosity seems to be completely absent. Although at very high magnification some pores became visible, these porous areas are not representative

of the overall structure of this formulation. Within these porous areas, pore dimensions can be estimated to be around 50-100 nm.

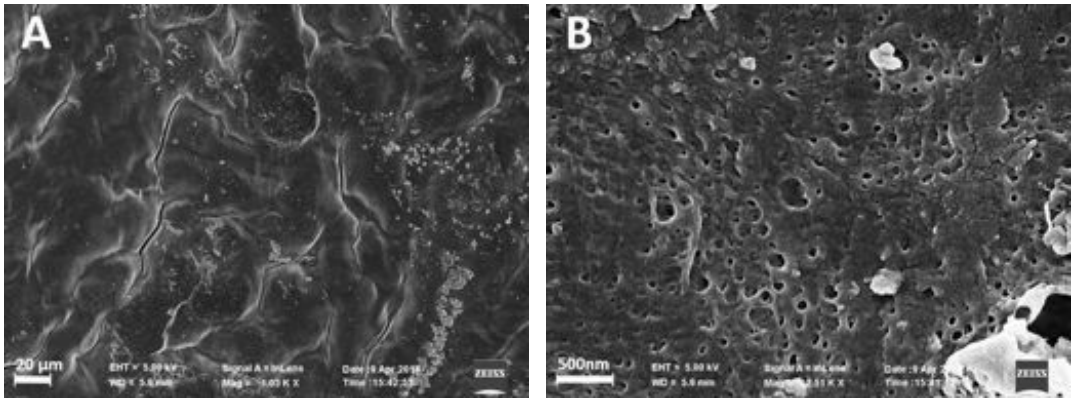

Fig. 8.9: SEM images of sample *PVA 12%* at different magnifications (A) 1000x, scale bar 20 µm; (B) 62500x, scale bar 500nm.

Absence of porosity can be attributed to collapse of the gel structure during drying. Considering that this formulation contains up to 74% of equilibrium water in the swollen state, water not contained into pores probably leads to formation of the so-called *molecular porosity* (Mattiasson et al., 2009), and hydrogels swelling is due to an increase of the space between network chains. Consequently, the water interacts strongly with polymer chains and is, thus, not available as free water, as confirmed by the previous thermal analysis performed on this sample and described in section 8.1.4.

In case of samples prepared by blending PVA with low molecular weight PVP, hydrogels surfaces appear inhomogeneous, being composed by darker, non-porous and clearer porous areas (Fig. 8.10). Pores are probably formed in PVP rich areas formed during a phase separation process occurring during drying, as a consequence of the washing out of the soluble PVP after extraction in water. Within the porous areas some orientation of the pores is visible, as following a concentration gradient, maybe originated during the drying process of the solution. Estimated pore dimensions are greater than for the pure PVA hydrogels, with pore diameters greater than 200 nm for both, sample *PVA/PVP*(3:1)* and *PVA/PVP*(1:1)*, and a more interconnected porous structure for the latter one,

characterized by a greater PVP content in the original solution (see Fig. 8.10 and 8.11).

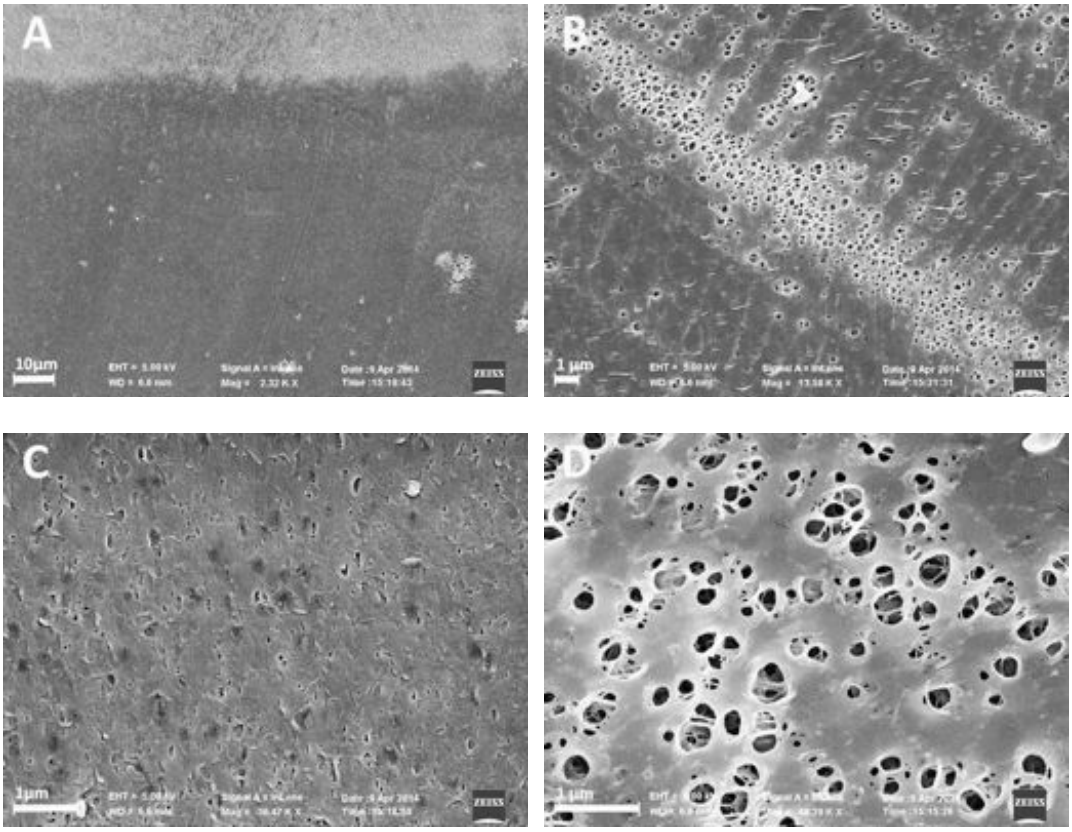

Fig. 8.10: SEM images of different areas of hydrogel *PVA/PVP*(3:1)*, prepared with low-molecular weight PVP; (A) 2300x, scale bar 10 µm; (B) 13600x, scale bar 1µm; (C) 36500x, scale bar 1µm; (D) 48300x, scale bar 1µm.

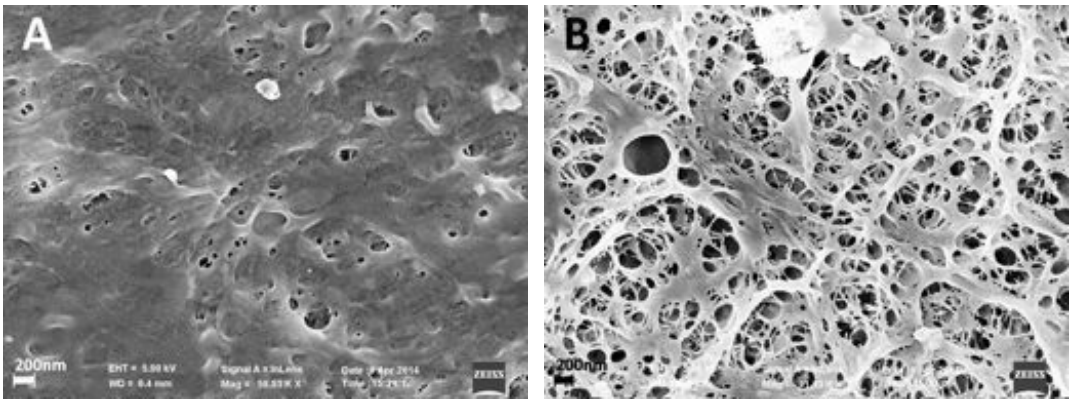

Fig. 8.11: SEM images of different areas of hydrogel *PVA/PVP*(1:1)*, prepared with low-molecular weight PVP; (A) 58500x, scale bar 200nm; (B) 51100x, scale bar 200nm.

Structure drastically changes for samples prepared with high molecular weight PVP. Some areas of great dimensions (hundreds of microns) seem to indicate a phase separation process during drying, as shown for sample *PVA/PVP(3:1)* in Fig. 8.12.(A). Within these areas a very homogeneous and highly interconnected porosity is observed, with pores exhibiting diameters of several microns (fig 8.12(B) and (C)).

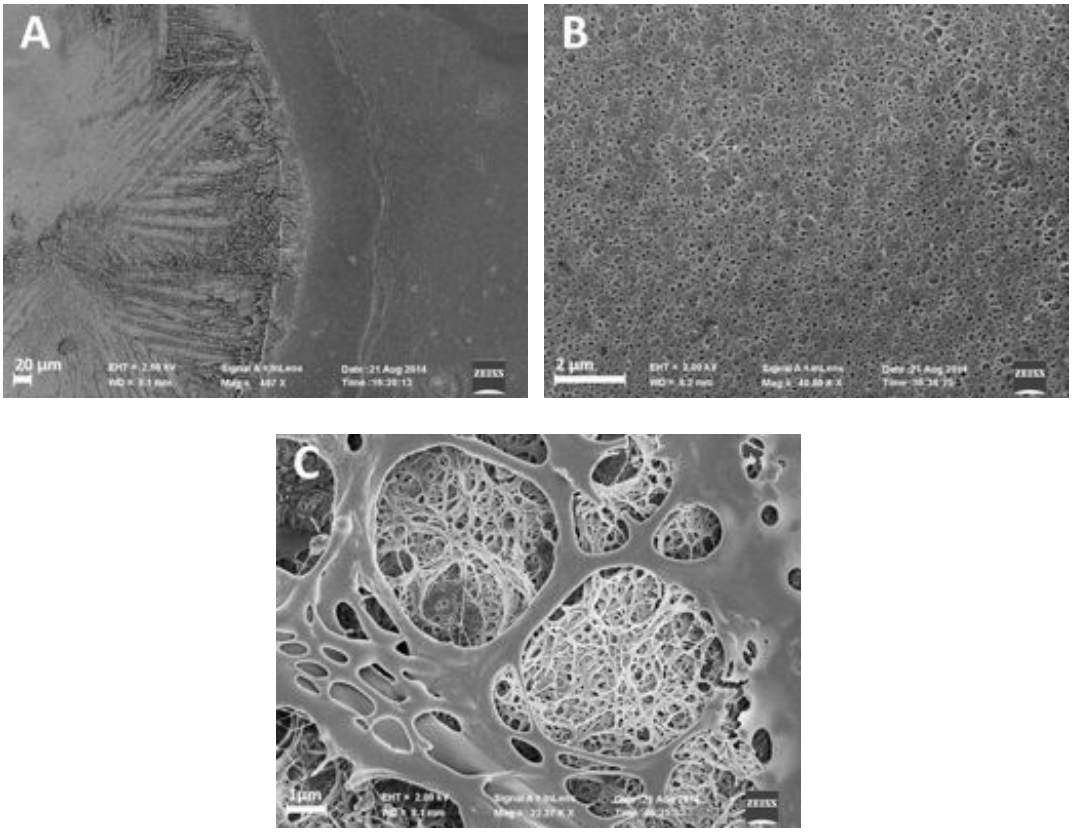

Fig. 8.12: SEM images of different areas of hydrogel *PVA/PVP(3:1)*, prepared with high-molecular weight PVP; (A) 500x, scale bar 20µm; (B) 5000x, scale bar 2µm; (C) 22300x, scale bar 1µm.

Lowering the PVA concentration to 6% in the original solution, as for sample *PVP/PVP(1:1)* yields structures characterized by an overall porosity, with no distinction in porous and non-porous areas (Fig. 8.13). Pores are organized in a very interconnected net-like structure and pore dimensions go up to several microns, although pore size distribution appears to be very broad (see figure 8.13 (B) and (C)).

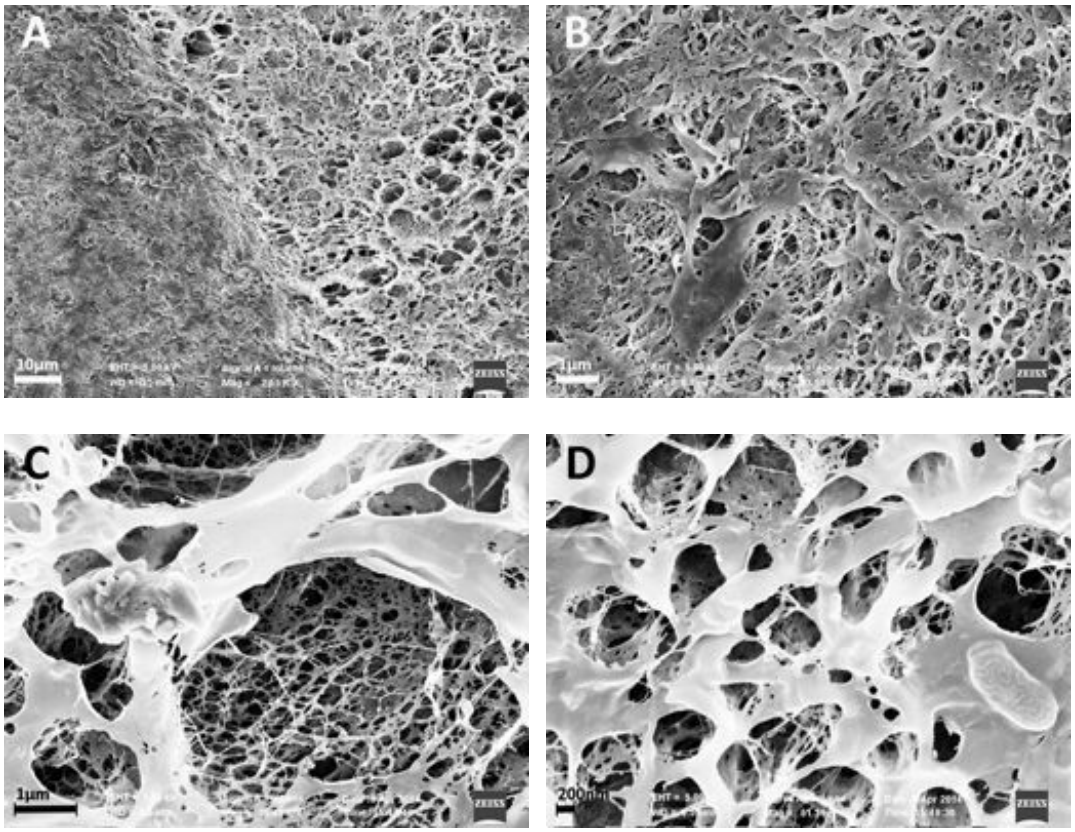

Fig. 8.13: SEM images of hydrogel *PVA/PVP(1:1)*, prepared with high-molecular weight PVP, at different magnifications; (A) 2.650x, scale bar 10µm; (B) 23500x, scale bar 1µm; (C) 35400x, scale bar 1µm; (D) 51300, scale bar 200nm.

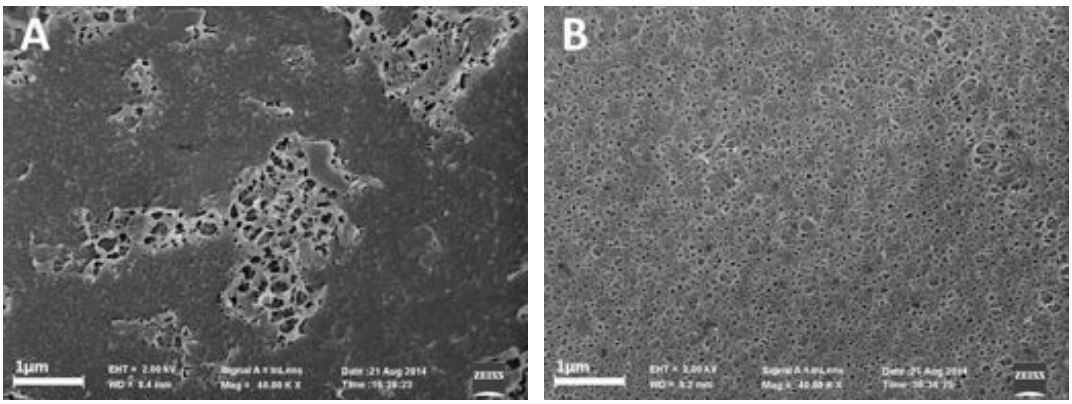

Fig. 8.14: SEM images of hydrogel *PVA/PVP(3:1)* after annealing process; both images (A) and (B) were collected at magnification 40000x, scale bar is 1µm.

SEM analysis permitted to evaluate the effect of annealing on the morphology of sample *PVA/PVP(3:1)*. The comparison of figures 8.14 (A) and (B) with figures 8.10-13 permits to verify that the heat treatment leads to o collapse of the structure: a generalized shrinking of the structure is observed and pore dimensions are sensibly reduced. The collapse of most part of the porosity may be the reason for the strong decrease in free water revealed by thermal analysis (see section 8.1.4).

8.1.8 Structure at the nanoscale: SAXS analysis

Small angle x-ray scattering (SAXS) experiments on hydrogels obtained through cast-drying method were performed to investigate the polymer structure at the nanoscale and the changes imposed by the addition of PVP and by heat treatment (annealing).

Panels (A) and (B) in figure 8.15 show the SAXS intensity distribution for samples PVA 9% and PVA/PVP (3:1) before and after annealing. Fitting of the scattering curves was performed according to a model (Horkay and Hammouda, 2008) that can be interpreted as a generalized version of the Debye-Bueche approach (Domingues et al., 2013). This model, used to fit both, neutral and charged polymeric solutions, presents, in its original form, a first low-q clustering term and a second high-q solvation contribution (Horkay and Hammouda, 2008):

$$\boldsymbol{I(q) = \frac{I_0}{q^n} + \frac{I_0}{1+(|q-q_0|\xi)^m} + B} \qquad \text{(Eq. 8.1)}$$

In Eq. 8.1, n and m are respectively the clustering and solvation Porod exponents, ξ is a correlation length, I_0 is the intensity for $q=0$ and q_0 is the interaction peak position (when applicable), q is the scattering vector. B is a q-independent background, due to the instrument setup.

Since in the acquired SAXS profiles no intensity increase was observed in the low-q region (see Fig. 8.15), the low-q clustering term was omitted and the SAXS curves

were modeled taking into account only the solvation term and the flat background, thus according to:

$$\boldsymbol{I(q) = \frac{I_0}{1+(|q-q_0|\xi)^m} + B} \qquad \text{(Eq. 8.2)}$$

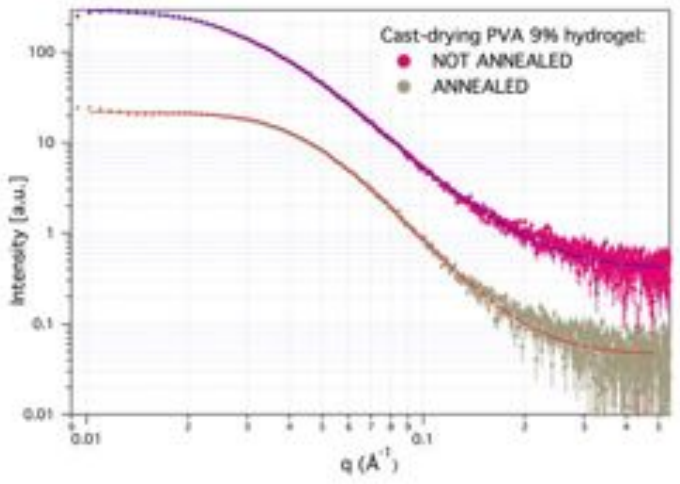

(A)

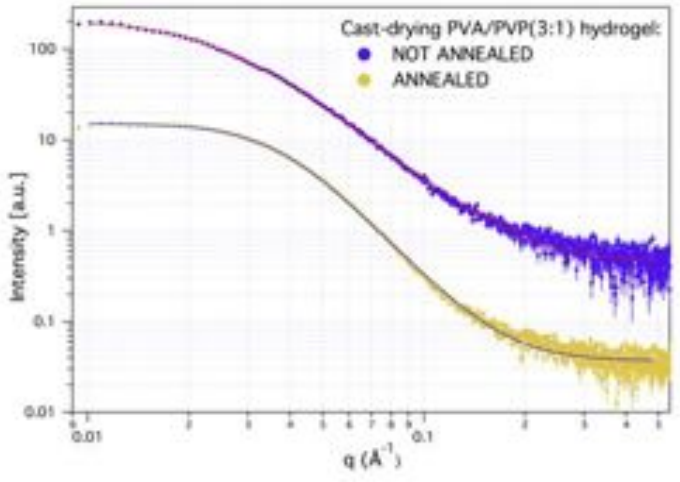

(B)

Fig. 8.15: log-log representation of the scattering intensity distribution for hydrogel samples before and after annealing treatment. (A) Sample PVA 9%; (B) sample PVA/PVP (3:1). Solid lines represent best fitting curves, obtained according to Eq. 8.2.

Table 8.9 lists the fitting parameters related to best fits shown in figure 8.15. As expected, accordingly to the uncharged nature of the used polymers q_0=0 for all investigated formulations. According to Porod's law, it is known that the

generalized Porod exponents vary from 1 (1D objects such as rods) to 4 (objects with smooth surfaces). For diffuse interfaces, such as polymer coils in a theta solvent, an exponent of 2 is expected. Best fits yield *m* parameters ranging from 2.90 to 3.94, reflecting the interfacial sharpness of the scattering centers. Increased *m* parameters for neat PVA and annealed samples can be interpreted as a sharpening of crystallite interfaces: during heat treatment interphases between the crystalline and amorphous phase are refined, while the presence of PVP interferes with this process.

	I(0) (cm^{-1})	***ξ*** (Å)	***m***	***q_0*** (1/Å)	**bkg** (cm^{-1})
not annealed					
PVA 9%	295.4±1.2	34.2±0.4	3.29±0.02	0	0.399±0.006
PVA/PVP (3:1)	207.0±1.8	41.2±0.6	2.90±0.03	0	0.4267±0.006
annealed					
PVA 9%	128.3±0.4	22.9±0.4	3.94±0.05	0	0.269±0.007
PVA/PVP (3:1)	256.2±0.6	27.4±0.3	3.88±0.03	0	0.621±0.005

Tab. 8.9: Parameters related to the best fits to SAXS profiles of neat PVA and blended PVA/PVP hydrogels before and after annealing.

The precise meaning of the correlation length ξ depends on the system microstructure, however, it can be generally regarded as an estimate of the average entanglement distance (Hammouda, 2010). Correlation length increases by 4.5-7 Å for blended PVA/PVP formulations, while a considerable decrease of 11-14 Å is observed as a consequence of the annealing process. Considering that crystallites represent the junction points throughout the polymer network, the increase in ξ related to PVP addition is in agreement with the lower crystallinity degree recorded for the blended systems by means of DSC, ATR and XRD measurements (see sections 8.1.6.1, 8.1.6.2 and 8.1.6.3), that reflects in a less entangled structure. On the other hand, as no increase in crystallinity was detected for the annealed samples, in this case the decrease in ξ cannot be considered as a consequence of higher cross-

linking degrees, but rather due to a contraction of the amorphous phase surrounding the crystalline cross-links.

8.2 Characterization of hydrogels obtained through freeze-thawing method

8.2.1 List of the prepared materials and general observations

Table 8.10 provides a list of the prepared polymer aqueous solutions subject freeze-thawing process. Solutions prepared with low-molecular weight PVP (i.e. $M_w \approx$ 40.000) or low hydrolysis degree PVA (i.e. HD=87-89%) are marked by an asterisk.

Name	PVA % (w/w)	PVP % (w/w)	Annotations
PVA*12% FT	12	0	*PVA 87-89% HD
PVA 12% FT	12	0	PVA 98-99% HD
PVA 9% FT	9	0	PVA 98-99% HD
PVA/PVP*(3:1) FT	9	3	*PVP Mw ≈ $4x10^4$
PVA/PVP*(1:1) FT	6	6	*PVP Mw ≈ $4x10^4$
PVA/PVP*(1:3) FT	3	9	*PVP Mw ≈ $4x10^4$
PVA/PVP(3:1) FT	9	3	PVP Mw ≈$1,3x10^6$
PVA/PVP(2:1) FT	9	4.5	PVP Mw ≈$1,3x10^6$
PVA/PVP(1:1) FT	6	6	PVP Mw ≈$1,3x10^6$
PVA/PEG (3:1) FT	9	3	PEG Mw≈$3,5x10^5$

Table 8.10: List of the hydrogels obtained through freeze-thawing method.

Freeze-thawed hydrogels can be prepared in different forms and shapes, depending on the form and volume of the mold in which they are casted before being subject to freezing. After freezing the samples are opaque and became translucent during thawing.

For each composition a minimum number of freezing cycles was needed to obtain a stable system. Increasing the number of freezing cycles *n*, permits to obtain hydrogels characterized by an increased stability. For a sufficiently large number of

cycles, depending on composition, hydrogels expel water to the surface and a slight contraction of the system is observed. After gelification samples are sticky due to non-crosslinked components; extraction in deionized water eliminates stickiness and very stable but soft and elastic hydrogels are obtained (see Fig. 8.16).
A macroscopic observation of the samples indicates that mechanical properties and adhesion are strongly affected by the number of freezing cycles, the composition of the hydrogels and the PVA concentration of the original solution.

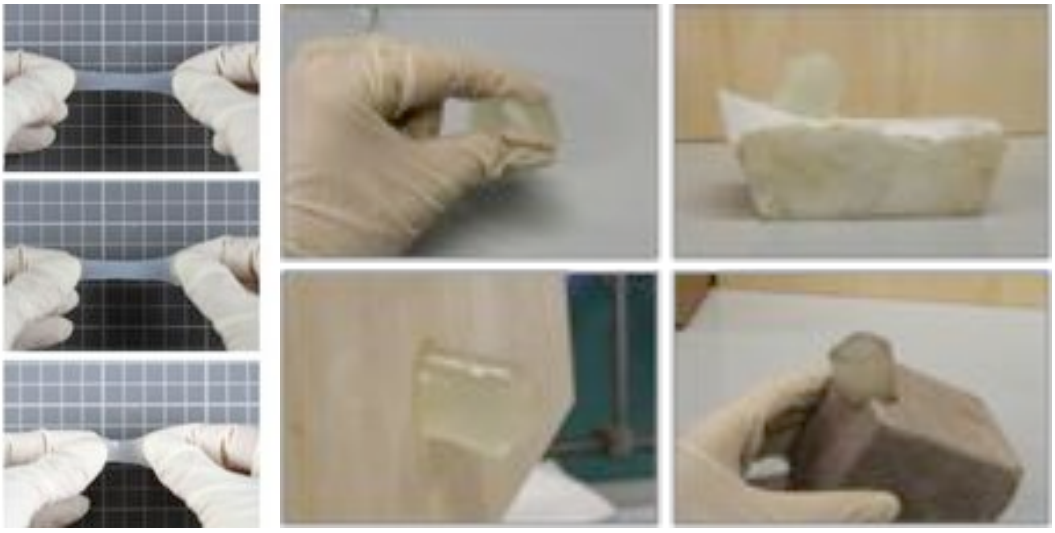

Fig. 8.16: (A) elastic properties of hydrogel *PVA 9% FT*; (B) ability of hydrogel *PVA/PVP(1:1) FT* to adhere to surfaces, also in presence of considerable irregularities.

As for cast-drying method, for synthesis of PVA/PEG blended hydrogel only the polymer-rich phase of the phase separated system was used. Therefore, since a consistent part of water was removed, interpretation of the results must take into account that concentration of the effective solution is higher than reported in Tab. 8.11.

Name	PVA % (w/w)	PVP % (w/w)	Annotations	Reason
PVA*12% FT	12	0	*PVA 87-89% HD	HD too low
PVA/PVP*(1:3) FT	3	9	*PVP Mw ≈ $4x10^4$	%PVA too low

Table 8.11: Formulations for which no gel formation through freeze-thawing method was observed.

As hydrogels prepared through cast-drying method, also freeze-thawed hydrogels are thermoreversible, that is, they dissolve if water is heated above 80°C.

No gel formation was observed for formulations *PVA*12% FT* and *PVA/PVP*(1:3) FT*, indicating that no stable network can be formed for too low PVA concentrations or through the use of PVA with a low HD, which is barely cristallizable.

8.2.2 Gel content G%

As already mentioned, it was observed that a minimum number of freezing and thawing cycles is necessary to achieve gelification, that is to attain a system that is almost partially insoluble in water at room temperature. The minimum number n_{min}, of freezing and thawing cycles to attain gelification is mainly related to PVA concentration in the original solution. The higher the concentration, the lower n_{min}: for *PVA 12% FT* $n_{min}=2$, while for sample *PVA 6% FT* $n_{min}=4$.

This behavior may be related to a more pronounced phase separation process during freezing for more concentrated solutions, which in fact promotes cross-linking through crystallites formation between neighboring PVA chains.

For solution with same PVA concentration, enhanced gelification is observed by increasing the number of freezing cycles.

Sample	Gel Fraction (G%)	
	n=3	**n=7**
PVA 12% FT	41.4 ±0.1	87.7 ±2.1
PVA/PVP*(3:1) FT	40.4 ±2.1	76.0 ±2.9
PVA/PVP*(1:1) FT	27.8 ±5.4	42.2 ±2.8
PVA/PVP (3:1) FT	71.1 ±4.2	91.1 ±3.2
PVA/PVP (2:1) FT	45.0 ±4.2	50.9 ±4.6
PVA/PVP (1:1) FT	25.4 ±1.3	35.9 ± 0.4

Table 8.12: Gel fraction for different hydrogel formulations obtained through freeze-thawing process and subject to n=3 and n=7 freezing cycles.

Table 8.12 reports calculated gel fractions for different formulations subject to *n=3* and *n=7* freezing cycles. Since PVA is the component responsible for network formation, gel faction G% depends on composition: gel fractions are lower for formulations containing PVP, that is embedded into network, but does not participate to crystallites formation. No relevant differences in G% are observed for samples prepared with low or high molecular weight PVP. Moreover, the gel fraction is strongly affected by the number of freezing cycles. Increasing freezing cycles from *n=3* to *n=7*, permits considerably to enhance gel fraction.

Figure 8.17 graphically summarizes the dependence of G% on PVP content and number of freezing cycles. It is interesting to note that an increase in gel fraction in respect to pure PVA (sample *PVA 12% FT*) is observed for composition containing 25% PVP (sample *PVA/PVP (3:1) FT*), while for all other formulations containing PVP G% is strongly reduced. This behavior may be related to the achievement of a good miscibility between the two polymers in this particular ratio.

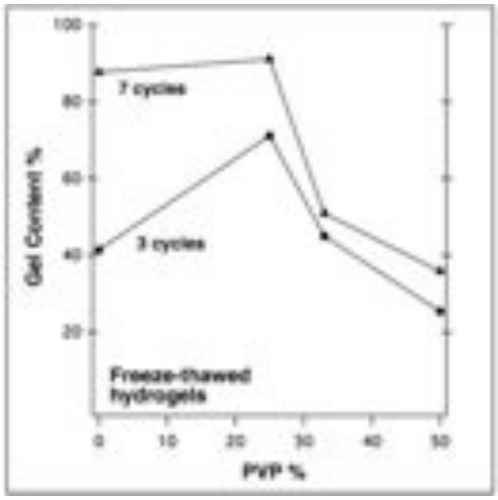

Fig. 8.17: Dependence of gel fraction G% on PVP content and number of freezing cycles.

8.2.3 Composition of hydrogels

To investigate possible differences in composition related to variation in efficiency of embedding the high- or low-molecular weight PVP, ATR-FTIR spectra of previously water-extracted and dried hydrogel films were collected.

Spectra of hydrogels prepared with high-molecular weight PVP (*PVA/PVP (3:1)FT*), low-molecular weight PVP (*PVA/PVP* (3:1)FT*) and neat PVA (*PVA12%FT*) are presented in Fig. 8.18.

As in case of hydrogels obtained through cast-drying method, the characteristic absorptions of PVP at 1658 and 1288 cm^{-1} are more evident in ATR-FTIR spectra of *PVA/PVP(3:1)FT* sample, indicating that longer PVP macromolecular chains are more efficiently embedded into the PVA network.

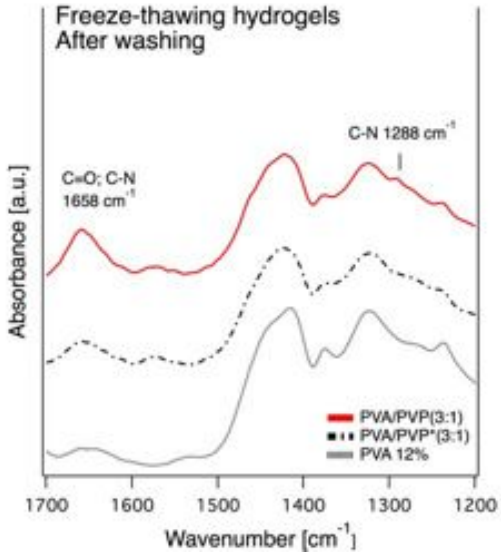

Fig. 8.18: ATR-FTIR spectra of samples *PVA/PVP(3:1)FT* prepared with PVP (M_w≈130000) (red line), *PVA/PVP*(3:1)FT* prepared with PVP M_w≈40000 (dotted line) and *PVA12%FT* (solid line). Spectra were normalized in respect to PVA absorption maximum at 1033 cm^{-1}.

However, differences in absorption seem not to account for the considerable difference ascertained in gel content analysis (see section 8.2.3), where sample *PVA/PVP (3:1)FT* displayed substantially increased values in respect to other

formulations. Though, a more in-depth and quantitative study of hydrogels composition should be considered.

8.2.4 Water content and free water

Equilibrium water content and free water index were calculated by thermal analysis for samples prepared with pure PVA and for blends containing different quantities of PVP or PEG. Results are listed in table 8.13.

Sample	**EWC (%)**	**FWI**
PVA 9% FT	95.3	0.92
PVA/PVP (3:1) FT	94.0	0.95
PVA/PVP (2:1) FT	96.1	0.93
PVA/PEG (3:1) FT	92.6	0.91

Table 8.13: Equilibrium water content (EWC) and free water index (FWI) for different freeze-thawing hydrogel formulations.

Unlike for hydrogels obtained through cast-drying method, in case of freeze-thawing hydrogels composition has little effect on both, equilibrium water content and free water index. The behavior of water within the hydrogel may in this case be governed to a greater extent by the porous structure of the gel, rather than by the interactions existing within the polymer chains. In fact, as will be elucidate in section 8.2.7, freeze-thawed hydrogels are characterized by a macroporous structure; thus, there will be only little interaction between water contained within pores and pore walls, reducing the effects of composition of the polymer lattice.

8.2.5 Crystallinity of hydrogels

Evaluation of the crystallinity degree in freeze-thawed hydrogels was performed by means of DSC, ATR-FTIR and XRD analysis, according to experimental conditions described in Chapter 7, section 7.4. The aim was to investigate the effects of blending (with PVP or PEG) and of the number of freezing cycles on crystallization behavior.

8.2.5.1 Determination of crystallinity through DSC

DSC measurements for the investigation of the crystallinity degree were performed on hydrogel samples characterized by different contents of a blended component (PVP or PEG).

As for hydrogels obtained through cast-drying method, the degree of crystallinity decreases considerably for increasing PVP content, indicating that the presence of this hydrophilic component interferes with the crystallization process (see Tab. 8.14).

	Melt Onset Temp. (°C)	Melt Peak Temp. (°C)	Enthalpy (J/g)	X_c (%)
PVA 9% FT	204.2	222.3	56.0	**34.8**
PVA/PVP (3:1) FT	199.1	221.6	47.2	**29.3**
PVA/PVP (2:1) FT	208.5	222.3	30.7	**19.1**
PVA/PEG (3:1) FT	204.4	222.1	60.1	**37.3**

Tab. 8.14: Crystallinity values obtained through DSC analysis on neat PVA samples and blended PVA/PVP or PVA/PEG hydrogels obtained through 3 freezing cycles. Represented values are the mean of two measurements.

A surprisingly high X_c value is observed for sample *PVA/PEG (3:1) FT*, which can probably be related to the higher concentration of the solution subject to freezing, originated from phase separation process occurring after cooling of the original

solution. The higher concentration of the solution favors crystallization process during freezing.

8.2.5.2 Determination of crystallinity through ATR-FTIR

ATR-FTIR analyses on hydrogels obtained through freeze-thawing method were performed to investigate the influence of blending, but also to evaluate the effect of increased number of freezing cycles, on crystallization process. The integrated intensity ratio I_{1141}/I_{850}, which is proportional to crystallinity degree, shows that the presence of PVP interferes with crystallization process by lowering the crystallinity. Fig. 8.19 shows an example of fits carried out on ATR FT-IR spectra to obtain the integrated intensity of I_{1141} and I_{850}.

As expected, increasing the number of freezing cycles from n=3 to n=7 leads to higher crystallinity of the hydrogels, confirming that nucleation and/or growth of crystals occurs within each freezing cycle (see Tab. 8.15).

The trend observed is in accordance with crystallinity values obtained on freeze-thawed hydrogels through DSC measurements, as described in previous section.

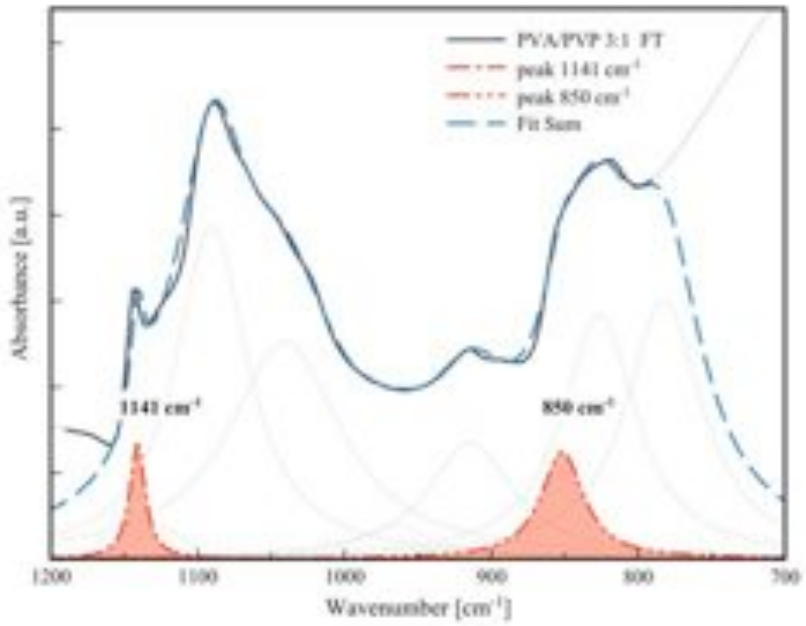

Fig. 8.19: ATR-FTIR spectra of sample *PVA/PVP (3:1) FT* for n=7 freezing cycles. Blue line represents the fit sum of the multi-peak fitting performed with MagicPlotPro®. Areas of the crystalline peak at 1141 cm^{-1} and of the amorphous peak at 850 cm^{-1} are highlighted in red.

	Peak area 1141 cm^{-1}	Peak area 850 cm^{-1}	$\mathbf{I_{1141}/I_{850}}$
3 freeze-thawing cycles			
PVA 9%	1.27	3.20	**0.39**
PVA/PVP (3:1)	1.75	5.56	**0.31**
PVA/PEG (3:1)	1.06	5.18	**0.20**
7 freeze-thawing cycles			
PVA 9%	1.46	3.26	**0.45**
PVA/PVP (3:1)	1.33	3.45	**0.37**
PVA/PVP* (1:1)	1.03	4.57	**0.23**

Tab. 8.15: Crystalline (1141 cm^{-1}) and amorphous (850 cm^{-1}) peak areas for the analyzed freeze-thawed hydrogel samples. I_{1141}/I_{850} represents a qualitative index, proportional to crystallinity of the samples.

8.2.5.3 Determination of crystallinity through XRD

X-ray diffraction profiles of freeze-thawed hydrogels were collected to highlight differences in crystallinity due to changes in composition of the samples. Thus, XRD measurements were performed on neat and blended (with PVP or PEG) hydrogel systems.

Fig. 8.20 shows a typical diffraction profile from freeze-thawed hydrogels, with indication of the integrated crystalline peak relative to $10\bar{1}$ reflection at $2\theta=19.4°$. Since water content of freeze-thawed hydrogels is higher than in hydrogels obtained through cast-drying method, only the maximum relative to $10\bar{1}$ reflection is visible, while no shoulder relative to 101 reflection at $2\theta=20°$ was detected.

Ratios $A_{cryst.}/A_{tot}$, that are a qualitative measure of the crystallinity for the investigated samples, are listed in Tab. 8.16. In accordance with results obtained from previous DSC and ATR-FTIR measurements, crystallinity decreases with

increasing PVP content. Sample obtained through blending with PEG displays an higher crystallinity due to higher concentration of the solution subject to freezing, due to phase separation process occurring after mixing.

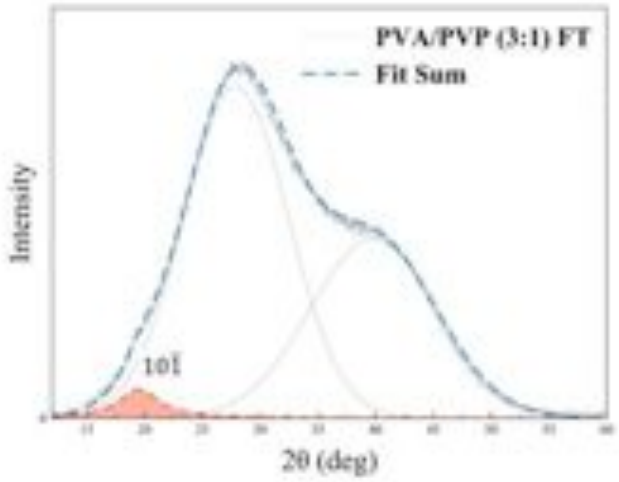

Fig. 8.20: X-ray powder diffraction profile of "wet" *PVA/PVP (3:1) FT* sample. The $10\bar{1}$ reflection at 2θ=19.4° is indicated.

	Area$_{cryst}$ (a.u.)	**Area$_{tot}$** (a.u.)	**A$_{cryst.}$/A$_{tot}$**
PVA 9% FT	4.929	136.107	**0.036**
PVA/PVP (3:1) FT	4.301	143.743	**0.030**
PVA/PVP (2:1) FT	2.643	120.793	**0.022**
PVA/PEG (3:1) FT	4.971	142.054	**0.035**

Tab. 8.16: Crystalline and total areas calculated from x-ray diffraction pattern of "wet" freeze-thawed hydrogel samples. The $A_{cryst.}/A_{tot}$ ratio gives a relative measure of crystallinity for comparative purposes.

8.2.6 Morphology and structure: SEM analysis

Figures 8.21-8.23 show SEM micrographs of different hydrogel formulations obtained through freezing-thawing technique. All hydrogels are characterized by heterogeneous and highly porous structures arising from freezing process occurring in the biphasic polymer-water system. In fact, solid ice crystals forming in the

unfrozen liquid polymer-rich phase act as pore-forming agents and are responsible for the macropourous structure of the gel after thawing. Ice crystal growth occurs until neighboring crystals come into tight contact with each other; thus, macropores are interconnected (Lozinsky and Plieva, 1998). Examination of the SEM images shows that morphology and porous structure is affected by the number of freezing cycles and by PVA concentration of the solution.

Figures 8.21 (A) and (B) show the porous structure of two hydrogels obtained through respectively *n=7* and *n=3* freezing cycles of pure PVA-water solutions. As already observed in previous researches, pore dimensions and pore walls are noticeably larger for the hydrogel obtained through the larger number of freezing cycles (Hatakeyema et al., 2005). This phenomenon was explained by the fact that repeated segregation caused by each freezing cycle makes the polymer-poor phase increasingly approach the composition of pure water, leading to formation of more and more defined ice crystals. As a consequence, the porous structure of the gel becomes more evident.

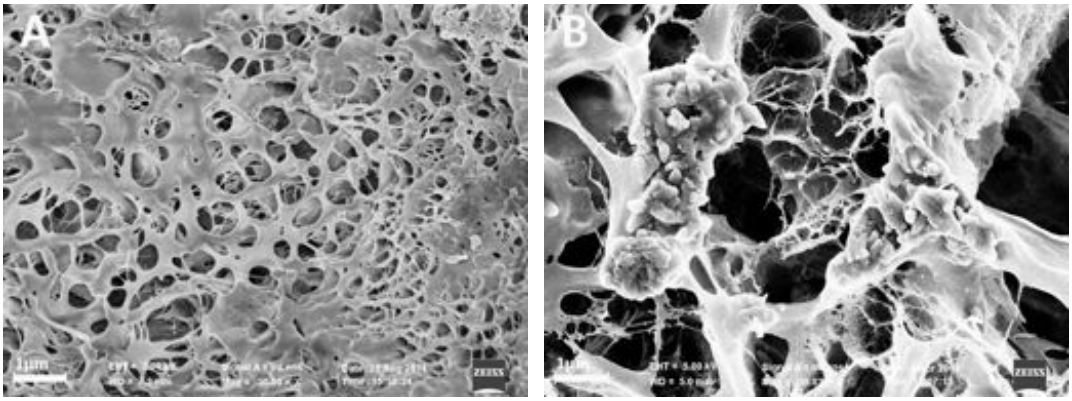

Fig. 8.21: SEM images of hydrogel *PVA 9% FT* after 3 freezing cycles (A) and hydrogel *PVA 12% FT* after 7 freezing cycles; magnification is 30000x and 30800x respectively, scale bar is 1 μm.

Similar behavior is observed for hydrogels obtained through blending with PVP: sample *PVA/PVP (3:1) FT* obtained after *n=3* freezing cycles exhibits a less defined porosity and reduced pore sizes than sample *PVA/PVP (1:1) FT* with *n=10*. Effect on pore dimensions and pore wall thickness is in this case also enhanced by the different PVA concentration of the two samples. As already stated by Lozinsky

et al., the higher the polymer concentration, the smaller the formed ice crystals, hence, by increasing the PVA concentration the amount and size of macropores decreases and pore wall thickness increases (Lozinsky and Plieva, 1998).

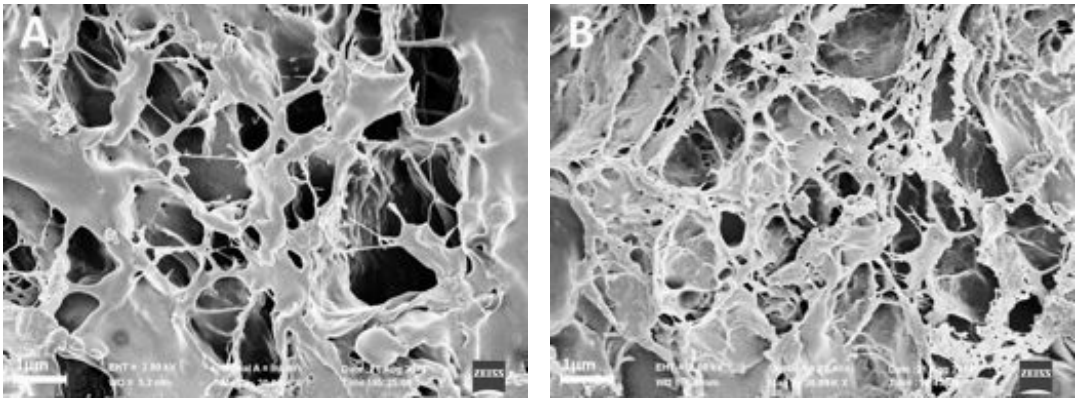

Fig. 8.22: SEM images of hydrogel *PVA/PVP (3:1)FT* with 3 freezing cycles (A) and hydrogel *PVA/PVP (1:1)FT* with 10 freezing cycles (B); magnification is 30000x, scale bar 1 μm.

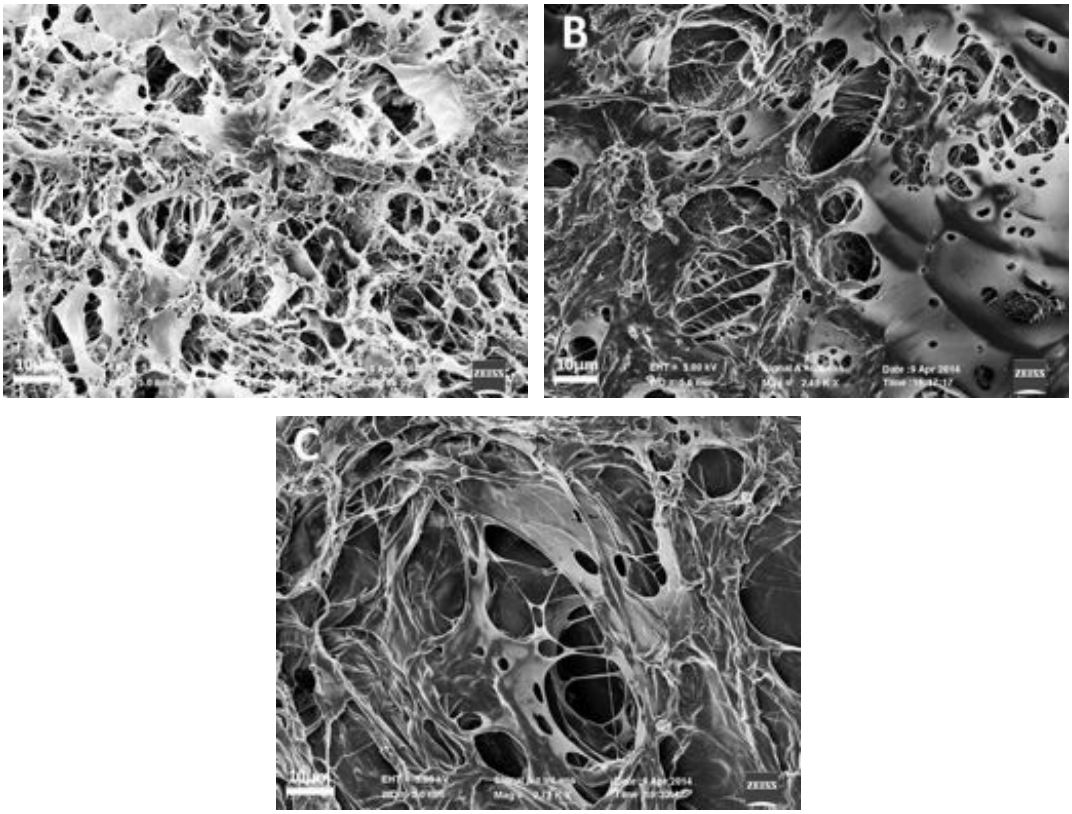

Fig. 8.23: SEM images of hydrogels *PVA 12% FT* (A), *PVA/PVP (3:1)FT* and *PVA/PVP (1:1)FT,* all with 7 freezing cycles; magnification are respectively 2600x, 2450x and 2.700x; scale bar is 1μm.

Effect of different PVA concentration is more evident in figure 8.23, where samples characterized by 12, 9 and 6% PVA concentration are presented (Fig. 8.23 (A), (B) and (C), respectively). SEM images show clearly that decreasing PVA concentration leads to formation of larger pores and thinner pore walls.
Observations in scanning electron microscopy show that regulation of the freezing regimes and the composition of the systems permits to control final porosity of the gel matrix.

8.2.7 Structure at the nanoscale: SAXS analysis

Figure 8.24 shows the SAXS intensity distribution for samples *PVA 9% FT*, *PVA/PVP (3:1) FT* and *PVA/PEG (3:1) FT* subject to n=3 freezing cycles.
SAXS curves of freeze-thawed hydrogels were modeled according to Eq. 8.2 (see section *8.1.8*) and related parameters are shown in Tab. 8.17.

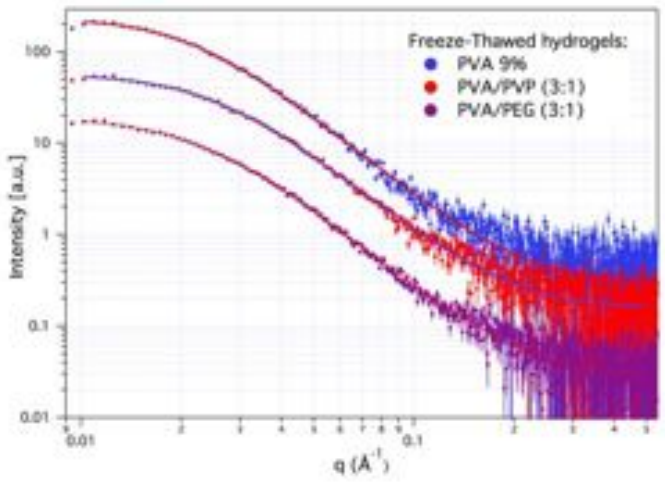

Fig. 8.24: log-log representation of the scattering intensity distribution for hydrogel samples *PVA 9% FT*, *PVA/PVP (3:1) FT* and *PVA/PEG (3:1) FT* obtained after n=3 freezing cycles. Solid lines represent best fitting curves, obtained according to Eq. 8.2.

For all investigated systems, the resulting parameter *m* has a constant value of ~2.9, which corresponds to "mass fractals" such as branched systems or networks

(Hammouda, 2010) and is thus in agreement with the typical structure of a gel system. Obtained *m* values for freeze-thawing hydrogels subject to n=3 freezing cycles are consistent with results of small-angle neutron scattering (SANS) experiments provided by previous research by Ricciardi et al., that evidenced a dependence of the slope in the high-*q* region from the number of freezing cycles. The parameter *m*, that governs the power-law followed by the curves, was found to be $m \cong 2$ for n=1; $m \cong 3$ for n=2 and n=3 and $m \cong 3.5$ for n=5 (Ricciardi et al., 2005). According to Porod's law, if the boundaries between phases are smooth, an *m* value of 4 is observed, values for this parameter lower than 4, as obtained in our case, suggest that boundaries of scattering objects are not well defined.

	I(0) (cm^{-1})	ξ (Å)	***m***	q_0 (1/Å)	**bkg** (cm^{-1})
PVA 9% FT	78.2±1.6	47.2±1.5	2.92±0.06	0	0.091±0.005
PVA/PVP (3:1) FT	56.6±1.2	40.4±1.4	2.87±0.07	0	0.152±0.006
PVA/PEG (3:1) FT	93.6±1.6	43.9±1.1	2.89±0.05	0	0.133±0.005

Tab. 8.17: Parameters related to the best fits to SAXS profiles of neat PVA and blended PVA/PVP and PVA/PEG hydrogels obtained through freeze-thawing method.

For the analyzed systems, the correlation length ξ falls in the range of 40-48 Å, indicating that the average size of the basic scattering unit does not change much as a consequence of blending process. The average mesh size is higher for freeze-thawing method hydrogels rather than for hydrogels obtained through cast-drying method. This is in accordance with previous results that evidenced higher water contents and swelling degrees for freeze-thawed hydrogels than for hydrogels obtained through cast-drying method.

References

Borodko, Y., Habas, S.E., Koebel, M., Yang, P., Frei, H., Somorjai, G.A., 2006. Probing the Interaction of Poly(vinylpyrrolidone) with Platinum Nanocrystals by UV−Raman and FTIR. J. Phys. Chem. B 110, 23052–23059.

Bunn, C.W., 1948. Crystal structure of Polyvinyl Alcohol. Nature 161, 929–930.

Burghoff, H.-G., Pusch, W., 1979. Characterization of water structure in cellulose acetate membranes by calorimetric measurements. J. Appl. Polym. Sci. 23, 473–484.

Cha, W.-I., Hyon, S.-H., Ikada, Y., 1993. Microstructure of poly(vinyl alcohol) hydrogels investigated with differential scanning calorimetry. Makromol. Chem. 194, 2433–2441.

Domingues, J.A.L., Bonelli, N., Giorgi, R., Fratini, E., Gorel, F., Baglioni, P., 2013. Innovative Hydrogels Based on Semi-Interpenetrating p(HEMA)/PVP Networks for the Cleaning of Water-Sensitive Cultural Heritage Artifacts. Langmuir 29, 2746–2755.

Hammouda, B., 2010. SANS from Polymers—Review of the Recent Literature. Polym. Rev. 50, 14–39.

Hatakeyema, T., Uno, J., Yamada, C., Kishi, A., Hatakeyama, H., 2005. Gel–sol transition of poly(vinyl alcohol) hydrogels formed by freezing and thawing. Thermochim. Acta, A collection of papers from the 40th Anniversary Japanese Conference on Calorimetry and Thermal Analysis held in Tokyo, Japan, October 12 - 14, 2004 431, 144–148.

Hodge, R.M., Edward, G.H., Simon, G.P., 1996. Water absorption and states of water in semicrystalline poly(vinyl alcohol) films. Polymer 37, 1371–1376.

Horkay, F., Hammouda, B., 2008. Small-angle neutron scattering from typical synthetic and biopolymer solutions. Colloid Polym. Sci. 286, 611–620.

Jang, J., Lee, D.K., 2003. Plasticizer effect on the melting and crystallization behavior of polyvinyl alcohol. Polymer 44, 8139–8146.

Kenney, J.F., Willcockson, G.W., 1966. Structure–Property relationships of poly(vinyl alcohol). III. Relationships between stereo-regularity, crystallinity, and water resistance in poly(vinyl alcohol). J. Polym. Sci. [A1] 4, 679–698.

Lee, J., Jin Lee, K., Jang, J., 2008. Effect of silica nanofillers on isothermal crystallization of poly(vinyl alcohol): In-situ ATR-FTIR study. Polym. Test. 27, 360–367.

Li, W., Xue, F., Cheng, R., 2005. States of water in partially swollen poly(vinyl alcohol) hydrogels. Polymer 46, 12026–12031.

Lozinsky, V.I., Plieva, F.M., 1998. Poly(vinyl alcohol) cryogels employed as matrices for cell immobilization. 3. Overview of recent research and developments. Enzyme Microb. Technol. 23, 227–242.

Mallapragada, S.K., Peppas, N.A., 1996. Dissolution mechanism of semicrystalline poly(vinyl alcohol) in water. J. Polym. Sci. Part B Polym. Phys. 34, 1339–1346.

Mansur, H.S., Sadahira, C.M., Souza, A.N., Mansur, A.A.P., 2008. FTIR spectroscopy characterization of poly (vinyl alcohol) hydrogel with different hydrolysis degree and chemically crosslinked with glutaraldehyde. Mater. Sci. Eng. C, Proceedings of the Symposium on Nanostructured Biological Materials, V Meeting of the Brazilian Materials Research Society (SBPMat) 28, 539–548.

Mattiasson, B., Kumar, A., Galeaev, I.Y., 2009. Macroporous Polymers: Production Properties and Biotechnological/Biomedical Applications. CRC Press.

Mooney, R.C.L., 1941. An X-Ray Study of the Structure of Polyvinyl Alcohol*. J. Am. Chem. Soc. 63, 2828–2832.

Peppas, N.A., 1977. Infrared spectroscopy of semicrystalline poly(vinyl alcohol) networks. Makromol. Chem. 178, 595–601.

Peppas, N.A., Merrill, E.W., 1976. Differential Scanning Calorimetry of Crystallized PVA Hydrogels. J. Appl. Polym. Sci. 20, 1457–1465.

Peppas, N.A., Tennenhouse, D., 2004. Semicrystalline poly(vinyl alcohol) films and their blends with poly(acrylic acid) and poly(ethylene glycol) for drug delivery applications. J. Drug Deliv. Sci. Technol. 14, 291–297.

Ricciardi, R., Auriemma, F., De Rosa, C., Lauprêtre, F., 2004. X-ray Diffraction Analysis of Poly(vinyl alcohol) Hydrogels, Obtained by Freezing and Thawing Techniques. Macromolecules 37, 1921–1927.

Ricciardi, R., Mangiapia, G., Lo Celso, F., Paduano, L., Triolo, R., Auriemma, F., De Rosa, C., Lauprêtre, F., 2005. Structural Organization of Poly(vinyl alcohol) Hydrogels Obtained by Freezing and Thawing Techniques: A SANS Study. Chem. Mater. 17, 1183–1189.

Watase, M., Nishinari, K., 1985. Rheological and DSC changes in poly(vinyl alcohol) gels induced by immersion in water. J. Polym. Sci. Polym. Phys. Ed. 23, 1803–1811.

Wolfe, J., Bryant, G., Koster, K.L., 2002. What is unfreezable water, how unfreezable is it and how much is there? CryoLetters 23, 157–166.

Chapter 9 – Application properties and preliminary tests

This chapter provides information related to practical application of the presented blended PVA-based hydrogel systems. Water release tests and evaluation of the adhesion features of different formulations are presented, along with some preliminary cleaning tests performed on different supports. Moreover, FT-IR analysis to assess on possible gel residues on porous and hydrophilic supports was also carried out.

9.1 Water release test

Water release tests provide useful information on retention properties of hydrogels. From a practical point of view and depending on the characteristics of the substrate that needs to be treated, the assessment on quantity of water that is released on a highly hydrophilic support (e.g. filter paper) permits a more conscious choice on the more suitable formulation.

For instance, if the materials constituting the artifact are highly water-sensitive, enhanced retention features are required and a formulation with low water release will be the most suitable. On the other hand, if the layer to be removed is very tough and hardened or difficult to solubilize, the gel must be able to exchange higher quantities of liquid phase with the surface; thus, a formulation with higher water release ability might better match this requirement.

For the evaluation of water release properties, fully swollen hydrogels were gently surface dried and then positioned on five sheets of Whatman® filter paper and covered with a lid to avoid water evaporation. The sheets of filter paper were

weighted before and after gel applications of 15min (for cast-drying method hydrogels) or 30 min (for freeze-thawing method hydrogels). Tables 9.1 and 9.2 show water release for different hydrogel formulations obtained through both, cast-drying and freeze-thawing method. In case of freeze-thawing method hydrogels, variation in water release properties depending of the number of freezing cycles *n* was also assessed. The released water is normalized by unit area.

Obtained data show lower water release values for cast-drying hydrogels in respect to formulations obtained through repeated freezing and thawing. In fact, freeze-thawing hydrogels are characterized by higher free-water content and greater pore dimensions (see sections 8.1.4, 8.17, 8.24, 8.2.6), which result in increased water mobility within the gel network.

We recall (see section 8.1.4) that for cast-drying hydrogels, only formulations characterized by the presence of a consistent amount of PVP present free-water contents making them suitable for cleaning purposes. In fact, water release values <5 mg/cm^2 registered for samples *PVA 6%*, *PVA 12%*, *PVA/PVP (3:1)* might be not sufficient for an homogeneous wetting and a uniform cleaning action. However, in practical applications, covering the hydrogel with a plastic wrap permits to reduce hydrogels dehydration, increasing the quantity of water released on the surface.

Cast-drying method hydrogels	Water release (mg/cm^2)
PVA 6%	4.5 ±1.4
PVA 12%	3.3 ±0.4
PVA/PVP (3:1)	4.1 ±0.7
PVA/PVP (1:1)	13.2 ±1.2

Tab 9.1: Water release on Whatman® filter paper for different formulations of cast-drying method hydrogels after 15 min contact.

The quantity of water released by freeze-thawing hydrogels depends on both, the composition and the number of freezing cycles. Water release generally decreases for increasing *n*. The effect is more pronounced for low *n* values (passing from *n=2* to *n=4*) while for higher *n* values probably a plateau will be reached (after *n=7*).

In general, lower PVA concentrations provide higher water release (see values for formulations *PVA 6% FT* and *PVA 12% FT*), while increasing PVP concentration leads increase of release water quantities. In fact, the water release of ~ 100mg/cm^2 displayed by the *PVA/PVP (1:1) FT* formulation, can be considered too high to obtain a controlled cleaning action on a sensitive substrate. Values of all other formulations fall in a range that makes them suitable for application as carriers for water-based cleaning methods.

Freeze-thawing method hydrogels	Water release (mg/cm^2)		
	n=2	***n=4***	***n=7***
PVA 6% FT	36.5 ±3.6	23.7 ±1.9	21.4 ±2.0
PVA 12% FT	26.9 ±3.5	14.9 ±1.4	14.2 ±2.6
PVA/PVP (3:1) FT	32.2 ±0.6	20.3 ±3.6	19.9 ±3.6
PVA/PVP (1:1) FT	n.a.	94.8 ±8.7	104.4 ±5.7
PVA/PEG (3:1) FT	19.1 ±1.1$^{(a)}$	n.a.	n.a.

Tab 9.2: Water release on Whatman® filter paper for different formulations of freeze-thawing method hydrogels after 30 min contact; *n* is the number of freezing cycles.
$^{(a)}$ hydrogel formulation *PVA/PEG (3:1) FT* was subject to *n=3* freezing cycles.

In conclusion, the performed water release tests show that retention properties of PVA-based hydrogels can be tuned by varying the PVA concentration, by addition of a further component (PVP, PEG) and, in case of freeze-thawing hydrogels, by varying the number of freezing cycles.

9.2 Adhesion features

In this section some of the enhanced adhesion features of blended PVA based hydrogels are presented. In fact, both, cast-drying and freeze-thawing method hydrogels are able to adhere to irregular or modeled surfaces, owing to their flexibility and elastic properties. Thanks to their strong cohesion forces they can be

easily removed without leaving gel residues.

Fig. 9.1 shows adhesion of *PVA/PVP (3:1)* cast-drying hydrogel on the moldings of a wooden frame. The transparent and flexible gel is able to adapt to the shape of the surface adhering like a second skin and granting a uniform adhesion, which is necessary for attaining a homogeneous cleaning action.

Fig. 9.1: Adhesion features of *PVA/PVP (3:1)* cast drying hydrogel, which is able to adapt his shape to the modeled surface of a wooden frame.

Fig. 9.2: Adhesion features of *PVA/PVP(3:1)FT* (freeze-thawing) hydrogel, thanks to its elasticity and softness it can penetrate within modeled holes on the surface of a gypsum bas-relief.

In Fig.9.2 hydrogel *PVA/PVP(3:1)FT*, obtained through freeze-thawing method, was applied on a gypsum bas-relief. The surface is modeled forming elevations, depressions including actual holes. These areas would be difficult to reach with a typical chemical gel formulation (characterized by a fixed shape), while using a physical gel with jam-like consistency would result in a difficult and incomplete removal. The blended PVA/PVP hydrogel perfectly adheres to the surface within the hole and can be gently removed after 15min of contact by the use of tweezers, without causing any stress to the surface.

Different formulations display different adhesion and different grades of mechanical "adjustability". The optical and tactile analysis of the samples permits to state that, as a rule of thumb, a decreased PVA concentration and an increased PVP concentration increase hydrogels adaptability to the surface they are put in contact with. The addition of PEG increases mechanical stability and makes the gel stiffer. Considering the formulations listed in section 9.1, adhesion features and mechanical adjustability of both, cast-drying and freeze-thawing hydrogels, can be evaluated as follows:

Adhesion features and mechanical adjustability
PVA/PVP (1:1) > ***PVA 6%*** > ***PVA/PVP (3:1)*** > ***PVA 12%*** > ***PVA/PEG (3:1)***

Tab. 9.3: Adhesion features and mechanical adjustability of different hydrogel formulations.

9.3 Preliminary cleaning tests

Hydrogels can be used for both, the cleaning or softening of hydrophilic materials and for removal of hydrophobic layers by means of water-based cleaning systems such as microemulsions. The use of microemulsions loaded within hydrogels has been extensively reported for several hydrogel formulations (Bonini et al., 2008; Domingues et al., 2013; Pizzorusso et al., 2012). In particular, Pizzorusso et al.

investigated the ability of hydrogel systems to load nanostructured fluids by means of SAXS measurements, which revealed that nanodroplets of solvents and surfactant can be actually included within the gel structure (Pizzorusso et al., 2012).

9.3.1 Cleaning with water

After synthesis hydrogels are stored in purified water, in which they are very stable, even for long periods (e.g. a year). After gentle surface drying to remove the excess water, such water-loaded hydrogels can be directly used for the removal of hydro-soluble surface grime, the softening of hardened hydrophilic layers, or for the controlled humidification of substrates.

Figure 9.3 shows the application of a freeze-thawed PVA/PVP (3:1) hydrogel on a hardened white layer that covers a gilded wooden frame. The solid white layer is quite compact, so its removal is possible only by means of a considerable mechanical action (see figure 9.3), which might be very stressful for the underlying gilded layer. 20 minutes humidification with PVA/PVP hydrogel results in a substantial softening of the white layer, that can be consequently removed by a gentle action with a cotton swab.

Fig. 9.3: Softening of a hardened layer by means of application of a freeze-thawed PVA/PVP hydrogel. After 20 min application, the layer can be gently removed using a cotton-swab.

Figure 9.5 presents a cleaning test on an ancient parchment sample provided by the National Archives at Kew, United Kingdom, dating back to the reign of King George the third (Fig. 9.4).

The surface is covered by a deposit, which strongly adheres on the undelaying parchment support. For the removal, a water-loaded *PVA/PVP(2:1)FT* hydrogel was used, application was 10 minutes. No further mechanical action was needed for the grime removal; cleaning result is highlighted by observation in UV-light (see Fig. 9.5). No deformation or swelling of the parchment surface due to contact with water was observed.

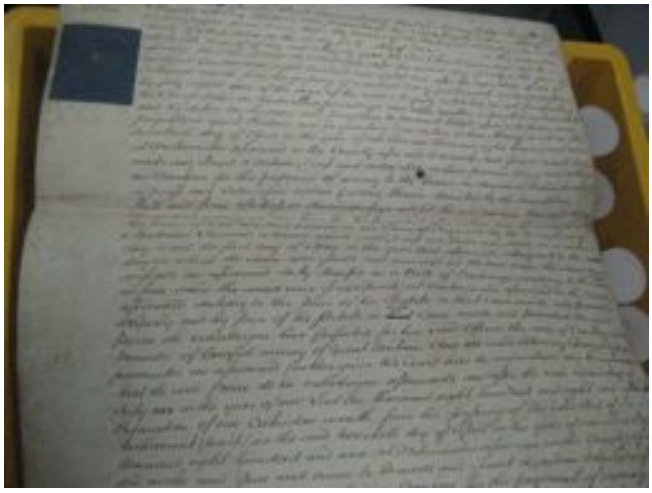

Fig. 9.4: Ancient parchment from National Archives at Kew, 18th century.

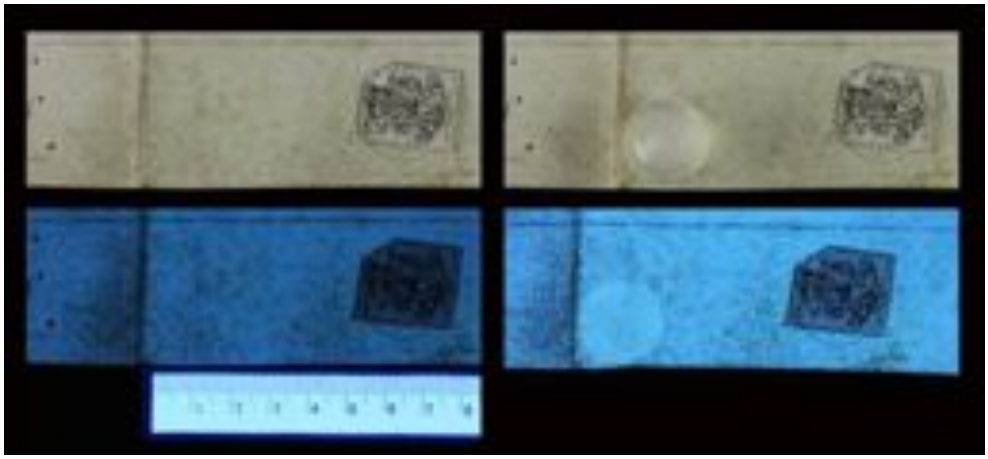

Fig. 9.5: Cleaning of hydrophilic surface grime from parchment, images were captured in diffuse visible light (t*op*) and UV-light (*bottom*).

9.3.2 Cleaning with microemulsions

Hydrogels can be loaded with microemulsions by immersion of the gel for at least 12h, to permit the system to reach equilibrium. After gentle surface drying to remove the liquid in excess, hydrogels can be applied to the surface to be cleaned.
Due to higher dehydration kinetics, in case of hydrogels obtained through cast-drying method, covering the gel with a plastic wrap during application permits to enhance cleaning performance.
Figures 9.6 and 9.7 presents cleaning results obtained after application of cast-drying and freeze-thawing method PVA/PVP hydrogels for the removal of an aged and yellowed terpenic varnish coating from a canvas painting. For this purpose, both hydrogels were loaded with a microemulsion containing ethylacetate (EA) and propylene carbonate (PC) as the dispersed phase. This microemulsive system, named EAPC, has proven to be an highly effective and versatile systems for the removal of various classes of polymers (Baglioni et al., 2012a, 2012b, 2010).

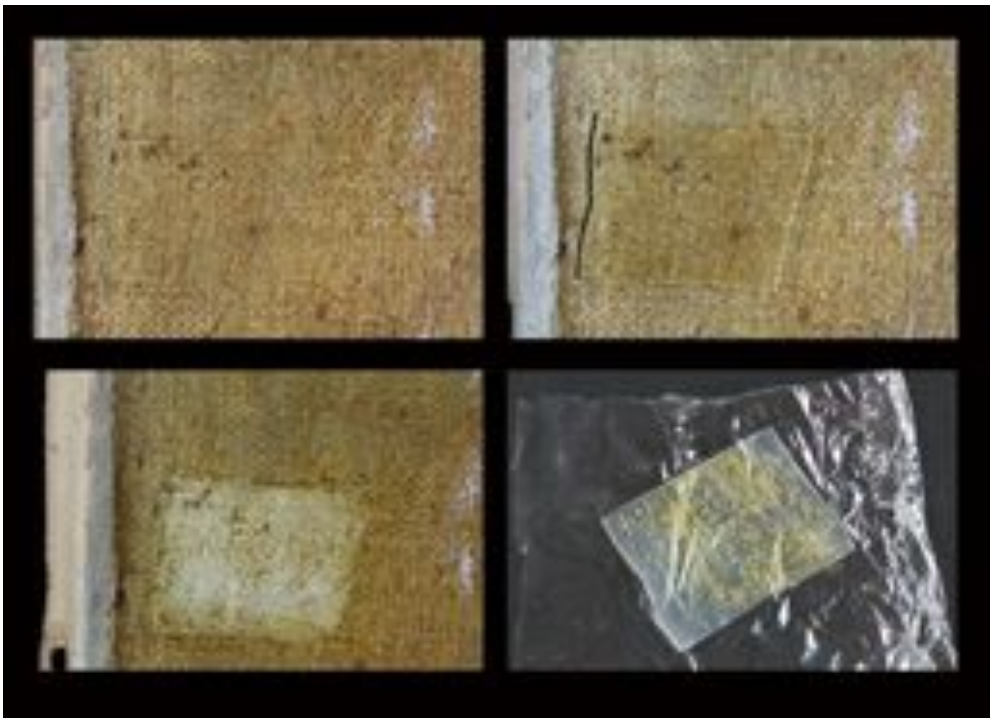

Fig. 9.6: Removal of a degraded a yellowed varnish from a canvas painting using cast-drying hydrogel *PVA/PVP (1:1).*

In both cases, applications of 10 minutes were sufficient to induce swelling of the polymer coating. The polymer resulted partially adhered (see Fig. 9.6, bottom) or soaked (see Fig. 9.7, bottom) by the gel. Swollen varnish residues remaining on the surface could be easily removed by gentle action with a cotton swab.

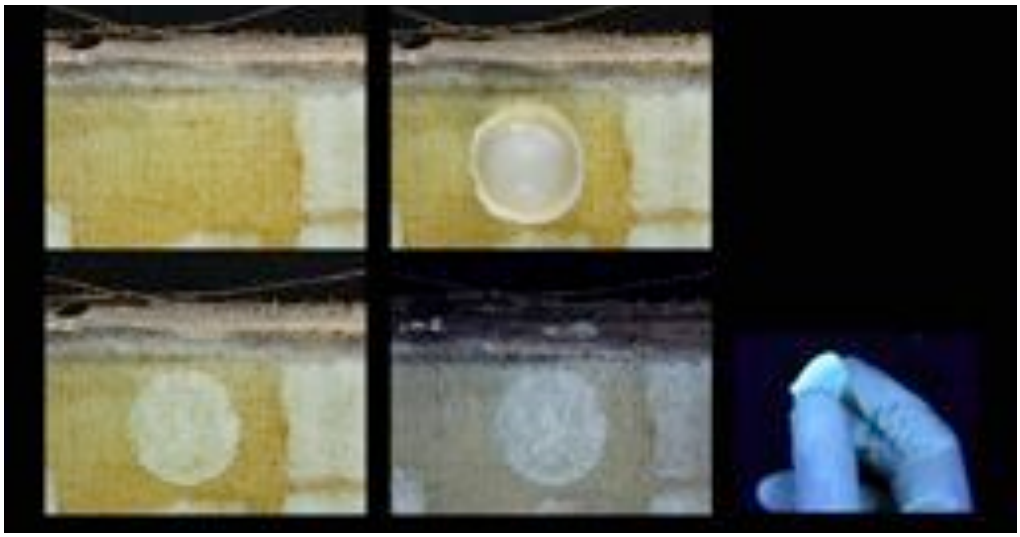

Fig. 9.6: Removal of a degraded a yellowed terpenic varnish from a canvas painting using freeze-thawing hydrogel *PVA/PVP (3:1) FT*. UV captured image highlights soaked varnish, which is highly fluorescent, within the hydrogel.

9.4 Evaluation of hydrogel residues after treatment

Assessment on gel residues after contact with a porous and hydrophilic surface were performed though ATR-FTIR analysis. Analysis were performed on Whatman® filter paper before and after 30 minutes of contact with different water-loaded hydrogel formulations. After treatment, filter paper samples were kept one week in a dessicator, to ensure complete drying. Tested formulations include neat PVA (sample *PVA 12%FT*) and blended hydrogels (*PVA/PVP (3:1)FT* and *PVA/PEG (3:1)FT*).

Fig. 9.7 shows obtained spectra, for comparison, spectra of blended PVA/PVP and PVA/PEG are also presented. As expected, no differences between spectra from

untreated and treated samples are observed, indicating that no detectable gel residues are left on the surfaces even after prolonged contact.

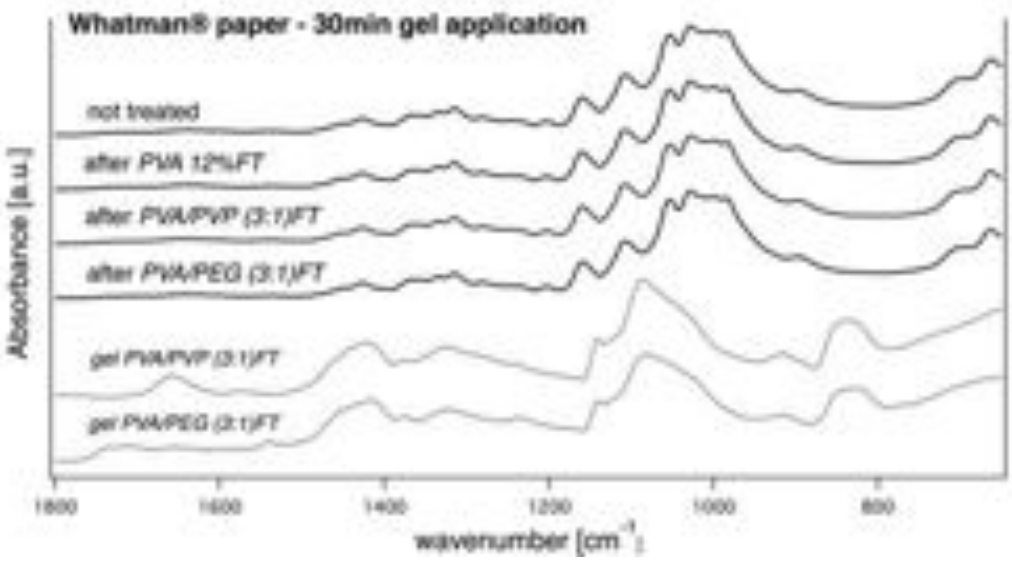

Fig. 9.7: ATR-FTIR spectra of Whatman® filter paper samples before and after 30 minutes contact with different hydrogels formulations (solid lines); for comparison, spectra of blended PVA/PVP and PVA/PEG hydrogels are also presented (dotted line).

References

Baglioni, M., Berti, D., Teixeira, J., Giorgi, R., Baglioni, P., 2012a. Nanostructured Surfactant-Based Systems for the Removal of Polymers from Wall Paintings: a SANS Study. Langmuir in press. doi:10.1021/la303463m

Baglioni, M., Giorgi, R., Berti, D., Baglioni, P., 2012b. Smart cleaning of cultural heritage: a new challenge for soft nanoscience. Nanoscale 4, 42–53. doi:10.1039/c1nr10911a

Baglioni, M., Rengstl, D., Berti, D., Bonini, M., Giorgi, R., Baglioni, P., 2010. Removal of acrylic coatings from works of art by means of nanofluids: understanding the mechanism at the nanoscale. Nanoscale 2, 1723–1732. doi:10.1039/c0nr00255k

Bonini, M., Lenz, S., Falletta, E., Ridi, F., Carretti, E., Fratini, E., Wiedenmann, A., Baglioni, P., 2008. Acrylamide-Based Magnetic Nanosponges: A New Smart Nanocomposite Material. Langmuir 24, 12644–12650. doi:10.1021/la802425k

Domingues, J.A.L., Bonelli, N., Giorgi, R., Fratini, E., Gorel, F., Baglioni, P., 2013. Innovative Hydrogels Based on Semi-Interpenetrating p(HEMA)/PVP Networks for the Cleaning of Water-Sensitive Cultural Heritage Artifacts. Langmuir 29, 2746–2755. doi:10.1021/la3048664

Pizzorusso, G., Fratini, E., Eiblmeier, J., Giorgi, R., Chelazzi, D., Chevalier, A., Baglioni, P., 2012. Physicochemical Characterization of Acrylamide/Bisacrylamide Hydrogels and Their Application for the Conservation of Easel Paintings. Langmuir 28, 3952–3961. doi:10.1021/la2044619

Conclusions

The cleaning of cultural heritage artifacts is one of the most controversial procedures in restoration practice due to its intrinsic irreversibility and potential intrusiveness. Efficacy, high selectivity, controllable action and low toxicity are the essential features that a system should have to grant an efficient ad safe cleaning performance. The use of non-confined organic solvents in cleaning procedures is considered to be too invasive nowadays, due to the lack in control of solvents penetration and spreading on artistic matrices, and to the insufficient selectivity, that can lead to dissolution, swelling or leaching of compounds that are part of the original substrate that needs to be preserved.

The use of polymeric matrices able to confine liquid cleaning systems, i.e. gels, is one of the most powerful strategies in order to attain both high control and reduced toxicity. Moreover, the use of aqueous cleaning methods has been receiving much attention in the last decades, since they permit to increase safety of the working environment. Among these, nanostructured fluids, such as oil-in-water microemulsions, have proved to be both efficient and selective tools for the removal of a wide array of materials from artistic substrates.

The synthesis of hydrogels, which consist of polymeric networks able to retain great amounts of water-based systems, supplies with a class of materials able to enhance the advantages derived from the use of aqueous methods by granting an increased control on their action.

The research performed at CSGI, in the Chemistry Department of the University of Florence, have largely contributed in the past ten years to several gel formulations, each with specific characteristics, addressed to particular cleaning issues. Special attention should be given to the mechanical properties, in addition to the cleaning

efficacy, in the design of gel systems for the cleaning of cultural heritage artifacts, which must ensure a residue-free treatment. Furthermore, the other essential aspect is to address the high retention features that are necessary for an actual controlled cleaning action.

In the present work the potential of a new class of PVA-based hydrogels, as confining tools for water-based cleaning systems, was investigated. Starting from aqueous PVA solutions, two different synthesis pathways, based on casting and air-drying or on repeated freezing and thawing, were identified. Both synthesis methods yield thermoreversible hydrogel systems, where network formation is achieved thanks to growth of microcrystalline regions that act as tie-points. Although the hydrogels belong to the class of physical gels, the cross-links made up by microcrystallites permit an enhancement of the systems' mechanical features, comparable with those typical for chemical gels. The characteristic strong cohesion forces permit the gels to perform, thus, a residue-free treatment.

In respect to the already existing gel systems, the development of these new hydrogels was addressed principally for the improvement of the mechanical adaptability of the hydrogel accounting for irregular or molded surfaces. In fact, the presented PVA-based hydrogels are characterized by pronounced elastic properties that permit the systems to be stressed and adapted to different surfaces and supports without loosing their mechanical integrity.

Moreover, the possibility of tuning hydrogels properties through blending process of PVA with further polymers (PVP, PEG) was also investigated.

The physico-chemical characterization of several formulations was performed to identify the synthesis parameters that affect the final properties of the gels; results for hydrogels obtained through cast-drying method and repeated freezing and thawing are discussed separately.

Hydrogels obtained through cast-drying method are thin, transparent and highly elastic, and are able to perfectly adhere on the surface they are put in contact with. The gravimetric analysis on the gel fraction performed on cast-drying hydrogels

permitted to evaluate that ability in network formation depends on initial PVA concentration and that PVP $M_w \approx 1300000$ is more efficiently embedded into the polymeric matrix than PVP $M_w \approx 40000$. This result was also confirmed by ATR-FTIR analysis. A thermal treatment above the glass-transition temperature of PVA (annealing) can increase the gel fraction.

Special attention was paid to the quantity and states of water within the hydrogels, since these features determine the suitability of a hydrogel to be used as a carrier for water-based systems on sensitive substrates, such as works of art. Analysis on water content and free water index (FWI) show that addition of PVP is of primary importance to yield hydrogels with suitable free water contents for cleaning purposes. Contrariwise, annealing process leads to a drastic decrease of FWI.

Moreover, an extensive study on hydrogels crystallinity was carried out, since this characteristic has a direct influence on the mechanical properties and stability of hydrogels. The crystallinity degree, studied by means of three different techniques (ATR-FTIR, DSC, XRD), was found to depend mainly on PVA concentration in the system, while the presence of PVP in the formulation decreases crystallinity. No increase in crystallinity was detected for annealed samples.

SEM images showed that cast-drying method hydrogels display a macroporous structure, with pore dimensions ranging from about 50 nm to several microns. Higher mean pore dimensions characterize formulations containing PVP, while in annealed samples the porosity appears to be collapsed.

The structural characterization performed through SAXS analysis evidenced shorter correlation lengths ξ for neat PVA samples rather than for blended systems, in accordance with the lower crystallinity of the latter ones, thus characterized by a less entangled structure.

Freeze-thawing method yields hydrogels that are rather soft and elastic, but contemporary very stable. The analysis on the gel fraction indicates that formation of an insoluble crosslinked structure depends in a measure on initial PVA concentration, but mostly on the number of freezing cycles.

The water content and the FWI are very high for all analyzed formulations and are not affected by changes in composition of the hydrogels. In fact, SEM analysis shows that freeze-thawing hydrogels are characterized by very large pore dimensions (up to 20μm), which are formed by the ice crystals during freezing. So, for this type of gels it is porosity, rather than the composition of the network, that governs the behavior of water within the gel structure.
The crystallinity degree is affected on the one hand by composition, being higher for neat PVA or blended PVA/PEG systems rather than for PVA/PVP hydrogels, on the other hand by the number of freezing cycles. Higher crystallinity degrees were detected by increasing the number of freezing cycles.
In accordance with higher swelling degrees and water content characterizing freeze-thawing method hydrogels, SAXS analysis revealed that they display a higher average mesh size with respect to hydrogels obtained through cast-drying method.

Finally application properties, such as water release and adhesion features, were investigated. Both are strictly related to composition and crystallinity of the hydrogels showing that hydrogels properties can be tuned through blending and by varying synthesis parameters, as for instance the number of freezing cycles.

Blended PVA-based hydrogel systems can be loaded with water or water-based cleaning systems (i.e. microemulsions). The preliminary cleaning tests, performed on different supports (wood, canvas, parchment) have proved that they are efficient tools for the controlled humidification and the removal of undesired layers (surface grime, aged varnishes) form artistic substrates and that hydrogels are able to adjust their shape in order to perfectly adhere also on irregular surfaces.

Acknowledgments

I would like to express my deepest appreciation to all those who provided me the possibility to complete this dissertation.

First and foremost, I would like to express my gratitude to my research supervisor and tutor, Prof. Piero Baglioni, who assisted and supported me throughout the process over the past three years. A special gratitude I give to Prof. Rodorico Giorgi whose contribution in stimulating suggestions and encouragement have substantially improved my work.

I wish to thank Dr. Francesca Ridi for the help with the thermal analysis experiments and Dr. Emiliano Fratini for his support in SAXS analysis and data fitting. For the XRD analysis Dr. Moira Ambrosi is acknowledged for introducing me to the *CRIST* facilities at the University of Florence, where I worked with Dr. Francesca Loglio, to whom I express my gratitude for assisting me during measurements.

In 2013 I had the occasion to spend several months at the *Instituto del Patrimonio Cultural de España (IPCE)* in Madrid. It was an extraordinary experience, so a special thanks goes to all the conservators and conservation scientists I had the luck to work with, especially Carmen Peña, Emma Sanchez and Dr. Elena Gonzalez Artèga.

The study presented in this dissertation is the result of three years of intensive work at the laboratories of *CSGI*, Chemistry Department of the University of Florence.

Thus, my most heartfelt thanks are dedicated to all my CSGI colleagues. In particular, I wish to thank Joana Domingues, for her personal and professional involvement in every step throughout the fulfillment of this work. A special thank is addressed to Giovanna Poggi and David Chelazzi, who helped and supported me with their kindness and experience, and to Erica Parisi for having patiently revised my dissertation.
I wish also to thank Eleonora for the precious help during synthesis and preparation of all the hydrogel samples.

The National Archives at Kew are acknowledged for providing the parchment samples used for the cleaning tests.

This work has been realized thanks to the *Progetto Pegaso* scholarship, financed by *Regione Toscana*. *CSGI* and *Nanoforart Project* are also acknowledged for the financial support.

Finally, I want to thank my family for their encouragement and support and for instilling in me a love of learning that I will carry throughout my life. And to my friends and specially Francesco, for being there through every part of this journey. I truly believe I could not have made it to where I am today without their constant love and support. Thank you.

Annex

List of publications

Domingues, J. A. L., Bonelli, N., Giorgi, R., Fratini, E., Gorel, F., Baglioni, P., Innovative Hydrogels Based on Semi-Interpenetrating p(HEMA)/PVP Networks for the Cleaning of Water-Sensitive Cultural Heritage Artifacts, *Langmuir*, 29 (8), 2013, pp. 2746-2755.

Giorgi, R., Domingues, J. A. L., Bonelli, N., Baglioni, P., Semi-Interpenetrating p(HEMA)/PVP Hydrogels for the Cleaning of Water-Sensitive Painted Artifacts: Assessment on Release and Retention Properties. In *Science and Technology for the Conservation of Cultural Heritage*, Proceedings of the International Congress on Science and Technology for the conservation of Cultural Heritage, Santiago de Compostela, Spain, October 2-5, 2012; Rogerio-Candelera, M. A.; Lazzari, M.; Cano, E., Eds.; CRC Press: Boca Raton, FL, 2013; pp. 291-294.

Domingues, J., Bonelli, N., Giorgi, R., Fratini, E., Baglioni, P., Innovative Method for the Cleaning of Water-Sensitive Artifacts: Synthesis and Application of Highly Retentive Chemical Hydrogels, *International Journal of Conservation Science*, 4, 2013, pp. 715-722.

Domingues, J., Bonelli, N., Giorgi, R., Baglioni, P., Chemical Semi-IPN Hydrogels for the Removal of Adhesives from Canvas Paintings, *Applied Physics A*, 114 (3), 2014, pp.705-710.

Poggi, G., Domingues, J. Bonelli, N., Giorgi, R., Baglioni, P., Nanomateriali Innovativi per la Conservazione dei Beni Culturali. Idrogel ad Alta ritenzione per la Pulitura di Opere d'Arte: l'Intervento sul Globo Terrestre della Biblioteca Civica Angelo Mai di Bergamo, *Bergomum* 2013, Bollettino della Civica Biblioteca Angelo Mai di Bergamo. 2014.

Langmuir

Article

pubs.acs.org/Langmuir

Innovative Hydrogels Based on Semi-Interpenetrating p(HEMA)/PVP Networks for the Cleaning of Water-Sensitive Cultural Heritage Artifacts

Joana A. L. Domingues,[†] Nicole Bonelli,[†] Rodorico Giorgi,[†] Emiliano Fratini,[†] Florence Gorel,[†,‡] and Piero Baglioni*[,†]

[†]Department of Chemistry "Ugo Schiff" and CSGI, University of Florence, Via della Lastruccia 3−50019 Sesto Fiorentino, Florence, Italy

[‡]Florence Gorel, Restauratice du patrimoine, 21, rue E. Goudchaux−57000 Metz, France

Supporting Information

ABSTRACT: Water-based detergent systems offer several advantages, over organic solvents, for the cleaning of cultural heritage artifacts in terms of selectivity and gentle removal of grime materials or aged varnish, which are known to alter the readability of the painting. Unfortunately, easel paintings present specific characteristics that make the usage of water-based systems invasive. The interaction of water with wood or canvas support favors mechanical stresses between the substrate and the paint layers leading to the detachment of the pictorial layer. In order to avoid painting loss and to ensure a fine control (layer by layer) of grime removal, water-based cleaning systems have been confined into innovative chemical hydrogels, specifically designed for cleaning water-sensitive cultural heritage artifacts. The synthesized hydrogels are based on semi-interpenetrating chemical poly(2-hydroxyethyl methacrylate)/poly(vinylpyrrolidone) networks with suitable hydrophilicity, water retention properties, and required mechanical strength to avoid residues after the cleaning treatment. Three different compositions were selected. Water retention and release properties have been studied by quantifying the amount of free and bound water (from differential scanning calorimetry); mesoporosity was obtained from scanning electron microscopy; microstructure from small angle X-ray scattering. To demonstrate both the efficiency and versatility of the selected hydrogels in confining and modulating the properties of cleaning systems, a representative case study is presented.

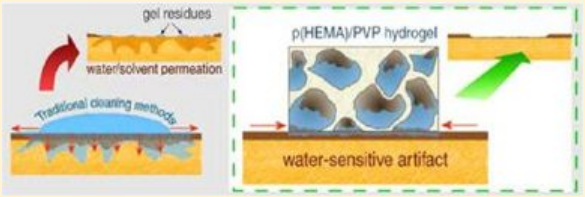

INTRODUCTION

Cleaning of cultural heritage artifacts represents one of the most delicate operations of restoration because it is potentially invasive and aggressive for the original materials as well as completely irreversible. The list of undesired materials to be removed from artifacts surface can include a wide group of substances: from deposits of pollutants and grime due to natural aging process, to aged and darkened varnish coatings. One of the most important issues for conservators and conservation scientists is the removal of materials that do not belong to the artwork, without affecting the original ones. In other words, high performing cleaning systems must be able to ensure a controlled and selective cleaning action.

In traditional conservation procedures, the removal of undesired materials is generally carried out through mechanical action or solubilization processes, mainly achieved with organic solvents. The main problems connected to the use of organic solvents concern their scarce environmental safety and their poor selectivity. The more similar are the characteristics (e.g., polarity) of the painting's original materials to those to be removed, the greater is the risk connected to the use of pure organic solvents. The confinement of solvent action is important to avoid diffusion processes of the dissolved substances into deeper and broader areas of the artifact. Furthermore, the uncontrolled penetration of pure solvents into the artifact's porous structure may cause swelling or leaching of binders and varnishes, with unknown long-term effects.[1,2]

In the past decades conservators devised several methods for the confinement of solvents, with the aim of increasing the control over the cleaning process. Penetration of the solvent via capillary action may be decreased using thickeners like cellulose ethers (e.g., hydroxypropyl cellulose—Klucel, ethyl cellulose) and polyacrylic acids (e.g., Carbopol). Unfortunately, the retention features of those systems are often unsatisfactory, and high evaporation rates of the solvents themselves can lead to formation of dry films of solid material on the treated surface.[3] Solvent gels (solvents in their thickened state) introduced by R. Wolbers,[4,5] are one of the most used cleaning tools. The capillary penetration of the solvent into the artifact is

Received: December 11, 2012
Revised: January 16, 2013
Published: January 18, 2013

dx.doi.org/10.1021/la3048664 | Langmuir 2013, 29, 2746−2755

reduced through immobilization of the solvent within the polymer network forming the solvent gel, characterized by weak intermolecular bonds that are responsible for the viscosity of the dispersion. The most important drawback concerning the use of solvent gels is related to the residues that might remain on the works of art after the cleaning. Following the treatment with a solvent gel system, it is always necessary to perform an appropriate cleaning procedure, which is usually carried out through organic solvent blends.[3] Furthermore, after mechanical removal and solubilization of the solvent gel system, residues of surfactant may remain on artifacts surface.[6]

A solution to the gel residue has been pursued by formulating completely innovative gel systems. Hence, some new confining systems such as highly viscous polymer solutions and physical gels (e.g., rheoreversible polyallylamine based organogels,[7] viscoelastic polyvinyl alcohol-borate based gels[8]) and chemical gels (e.g., polyacrylamide networks, which can be functionalized with magnetic nanoparticles) have been recently developed in our research group.[9−11] In the latter class of gelled systems (chemical gels), the polymeric network is characterized by the presence of covalent bonds. With respect to physical gels, chemical gels exhibit improved mechanical properties; they can be shaped in a well-defined form and can swell in a liquid medium without gel solubilization.

The present study was focused on designing low environmental toxicity hydrogels that fulfill all the mentioned desired characteristics. These gels can be loaded with water or water-based detergent systems (micellar systems, microemulsions), which allow replacing the traditional pure organic solvents.

Because of its high biocompatibility, poly(2-hydroxyethyl methacrylate)—p(HEMA)—hydrogels have been extensively studied in medical and pharmaceutical areas.[12,13] However, hydrophilicity of p(HEMA) is not sufficient for loading water-based cleaning systems for application to cultural heritage conservation. Poly(vinylpyrrolidone)—PVP—is a high hydrophilic polymer, widely used in the pharmaceutical, cosmetic, and food industries,[14] whose cross-linked hydrogels have scarce mechanical features.[15] In this paper we describe how the features of these two polymers can be combined to improve the capability of p(HEMA) to form stable networks with high hydrophilicity, assisted by the presence of hydrophilic PVP chains.

To benefit from both mechanical strength and hydrophilicity, the polymerization reaction was carried out to obtain semi-interpenetrating polymer network (semi-IPN) hydrogels. In fact, the synthesis of classical "copolymer hydrogels" leads to compounds with characteristics usually quite different from those resulting from the sum of single homopolymer properties. Semi-IPNs are based on polymer blends in which linear or branched polymers are embedded into one or more polymer networks during the polymerization reaction, without any chemical reaction occurring between them;[16,17] thus, the obtained hydrogel presents properties similar to the average of the single homopolymer properties. Linear polymers incorporated into a cross-linked network can act as dangling chains, producing softer gel systems, as expressed by the reduction of the friction coefficient.[18] We developed a semi-interpenetrating p(HEMA)/PVP network hydrogel where free chains of PVP macromolecules are embedded into a p(HEMA) network. We tuned the p(HEMA)/PVP ratio and the amount of water added to the reaction mixture to achieve the ideal properties for applications in cleaning of cultural heritage artifacts, i.e., good adhesion with the artifacts surface, high retention of the detergent system combined with efficient cleaning, cleaning action confined exclusively on gel contact area, no gel residues, and capacity of swell in different aqueous cleaning systems (e.g., mixed solvent systems, micellar solutions, microemulsions, etc.). Three semi-IPN hydrogels, differing from each other in the mechanical properties and release/retention capability, are presented in this paper. In order to evaluate the effectiveness of the investigated gel systems, the removal of hydrophilic layers was performed on a water-sensitive substrate. These gels can be also used to remove hydrophobic layers (such as adhesives, polymers, etc.) from water-sensitive materials. For this purpose, semi-IPN p(HEMA)/PVP hydrogels can be loaded with micellar systems or microemulsions, which have shown to be highly performing aqueous systems for the cleaning of cultural heritage artifacts[19−25] and can be efficiently confined in the chemical hydrogels.[9−11]

We show that these novel systems have outstanding cleaning capacity for water-sensitive works of art, and in particular for watercolor paintings that are extremely difficult to clean with conventional methods.

EXPERIMENTAL SECTION

Materials. 2-Hydroxyethyl methacrylate (HEMA) (assay 97%) and poly(vinylpyrrolidone) (PVP) (average $M_w \approx 1300$ kDa) were obtained from Sigma-Aldrich. α,α'-Azoisobutyronitrile (AIBN) (assay 98%) and *N*,*N*-methylene-bis(acrylamide) (MBA) (assay 99%) were obtained from Fluka, AIBN was recrystallized twice from methanol prior to use. All the other chemicals were used as received. Water was purified by a Millipore MilliRO-6 Milli-Q gradient system (resistivity >18 MΩ cm).

Hydrogels Synthesis. The semi-IPN hydrogels were prepared by physically embedding linear PVP into the hydrogel network. This was achieved by free radical polymerization of HEMA monomer and the cross-linker MBA in a water solution containing linear PVP. Series of different hydrogels were designed by varying the proportions of monomer/cross-linker ratio with PVP and water percentages. The composition of the best systems selected for the cleaning trials is presented in Table 1. In particular, these semi-IPN hydrogels can be designed by varying their component ratios (water, PVP, HEMA, and cross-linker quantities) in order to tune their characteristics in terms of mechanical behavior (softness, elasticity, and resistance to tensile strength) and affinity to water.

Table 1. Compositions (w/w) of the Selected Semi-IPN Hydrogels; Monomer/Cross-Linker and HEMA/PVP Ratio[a]

	H50	H58	H65
HEMA	25.0%	16.8%	10.5%
MBA	0.20%	0.20%	0.21%
PVP	24.9%	25.1%	24.5%
water	49.9%	57.9%	64.9%
monomer/cross-linker ratio	$1:1 \times 10^{-2}$	$1:1.5 \times 10^{-2}$	$1:2 \times 10^{-2}$
HEMA/PVP ratio	50/50	40/60	30/70

[a]H58 formulation was specifically designed for the cleaning of the Thang-Ka model samples. The acronym H*XX* refers to the percentage of water (*XX*) in the reaction mixture.

Hydrogels synthesis was carried out in two different types of molds to obtain (i) hydrogels with 2.5 × 2.5 × 1 cm parallelepiped shape used for the physicochemical analyses and (ii) flat hydrogel films having 2 mm thickness used for the cleaning tests. All the products (see Table 1) and radical initiator AIBN (1:0.01 monomer/initiator molar ratio) were mixed together, and the solution was bubbled with nitrogen for 5 min to remove dissolved oxygen that could inhibit the radical polymerization of HEMA. The solutions were gently sonicated for 30 min in pulsed mode to eliminate the formed gas bubbles.

dx.doi.org/10.1021/la3048664 | *Langmuir* 2013, 29, 2746−2755

The polymerization reaction, initiated by thermal homolysis of AIBN, occurred at 60 °C for 4 h. After polymerization, hydrogels were washed and placed in containers filled with distilled water. The water was renewed twice a day for 7 days to remove any residue of unreacted monomer and the free PVP.

Physicochemical Characterization of Hydrogel. Each of the following parameters was calculated from at least three different measurements.

The gel content (G) gives the ratio between the mass of the final semi-IPN p(HEMA)/PVP hydrogel and the mass of the two components in the initial mixture, which can be calculated as follows[26]

$$G(\%) = \frac{W_d}{W_0} \times 100 \tag{1}$$

where W_d is the dry weight of the hydrogel and W_0 is the weight of HEMA and PVP in the initial reaction mixture. The dry weight was obtained by heating at 70 °C for 5 h and then increasing the temperature to 120 °C for 48 h. The obtained xerogels were placed in a desiccator to cool down to room temperature before weighing.

The equilibrium water content (EWC) of hydrogels gives information on the polymer network hydrophilicity and can be calculated as follows[27]

$$\mathrm{EWC} = \frac{W_W - W_d}{W_W} \times 100 \tag{2}$$

where W_W is the weight of the water swollen hydrogel in equilibrium, obtained at least 7 days after polymerization reaction.

Gel samples of 12−18 mg were analyzed in closed aluminum pans to determine both free water index (FWI) and freeze-bound water index (FBWI). The water content expressed as weight fraction in the gel, A, was determined by differential thermogravimetry (DTG), using a SDT Q600 (TA Instruments) apparatus. The temperature scan was from 20 to 450 °C with a heating rate of 10 °C/min. Melting enthalpies were calculated from differential scanning calorimetry (DSC) thermograms using a Q1000 (TA Instruments) apparatus. The temperature range scan was from −80 to 20 °C with 0.5 °C/min rate. The FWI was calculated as follows[28]

$$\mathrm{FWI} = \frac{\Delta H_{exp}}{\mathrm{WC} \times \Delta H_{theo}} \tag{3}$$

where the ΔH_{exp} (J/g) represents the melting enthalpy variation for free water and can be determined by integration of the DSC peak around 0 °C, WC is the water weight fraction in the fully hydrated hydrogel, and ΔH_{theo} is the theoretical value of the specific enthalpy of fusion for bulk water (333.61 J/g).[29]

Since the FWI gives the fraction of free water with respect to the total amount of water in the hydrogel, it is relevant to calculate the amount of free (R_{fx}) and total bound (R_{bx}) water per gram of dry hydrogel. These parameters can be determined according to the following equations:[11]

$$R_{fx} = \frac{W_W \times \mathrm{WC} \times \mathrm{FWI}}{W_d} \tag{4}$$

$$R_{bx} = \frac{W_W \times \mathrm{WC} \times (1 - \mathrm{FWI})}{W_d} \tag{5}$$

Partially rehydrated hydrogels were prepared to determine the freeze-bound water fraction. About 15 mg of sample were first equilibrated at 75% and then at 100% relative humidity (RH) for 6 days.[30] The freeze-bound water amount was determined from the relationship[28]

$$\mathrm{FBWI} = \frac{\Delta H_{exp}}{\mathrm{WC} \times \Delta H_{bound}} \tag{6}$$

where ΔH_{bound} (J/g) is the theoretical value of the melting enthalpy of water at the specific temperature below 0 °C, and it was calculated as described in the literature.[31]

The amounts of freeze-bound, R_{fbx}, and nonfreezable water, R_{nfx}, per gram of dry hydrogel are obtained from

$$R_{fbx} = \frac{W_W \times \mathrm{WC} \times \mathrm{FBWI}}{W_d} \tag{7}$$

$$R_{nfx} = \frac{W_W \times \mathrm{WC} \times (1 - \mathrm{FWI} - \mathrm{FBWI})}{W_d} \tag{8}$$

Xerogels, obtained through a freeze-drying process, were used to determine mesoporosity. A FEG-SEM ΣIGMA (Carl Zeiss, Germany) was used to acquire the images using an acceleration potential of 1 kV and a working distance of 1.4 mm. The metallization of the samples was not necessary with these experimental conditions.

SAXS measurements were carried out with a HECUS S3-MICRO camera (Kratky-type) equipped with a position-sensitive detector (OED 50M) containing 1024 channels of width 54 μm. Cu Kα radiation of wavelength λ = 1.542 Å was provided by an ultrabrilliant point microfocus X-ray source (GENIX-Fox 3D, Xenocs, Grenoble), operating at a maximum power of 50 W (50 kV and 1 mA). The sample-to-detector distance was 269 mm. The volume between the sample and the detector was kept under vacuum during the measurements to minimize scattering from the air. The Kratky camera was calibrated in the small angle region using silver behenate (d = 58.38 Å).[32] Scattering curves were obtained in the q-range between 0.01 and 0.54 Å^{-1}, assuming that q is the scattering vector, $q = 4\pi/\lambda \sin\theta$, and 2θ the scattering angle. Gel samples were placed into a 1 mm demountable cell having Mylar films as windows. The temperature was set to 25 °C and was controlled by a Peltier element, with an accuracy of 0.1 °C. All scattering curves were corrected for the empty cell contribution considering the relative transmission factor.

The presence of gel residues over the cleaned surface was checked with attenuated total reflectance Fourier transform infrared spectroscopy (ATR-FTIR) on canvas or paper samples kept in contact with the hydrogel for 4 h. A Thermo Nicolet Nexus 870 FTIR spectrometer equipped with a Golden Gate diamond cell was used. Data were collected with an MCT detector with a sampling area of 150 μm^2. The spectra were obtained from 128 scans with 4 cm^{-1} of optical resolution.

Gel Retention Capability. Dehydration kinetics and water release provide a better understanding of the retention capability of each gel. To determine the dehydration kinetics, expressed as water decrease over time (WD), swollen hydrogel films were weighted and placed in a humidity chamber at 53% RH until equilibrium was reached. The weight decrease as a function of time was calculated as follows

$$\mathrm{WD} = \frac{W_i - W_d}{W_W - W_d} \times 100 \tag{9}$$

where W_i is the hydrogel weight at the specific time i.

For the evaluation of water release properties, fully swollen hydrogels were gently surface dried and then positioned on four sheets of Whatman filter paper and covered with a lid to avoid water evaporation. The sheets of filter paper were weighted before and after 30 min of gel application. The released water is normalized by unit area.

Removal of Hydrophilic Surface Grime. To assess the gel performance, a Thang-Ka mock-up was prepared. A Thang-Ka consists of a multilayer structure in which a cotton canvas is covered with a preparation layer containing $CaCO_3$ and animal glue. The painting technique is a tempera magra; i.e., pigments and colorants are mixed with animal glue dissolved in water. In the prepared model, calcium carbonate was used as the white pigment; malachite was used to obtain the green color; the blue colorant is indigo; the golden lines are obtained from shell gold. To carry out cleaning tests, the mock-up surface was previously covered with an artificial grime mixture. The grime was applied in a 4.5% v/v solution of mineral oil in chloroform using a paintbrush. The synthetic grime mixture has a hydrophilic composition and was designed by R. Wolbers.[33] The progress of the cleaning process was determined using a spectrophotocolorimetric analysis. The light reflected from the sample was collected by a fiber-

dx.doi.org/10.1021/la3048664 | Langmuir 2013, 29, 2746−2755

optic cable (FRP series) connected to a high sensitivity CCD camera (−10 °C TE cooled Prime X back-thinned) in a 350−1000 nm range. The light spot was around 1 mm in diameter. Reflectance spectra were acquired at a distance of 3 mm from the surface. Colorimetric data were collected using standard illuminant C and standard observer CIE 1931 (2°) in a λ range of 400−700 nm (with 10 nm of resolution) and with a 0°/0° geometry. The degree of cleaning was evaluated through color difference from the ΔE^* parameter

$$\Delta E^* = [(\Delta L^*)^2 + (\Delta a^*)^2 + (\Delta b^*)^2]^{1/2} \quad (10)$$

where ΔE^* is the color difference in the colorimetric space CIELAB 1976 and L^*, a^*, and b^* are the related colorimetric coordinates.[34,35]

RESULTS AND DISCUSSION

The innovative application of a chemical gel for the cleaning of the front of a canvas painting is presented here, as far as we know, for the first time. An artificially soiled Thang-Ka mock-up was considered to assess the efficiency of hydrophilic grime removal from a water-sensitive substrate. A Thang-Ka is a Tibetan votive artifact based on tempera magra painting on canvas, where the binder is animal glue (see Figure 1). This

Figure 1. Detail of a Thang-Ka from the 18th century.

painting technique is characterized by a high pigment volume concentration (PVC), equal or slightly higher than critical PVC, at which there is just sufficient binder to wet the pigment particles. This leads to a very low cohesive paint layer, where the scarce quantity of binder is water-sensitive,[36] making the removal of hydrophilic surface grime, which is trapped into the painting "porosity", a challenge for conservators. Because paint layer is water-soluble, the traditional use of a water-impregnated cotton swab has a nonselective action for hydrophilic grime removal. So it is necessary to achieve a layer by layer removal through the precise confinement of the solvent. Hence, the Thang-Ka represents an appropriate case study to test semi-IPN hydrogel capability to perform an efficient and high-controlled cleaning action.

All the semi-IPN hydrogel formulations were found to have interesting macroscopic characteristics and improved mechanical properties with respect to a p(VP) homopolymer hydrogel. The semi-IPN p(HEMA)/PVP hydrogels properties are strictly dependent on the quantitative ratios of their components. Two formulations having different hydrophilicity, H65 and H50, were investigated. The acronym H*XX* refers to the *XX* percentage of water in the reaction mixture, which is proportional to the hydrophilic character of the hydrogel, enhanced by the addition of linear PVP chains.

The investigated hydrogels are transparent or translucent and easy to manipulate. Specifically, the H50 is the most rigid, homogeneous, and completely transparent, while the H65 hydrogel is opalescent, translucent, pliable and exhibits a reversible enhanced deformability when some mechanical stress is applied. This feature is important to attain better adhesion to rough surfaces. In addition, both hydrogels are to some extent softer than ordinary chemical gels and maintain high water retention capability.

Semi-IPN hydrogels are polymer blends, and during synthesis there is no chemical reaction between monomer and linear polymer. Therefore linear PVP could be separated from the constituent polymer network of HEMA without breaking chemical bonds.[16] Formation of hydrogen bonds between the carbonyl group of PVP and the hydroxyl group of HEMA has already been reported in the literature.[37] This kind of interaction leads to an efficient embedding of linear PVP into the network of p(HEMA). The gel content (G) is 90% for H50 and 74% for H65. Even if the p(HEMA)/PVP ratio in H50 is 50/50, its gel content is substantially high. Increasing linear PVP content lowers G values. This means that the available area of the HEMA network, which interacts with PVP chains, at a specific HEMA/PVP ratio will not be enough to contain further PVP. Hence, besides water, PVP in excess is a further component that contributes to the final porosity of the hydrogel and to a more heterogeneous microporosity, as confirmed by FEG-SEM images.

The EWC in semi-IPN hydrogels is due to both porosity and hydrophilic character of the final polymer network. The water content of H50 and H65 hydrogels increased from the initial 50% to 72% and from 65% to 87%, respectively, without any loss of transparency. This is a noteworthy feature considering that there is a water content limit for the reaction mixture: larger amounts of water produce phase separation during polymerization leading to a totally white opaque hydrogel.[17,38] In fact, p(HEMA) hydrogels have an EWC approximately of 39%.[39] Therefore, to obtain transparent p(HEMA) hydrogels, the maximum water content in the reaction mixture must be lower than this value. By adding highly hydrophilic linear PVP into the reaction mixture, it is possible to increase both the water content and the network hydrophilicity with the result of an increase in the final porosity.

Water inside swollen hydrogels can be classified into three different states: free, bound-freezable, and unfreezable water. This classification takes into account the extent of interactions of water molecules with the polar part of the polymer chains: free water is defined as the water with the same thermodynamic properties of bulk water; freeze-bound water interacts weakly with the polymer chains of the hydrogels so that its freezing point is lower than 0 °C; unfreezable water is strongly hydrogen bonded, and no phase transition is observed from −70 to 50 °C.[40,41] Because only free water is contributing to the cleaning process, the knowledge of the bound-freezable and free water fractions inside hydrogels is important to quantify the hydrogel capability to exchange the solvent at the surface and thus to prevent any excessive wetting. The distribution of "water states" inside hydrogels can be estimated through the calculation of freezable water, from the free water index (FWI) and freeze-bound water index (FBWI) parameters, both determined via DSC. In the DSC thermograms, free water shows a freezing point equal to that of bulk water, while the freezing point of bound-freezable water is lower than 0 °C, due

to the water interactions with polymer chains or the confinement in the mesoporosity.[41]

The DSC thermograms, obtained from the swollen H50 and H65 hydrogels, are shown in Figure 2. Two distinct protocols

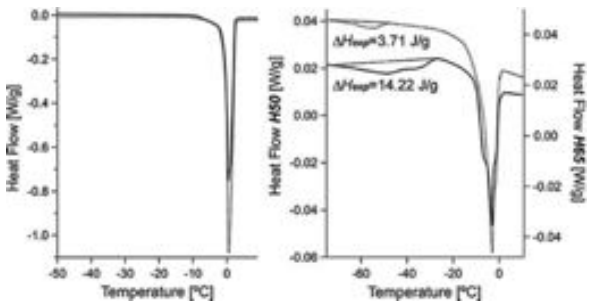

Figure 2. DSC thermograms for the fully swollen hydrogels (left) and partially rehydrated hydrogels (right) for H50 (solid line) and H65 (dotted line). Both thermograms were normalized to sample weight.

were used to determine both FWI and FBWI parameters as described in the Experimental Section. The DSC thermograms in Figure 2 (left panel) show a shoulder below 0 °C, which is associated with a minor fraction of free water that has indirect interactions with the polymer network and, therefore, has a behavior close to freeze-bound water.

The FWI results are reported in Table 2. Freeze-bound water is evidenced by the broad freezing peak visible between −70 and −20 °C in Figure 2 (right panel), in addition to the more intense freezing peak for free water. It is evident that the area associated with the freeze-bound water peak is larger for H50.

The FWI values obtained highlight that free water inside swollen hydrogels is to a large extent higher than bound water. Therefore, aqueous systems inside hydrogels behave mostly as free water. In fact, the free water content is around 73% in H50 and 77% in H65 with respect to the total water inside the swollen hydrogels. In order to point out the evident difference between hydrogels hydrophilicity, it was relevant to analyze both R_{fx} and R_{bx} parameters. From these parameters it is possible to assess the real amount of free water available per each gram of dry hydrogel. As expected, both parameters are higher for H65 (4.72 of R_{fx} and 1.41 of R_{bx}) than for H50 (2.30 of R_{fx} and 0.85 of R_{bx}). This feature is due to the higher amount of PVP in the H65 hydrogel. In fact, higher content of PVP contributes to a more swollen hydrogel that recalls more water molecules per unit mass of polymer, increasing both R_{fx} and R_{bx} parameters.

On the other hand, to better understand the freeze-bound water behavior in hydrogels, FBWI was calculated from the freeze-bound water fusion peak presented in Figure 2 B. The results are listed in Table 2.

H50 has a higher FBWI than H65 as a consequence of a greater number of water molecules in contact with pore walls due to smaller pore dimensions and the higher surface to volume ratio. Furthermore, since the R_{bx} parameter gives the amount of total bound water per gram of xerogel, it was important to split it into the amount of freeze-bound and nonfreezable water per gram of xerogel inside partially rehydrated hydrogels (R_{fbx} and R_{nfx}, respectively). It is evident that the more hydrophilic hydrogel H65 shows a higher R_{nfx} value, while the amount of freeze-bound water is significantly lower.

Table 2. Free Water Index (FWI), Freeze-Bound Water Index (FBWI), and Correlated Parameters for Fully Swollen (HXX) and Partially Rehydrated Hydrogels (HXX*)[a]

	FWI					FBWI			
	A	ΔH_{exp} (J/g)	FWI	R_{fx} (g/g)	R_{bx} (g/g)	ΔH_{exp} (J/g)	FBWI	R_{fbx}	R_{nfx}
H50	0.758 ± 20 × 10^{-3}	184.7 ± 5.9	0.730 ± 4 × 10^{-3}	2.30 ± 0.26	0.85 ± 0.08	–	–	–	–
H65	0.859 ± 13 × 10^{-3}	220.8 ± 0.6	0.770 ± 9 × 10^{-3}	4.72 ± 0.44	1.41 ± 0.20	–	–	–	–
H50*	0.396 ± 22 × 10^{-3}	40.7 ± 5.8	0.309 ± 63 × 10^{-3}	0.20 ± 0.02	0.46 ± 0.08	13.7 ± 1.7	0.161 ± 18 × 10^{-3}	0.10 ± 0.02	0.36 ± 0.06
H65*	0.475 ± 33 × 10^{-3}	47.1 ± 2.6	0.304 ± 6 × 10^{-3}	0.27 ± 0.03	0.61 ± 0.09	4.1 ± 0.6	0.045 ± 4 × 10^{-3}	0.04 ± 0.01	0.57 ± 0.08

[a] A is the weight fraction of water. FBWI was calculated using the partially rehydrated hydrogels as reported in the Experimental Section.

dx.doi.org/10.1021/la3048664 | Langmuir 2013, 29, 2746−2755

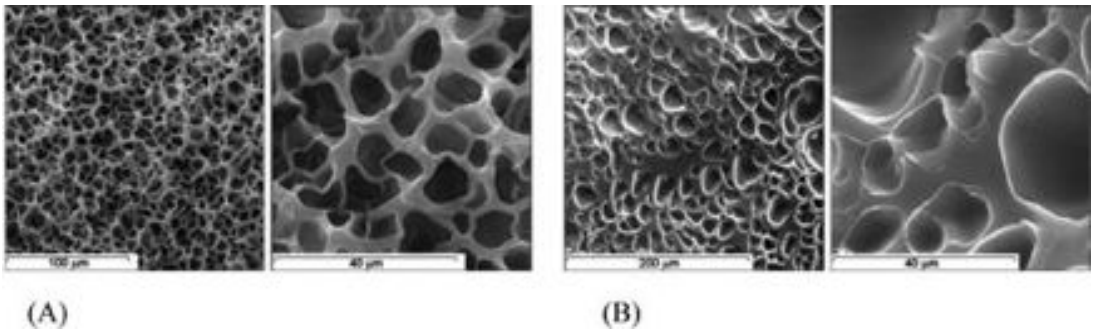

Figure 3. SEM images of H50 (A) and H65 (B) xerogels obtained at two different magnifications.

FEG-SEM images were acquired to detail the structure and porosity of the lyophilized hydrogel (xerogel). Since xerogel state is required for FEG-SEM image acquisition, EWC was determined in the fully rehydrated xerogels as well, to evaluate if the freeze-drying process compromises the microstructure of the hydrogel. A decrease of the EWC was observed in both cases: 0.16% and 8.28% for H50 and H65, respectively. In the case of H50 the variation is almost negligible, while for H65 the difference of EWC is considerable, which means that ca. 8% of microporosity is collapsed during freeze-drying as a consequence of the water to ice expansion associated with the freezing step necessary for the lyophilization. This difference is, thus, relevant to be considered when dealing with FEG-SEM results.

FEG-SEM images are shown in Figure 3 for H50 and H65 xerogels. A spongelike structure is observed for both samples, and pore dimensions are approximately comprised in the range from 5 to 40 μm. A more heterogeneous structure is clearly noted for H65 with respect to H50 xerogel. Pore wall thickness in H50 xerogel presents an average value of $\approx 2.4 \pm 1.3$ μm. In accordance with the heterogeneity of the H65 structure, there is a broader distribution of pore wall thickness.

In ordinary cross-linked chemical hydrogels, the amount of water in the reaction mixture is the major contributor to final porosity. FEG-SEM images clearly show smaller pores for H50 formulation compared with H65. To further quantify this aspect, a pore size distribution was extracted from several FEG-SEM images using ImageJ analysis software. The obtained histogram is presented in Figure 4.

H65 hydrogel displays a broader distribution with pore diameters going from 5 to 39 μm. As for H50, a more homogeneous distribution is noted with the main pore diameters comprised between 6 and 11 μm. Furthermore, the porosity was estimated to be approximately 10375 pores/mm^2 for H50 and 2600 pores/mm^2 for H65 xerogel. The difference of porosities between the two hydrogels is due to three main factors: the water content in the initial polymerization mixture, which is the main factor responsible for final gel porosity and dimension of pores; the PVP release after polymerization; and the cross-linker content, which contributes, for the same PVP/HEMA/H_2O ratios, to more compact network structures.

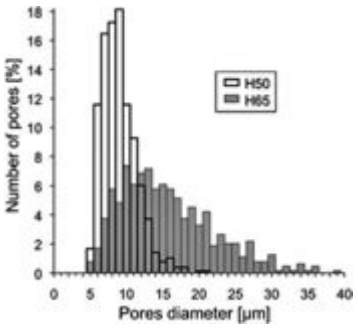

Figure 4. Pore size distributions for H50 and H65 semi-IPN xerogels.

SAXS investigations were carried out to detail the structural changes imposed at the nanoscale by the PVP addition. The investigated hydrogel formulations were compared to a cross-linked p(HEMA) hydrogel as a reference. p(HEMA) hydrogel is prepared analogously to H50 except for the addition of PVP. Thus, the cross-linked p(HEMA) network percentage in p(HEMA) hydrogel is higher than in semi-IPN formulations (50% w/w in the composition of p(HEMA) compared with a maximum of 25% w/w in semi-IPN compositions), and the water-phase was maintained at 50% w/w of the total. This excess of water leads to phase separation during polymerization of p(HEMA) hydrogel, as reported in the literature.[38]

SAXS curves, as shown in Figure 5, were modeled using the Debye−Bueche approach.[42] In this model, SAXS intensity distribution is split in two q-dependent contributions and an instrumental flat background:

$$I(q) = I_{\text{Lorentz}}(q) + I_{\text{excess}}(q) + \text{bkg} \tag{11}$$

The first contribution, $I_{\text{Lorentz}}(q)$, is a Lorentzian term accounting for the scattering associated with a tridimensional network with a characteristic mesh size. It can be expressed as follows

$$I_{\text{Lorentz}}(q) = \frac{I_{\text{Lorentz}}(0)}{1 + q^2\zeta^2} \tag{12}$$

where $I_{\text{Lorentz}}(0)$ is the Lorentzian intensity at $q = 0$ and ζ is the average mesh dimension of the network. The second contribution, I_{excess}, the excess scattering, concerns the scattering at low q produced by inhomogeneities, as for example, solidlike polymer domains.

$$I_{\text{excess}}(q) = \frac{I_{\text{excess}}(0)}{(1 + q^2a^2)^2} \tag{13}$$

where $I_{\text{excess}}(0)$ is the excess intensity at $q = 0$ and a is the average dimension of the inhomogeneity domains accessible by the SAXS experiment.

dx.doi.org/10.1021/la3048664 | *Langmuir* 2013, 29, 2746−2755

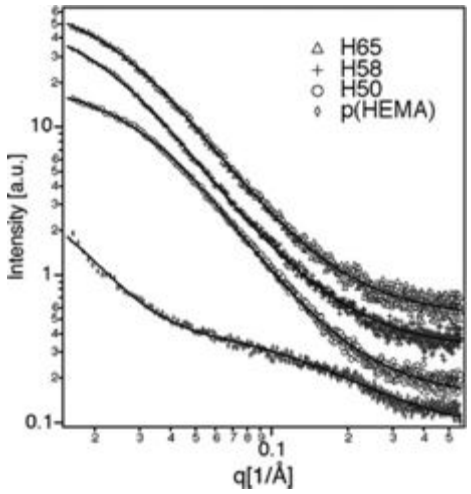

Figure 5. SAXS intensity distribution in a log–log scale for all semi-IPN hydrogels investigated. A cross-linked p(HEMA) hydrogel is reported as a reference. The solid lines are the fits with the Debye–Bueche model. The curves are shifted upward by an arbitrary factor to avoid overlap.

Best fitting curves are reported as solid lines in Figure 5, while the extracted parameters from the Debye–Bueche model are listed in Table 3.

Table 3. Debye–Bueche Parameters Obtained from the SAXS Curves of the Investigated Hydrogels

	p(HEMA)	H50	H58	H65
$I_{Lorentz}(0)$	1.7	12.1	8.2	7.8
ζ (nm)	0.7	2.5	2.8	3.1
$I_{excess}(0)$	27.4	40.2	45.3	25.1
a (nm)	6.0	2.5	3.6	3.3
bkg	0.50	0.39	0.30	0.23
$I_{excess}(0)/I_{Lorentz}(0)$	16.1	3.3	5.5	3.2

The SAXS profiles in Figure 5 show a neat difference between p(HEMA) and semi-IPN hydrogels. According to the literature,[43] mesh dimension depends mainly on the equilibrium water content, which in the present case is proportional to the p(HEMA)/PVP ratio in the reaction mixture. H50 semi-IPN hydrogel has a mesh size of 2.5 nm while the H58 of 2.8 nm and H65 of 3.1 nm. In fact, mesh size increase for each semi-IPN formulation is accompanied by a comparable increase of EWC. Namely, the mesh volume increase over H50 is 41% and 91% in H58 and H65, respectively, which is in agreement to the EWC increase of 11% and of 21% in the same formulations.

The increase of average mesh size is also related to the decrease in cross-linker concentration, as reported in the literature.[44] Despite cross-linker content decreases, H50 shows a smaller ζ than H65. This is due to the decreasing percentage of PVP from H65 to H50, which leads to a less swollen network.

As reported in the literature[45−47] less homogeneous structures are likely to form when the syntheses are conducted at higher polymer volume fractions (water-poor systems) and/or at higher cross-linker concentration. The variation on inhomogeneity dimension, a, is not clear for the three semi-IPN formulations since the more water-poor system (H50) has the lower number of cross-links, while the formulation with higher EWC (H65) is characterized by a higher cross-linker content. So the effect of these two components is disguised. As a matter of fact, H50 has the smallest a dimension in the series thus resulting in the most homogeneous both in the nanometer-scale length and in the micrometer-scale length as already shown by the porosity distribution extracted from the SEM images. The increase of inhomogeneities dimension is clearly noticed in the water-poor p(HEMA) system.

The $I_{excess}(0)/I_{Lorentz}(0)$ ratio is proportional to inhomogeneity/mesh volume fractions. In this regard, the collected SAXS data agree with the increase of inhomogeneity abundance related to the higher polymer volume fraction. In fact, there is an increase of inhomogeneities of a factor 4 for p(HEMA) hydrogel with respect to semi-IPN formulations.

Application of Hydrogels. Due to higher transparency and ease of handling, hydrogels shaped as a film were preferred for carrying out the cleaning tests on model samples. The dehydration kinetics of the hydrogels was evaluated at 55% RH and 20 °C to verify if during the time required for the cleaning process, the amount of water is enough.

Dehydration curves of H50 and H65 hydrogel films are presented in Figure 6. The same amount of water contained in the hydrogel was put in a beaker inside the dehydration chamber to have a comparison with the evaporation kinetics of bulk water.

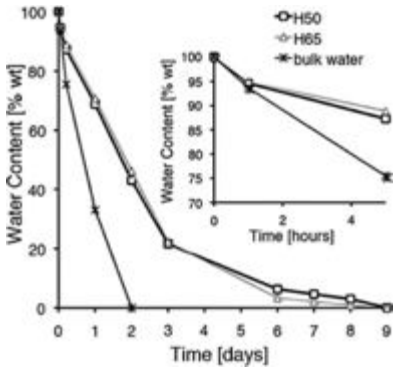

Figure 6. Dehydration curves for H50 and H65 semi-IPN hydrogels and for bulk water. Inset: dehydration curves within the first 5 h.

The dehydration kinetics confirmed that for some hours the amount of water inside hydrogels is still above 95% of the initial value (see inset of Figure 6), while the dehydration equilibrium was reached after 6 days.

A release test was performed using two hydrogel formulations (H50 and H65) to assess the real amount of water released to a highly hydrophilic surface such as paper. Both hydrogels performed a homogeneous release of water restricted to the paper contact area. After 30 min of contact, H50 released 16 ± 1 mg/cm^2 while H65 released 33 ± 3 mg/cm^2. The evident difference of water release between both hydrogels is in accordance with the results of DSC analysis.

To confirm that no gel residues are left after cleaning with semi-IPN hydrogels, ATR-FTIR spectra from a highly hydrophilic material such as cotton canvas were collected.

In Figure 7 the characteristic intense bands assigned to the carbonyl stretching vibration of both HEMA and PVP

dx.doi.org/10.1021/la3048664 | Langmuir 2013, 29, 2746−2755

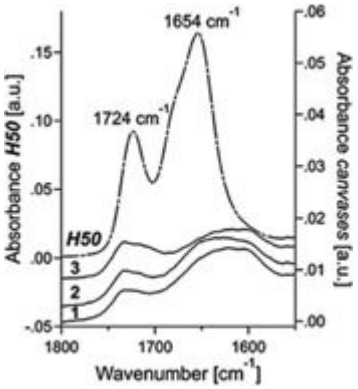

Figure 7. ATR-FTIR spectra of H50 hydrogel (slash-dotted line), of canvases previously in contact with H65 (1) and H50 (2) hydrogels and of canvas as it is (3).

(respectively 1724 and 1654 cm^{-1}) are clearly not present in the other spectra (1 and 2), which confirmed that no residues were left on canvas after treatment.

The application of semi-IPN hydrogels for the removal of hydrosoluble surface grime from a Thang-Ka mock-up is presented below. Cleaning tests were performed using H50 and H65 hydrogels. Since the first gel was not efficient enough and the latter showed an excessive wetting action, water-loaded H58 hydrogel (tailored for this case study; for chemical composition see Table 1) was chosen because it presents retention/release characteristics in between H50 and H65.

To obtain a gradual and controlled cleaning action, the most efficient procedure was the use of water-loaded hydrogel H58 in two short applications, each of about 20 min. Furthermore, the application procedure does not include any mechanical action, while in traditional cleaning methods this is a mandatory step. The ease of handling of this hydrogel film is shown in Figure 8. To evaluate the ability of semi-IPN hydrogels to

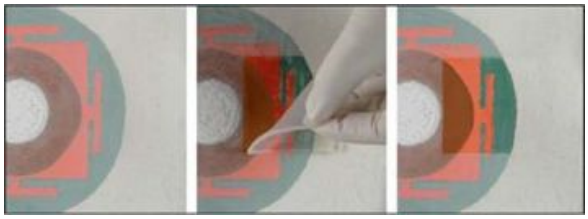

Figure 8. Stages of cleaning on Thang-Ka mock-up (see video in the Supporting Information).

restrain cleaning action while offering an efficient treatment, a comparison with a recently used material for art conservation, i.e., agar–agar gel,[48] was carried out. Semi-IPN p(HEMA)/PVP and agar–agar hydrogels were left in contact for 5 min with paper painted with a water-soluble ink (brazilwood ink). Color leaching, due to an excessive wetting of the treated surface, is highlighted by the diffusion of the colorant that is clearly visible after contact with agar–agar gel, while the color front is still sharp in the case of semi-IPN p(HEMA)/PVP hydrogels (Figure 9).

Figure 10 shows the homogeneous and confined cleaning obtained using H58 hydrogel, resulting in a gradual depletion of the grime coating without any color leaching.

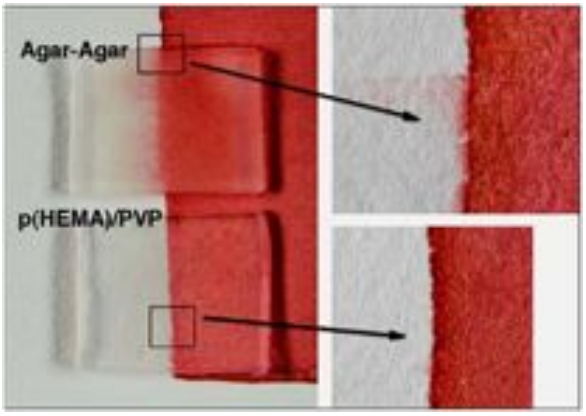

Figure 9. Five minutes application of agar–agar (2% w/w) and semi-IPN p(HEMA)/PVP hydrogels on paper painted with brazilwood ink.

UV–vis reflectance spectra further provide qualitative confirmation of the cleaning results (see Figure 11). Reflectance spectra of artificial soiled areas show enhanced reflectance values in the whole investigated range. This is due to the scattering of incident light caused by grime particles, resulting in a whitish, and thus more reflective, surface. In fact, the reflectance spectra from the cleaned areas show a progressive approximation to the reflectance values of reference areas (not soiled color).

To quantify this approximation, the color difference ΔE^* was calculated for soiled and cleaned surface areas with respect to reference area. Table 4 presents colorimetric data concerning the indigo colorant, the most sensitive paint layer of the Thang-Ka mock-up. The calculated values of ΔE^* show a significant reduction in the treated areas with respect to the artificially soiled area. The same trend is observed for the single colorimetric coordinates. This demonstrates that improved cleaning control can be achieved by using semi-IPN hydrogels based on p(HEMA) and linear PVP. The surface grime is gradually removed, and the original water-sensitive paint layers are not affected.

CONCLUSIONS

In this paper the synthesis and characterization of high retentive semi-IPN hydrogels developed specifically for application in art conservation is presented. Semi-IPN hydrogels have been prepared by free radical polymerization of HEMA monomer embedding linear PVP into the hydrogel network and varying the components ratios (water, PVP, HEMA, and cross-linker quantities) to tune their characteristics in terms of mechanical behavior (softness, elasticity, and resistance to tensile strength) and affinity to water. The water inside swollen hydrogels was characterized by differential scanning calorimetry and classified as unfreezable, bound-freezable, and free water, depending on the extent of interactions with the polar part of the polymer chains. The hydrogels possess suitable water release and retention properties for a controlled and efficient cleaning of water-sensitive artifacts. Moreover, the gels' mechanical properties and the water "mobility" can be tailored to the required characteristics for specific conservation issues by changing gels' composition, making these new polymeric hydrogels the most advanced systems for the cleaning of water-sensitive artifacts.

dx.doi.org/10.1021/la3048664 | *Langmuir* 2013, 29, 2746–2755

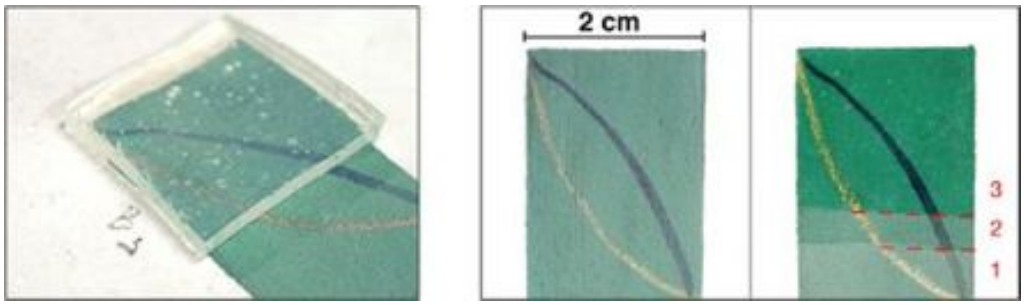

Figure 10. Artificial grime removal using water-loaded H58 hydrogel from a Thank-Ka mock-up. Right image presents different levels of cleaning: not cleaned (1); after 20 min of hydrogel application (2); after further 20 min of hydrogel application (3).

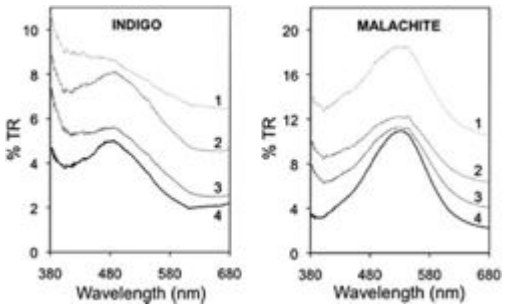

Figure 11. UV−vis reflectance spectra acquired from indigo and malachite painted areas: (1) artificial soiled surface; (2) after 20 min cleaning; (3) after ulterior 20 min cleaning; (4) reference painted area.

Table 4. Colorimetric Coordinates L^*, a^*, b^*, and ΔE^* Values for the Reference Area, Not Cleaned Area, and Different Applications of H58 Hydrogel[a]

indigo	L^*	a^*	b^*	ΔE^*
reference area (not soiled)	21.5 ± 1.9	−7.2 ± 0.4	−7.0 ± 0.4	0
before cleaning	32.8 ± 0.6	−2.6 ± 0.8	−3.7 ± 0.7	12.6
20 min H58 hydrogel application	31.7 ± 1.3	−5.0 ± 0.4	−4.7 ± 0.8	10.6
further 20 min H58 hydrogel application	21.8 ± 1.4	−5.2 ± 0.3	−6.9 ± 0.6	2.1

[a]Each of the colorimetric coordinates presented is the average value of at least 10 measurements.

■ ASSOCIATED CONTENT

Ⓢ Supporting Information

Movie on the cleaning of water-sensitive surface. This material is available free of charge via the Internet at http://pubs.acs.org.

■ AUTHOR INFORMATION

Corresponding Author

*Phone: +39 055 457 3033. Fax: +39 055 457 3032. E-mail: baglioni@csgi.unifi.it. URL: www.csgi.unifi.it.

Author Contributions

The manuscript was written through contributions of all authors. All authors have given approval to the final version of the manuscript.

Notes

The authors declare no competing financial interest.

■ ACKNOWLEDGMENTS

The authors acknowledge Dr. F. Ridi for the thermal analysis experiments and Dr. M. Potenza for the spectrophotocolorimetric measurements. J.A.L.D. acknowledges financial support provided by *Fundação para a Ciência e a Tecnologia* (FCT) through a Ph.D. research grant (SFRH/BD/73817/2010). This work was partly supported by CSGI and the European Union, Project NANOFORART (FP7-ENV-NMP-2011/282816).

■ REFERENCES

(1) Stolow, N. Application of Science to Cleaning Methods: Solvent Action Studies on Pigmented and Unpigmented Linseed Oil Films. In *Recent Advances in Conservation*, Proceedings of the IIC Rome Conference, Rome, Italy, 1961; Butterworths: London, U.K., 1963; pp 84−88.

(2) Phenix, A.; Sutherland, K. The Cleaning of Paintings: Effects of Organic Solvents on Oil Paint Films. *Rev. Conserv.* **2001**, *2*, 47−60.

(3) Cremonesi, P. *L'Uso di Tensioattivi e Chelanti nella Pulitura di Opere Policrome*; Il Prato: Padua, Italy, 2004.

(4) Wolbers, R.; Sterman, N.; Stavroudis, C. *Notes for the Workshop on New Methods in the Cleaning of Paintings*; The Getty Conservation Institute: Marina del Rey, CA, 1988.

(5) Wolbers, R. *Cleaning Painted Surfaces: Aqueous Methods*; Archetype: London, U.K., 2000.

(6) Burnstock, A.; Kieslich, T. A Study of the Clearance of Solvent Gels Used for Varnish Removal from Paintings. In *ICOM Committee for cConservation*, Proceedings of the 11th Triennial Conference, Edinburgh, Scotland, Sept 1−6, 1996; James & James: London, U.K., 1996; pp 253−262.

(7) Carretti, E.; Bonini, M.; Dei, L.; Berrie, B. H.; Angelova, L. V.; Baglioni, P.; Weiss, R. G. New Frontiers in Materials Science for Art Conservation: Responsive Gels and Beyond. *Acc. Chem. Res.* **2010**, *43*, 751−760.

(8) Carretti, E.; Grassi, S.; Cossalter, M.; Natali, I.; Caminati, G.; Weiss, R. G.; Baglioni, P.; Dei, L. Poly(vinyl alcohol)−Borate Hydro/Cosolvent Gels: Viscoelastic Properties, Solubilizing Power, and Application to Art Conservation. *Langmuir* **2009**, *25*, 8656−8662.

(9) Bonini, M.; Lenz, S.; Giorgi, R.; Baglioni, P. Nanomagnetic Sponges for the Cleaning of Works of Art. *Langmuir* **2007**, *23*, 8681−8685.

(10) Bonini, M.; Lenz, S.; Falletta, E.; Ridi, F.; Carretti, E.; Fratini, E.; Wiedenmann, A.; Baglioni, P. Acrylamide-Based Magnetic Nanosponges: A New Smart Nanocomposite Material. *Langmuir* **2008**, *24*, 12644−12650.

(11) Pizzorusso, G.; Fratini, E.; Eiblmeier, J.; Giorgi, R.; Chelazzi, D.; Chevalier, A.; Baglioni, P. Physicochemical Characterization of Acrylamide/Bisacrylamide Hydrogels and Their Application for the Conservation of Easel Paintings. *Langmuir* **2012**, *28*, 3952−3961.

(12) Tighe, B. J. Hydrogels as Contact Lens Materials. In *Hydrogels in Medicine and Pharmacy*; Peppas, N. A., Ed.; CRC Press: Boca Raton, FL, 1987; Vol. *III*, Properties and Applications, pp 53−82.

(13) Mack, E. J.; Okano, T.; Kim, S. W. Biomedical Applications of Poly(2-Hydroxyethyl Methacrylate) and its Copolymers. In *Hydrogels in Medicine and Pharmacy*; Peppas, N. A., Ed.; CRC Press: Boca Raton, FL, 1987; Vol. *II*, Polymers, pp 65−93.
(14) Haaf, F.; Sanner, A.; Straub, F. Polymers of N-Vinylpyrrolidone: Synthesis, Characterization and Uses. *Polym. J.* **1985**, *17*, 143−152.
(15) Wang, J.; Sun, F.; Li, X. Preparation and Antidehydration of Interpenetrating Polymer Network Hydrogels Based on 2-Hydroxyethyl Methacrylate and N-Vinyl-2-Pyrrolidone. *J. Appl. Polym. Sci.* **2010**, *117*, 1851−1858.
(16) McNaught, M.; Wilkinson, A. Definitions of Terms Relating to the Structure and Processing of Sols, Gels, Networks, and Inorganic-Organic Hybrid Materials. In *IUPAC Compendium of Chemical Terminology* [Online]; Blackwell Scientific Publications: Oxford, U.K., 1997; p 1815. http://goldbook.iupac.org/PDF/goldbook.pdf (accessed Oct 10, 2012).
(17) Yanez, F.; Concheiro, A.; Alvarez-Lorenzo, C. Macromolecule Release and Smoothness of Semi-Interpenetrating PVP−pHEMA Networks for Comfortable Soft Contact Lenses. *Eur. J. Pharm. Biopharm.* **2008**, *69*, 1094−1103.
(18) Gong, J. P.; Osada, Y. Surface Friction of Polymer Gels. *Prog. Polym. Sci.* **2002**, *27*, 3−38.
(19) Carretti, E.; Dei, L.; Baglioni, P. Solubilization of Acrylic and Vinyl Polymers in Nanocontainer Solutions. Application of Microemulsions and Micelles to Cultural Heritage Conservation. *Langmuir* **2003**, *19*, 7867−7872.
(20) Carretti, E.; Giorgi, R.; Berti, D.; Baglioni, P. Oil-in-Water Nanocontainers as Low Environmental Impact Cleaning Tools for Works of Art: Two Case Studies. *Langmuir* **2007**, *23*, 6396−6403.
(21) Carretti, E.; Fratini, E.; Berti, D.; Dei, L.; Baglioni, P. Nanoscience for Art Conservation: Oil-in-Water Microemulsions Embedded in a Polymeric Network for the Cleaning of Works of Art. *Angew. Chem., Int. Ed.* **2009**, *48*, 8966−8969.
(22) Giorgi, R.; Baglioni, M.; Berti, D.; Baglioni, P. New Methodologies for the Conservation of Cultural Heritage: Micellar Solutions, Microemulsions, and Hydroxide Nanoparticles. *Acc. Chem. Res.* **2010**, *43*, 695−704.
(23) Baglioni, M.; Rengstl, D.; Berti, D.; Bonini, M.; Giorgi, R.; Baglioni, P. Removal of Acrylic Coatings from Works of Art by Means of Nanofluids: Understanding the Mechanism at the Nanoscale. *Nanoscale* **2010**, *2*, 1723−1732.
(24) Baglioni, M.; Giorgi, R.; Berti, D.; Baglioni, P. Smart Cleaning of Cultural Heritage: A New Challenge for Soft Nanoscience. *Nanoscale* **2012**, *4*, 42−53.
(25) Baglioni, M.; Berti, D.; Teixeira, J.; Giorgi, R.; Baglioni, P. Nanostructured Surfactant-Based Systems for the Removal of Polymers from Wall Paintings: A Small-Angle Neutron Scattering Study. *Langmuir* **2012**, *28*, 15193−15202.
(26) Ming Kuo, S.; Jen Chang, S.; Jiin Wang, Y. Properties of PVA-AA Cross-Linked HEMA-Based Hydrogels. *J. Polym. Res.* **1999**, *6*, 191−196.
(27) Liu, Q.; Hedberg, E. L.; Liu, Z.; Bahulekar, R.; Meszlenyi, R. K.; Mikos, A. G. Preparation of Macroporous Poly(2-Hydroxyethyl Methacrylate) Hydrogels by Enhanced Phase Separation. *Biomaterials* **2000**, *21*, 2163−2169.
(28) Nakamura, K.; Hatakeyama, T.; Hatakeyama, H. Relationship between Hydrogen Bonding and Bound Water in Polyhydroxystyrene Derivatives. *Polymer* **1983**, *24*, 871−876.
(29) Lide, D. R. *CRC Handbook of Chemistry and Physics*, 79th ed.; CRC Press: Boca Raton, FL, 1998.
(30) Faroongsarng, D.; Sukonrat, P. Thermal Behavior of Water in the Selected Starch- and Cellulose-Based Polymeric Hydrogels. *Int. J. Pharm.* **2008**, *352*, 152−158.
(31) Landry, M. R. Thermoporometry by Differential Scanning Calorimetry: Experimental Considerations and Applications. *Thermochim. Acta* **2005**, *433*, 27−50.
(32) Blanton, T.; Huang, T. C.; Toraya, H.; Hubbard, C. R.; Robie, S. B.; Louer, D.; Gobel, H. E.; Will, G.; Gilles, R.; Raftery, T. JCPDS—International Centre for Diffraction Data Round Robin Study of Silver Behenate. A Possible Low-Angle X-Ray Diffraction Calibration Standard. *Powder Diffr.* **1995**, *10*, 91−95.
(33) Wolbers, R. The Use of a Synthetic Soiling Mixture as a Means for Evaluating the Efficacity of a Aqueous Cleaning Materials on Painted Surfaces. *Conservation−Restauration Biens Culturels* **1992**, *4*, 22−29.
(34) Wyszecki, G.; Stiles, W. S. *Color Science: Concepts and Methods, Quantitative Data and Formulae*, 2nd ed.; John Wiley & Sons: New York, 2000.
(35) Kolar, J.; Strlic, M.; Marincek, M. IR Pulsed Laser Light Interaction with Soiled Cellulose and Paper. *Appl. Phys. A: Mater. Sci. Process.* **2002**, *75*, 673−676.
(36) Jackson, D. P.; Jackson, J. A. *Tibetan Thangka Painting: Methods & Materials*, 2nd ed.; Serindia: London, U.K., 1988.
(37) Huang, Y.; Yang, J. *Novel Colloidal Forming of Ceramics*; Springer: Berlin Heidelberg, Germany, 2011.
(38) Lou, X.; Munro, S.; Wang, S. Drug Release Characteristics of Phase Separation pHEMA Sponge Materials. *Biomaterials* **2004**, *25*, 5071−5080.
(39) Okay, O. Macroporous Copolymer Networks. *Prog. Polym. Sci.* **2000**, *25*, 711−779.
(40) Wolfe, J.; Bryant, G.; Koster, K. L. What is Unfreezable Water, How Unfreezable Is It and How Much is There? *CryoLetters* **2002**, *23*, 157−166.
(41) Li, X.; Cui, Y.; Xiao, J.; Liao, L. Hydrogel−Hydrogel Composites: The Interfacial Structure and Interaction between Water and Polymer Chains. *J. Appl. Polym. Sci.* **2008**, *108*, 3713−3719.
(42) Debye, P.; Bueche, A. M. Scattering by an Inhomogeneous Solid. *J. Appl. Phys.* **1949**, *20*, 518−525.
(43) Canal, T.; Peppas, N. A. Correlation between Mesh Size and Equilibrium Degree of Swelling of Polymeric Networks. *J. Biomed. Mater. Res., Part A* **1989**, *23*, 1183−1193.
(44) Peppas, N. A.; Hilt, J. Z.; Khademhosseini, A.; Langer, R. Hydrogels in Biology and Medicine: From Molecular Principles to Bionanotechnology. *Adv. Mater.* **2006**, *18*, 1345−1360.
(45) Panyukov, S.; Rabin, Y. Statistical Physics of Polymer Gels. *Phys. Rep.* **1996**, *269*, 1−131.
(46) Benguigui, L.; Boue, F. Homogeneous and Inhomogenous Polyacrylamide Gels As Observed by Small Angle Neutron Scattering: A Connection with Elastic Properties. *Eur. Phys. J. B* **1999**, *11*, 439−444.
(47) Ikkai, F.; Shibayama, M. Inhomogeneity Control in Polymer Gels. *J. Polym. Sci., Part B* **2005**, *43*, 617−628.
(48) Campani, E.; Casoli, A.; Cremonesi, P.; Saccani, I.; Signorini, E. *Quaderni del Cesmar7: L'Uso di Agarosio e Agar per la Preparazione di "Gel Rigidi"−Use of Agarose and Agar for Preparing "Rigid Gels"*, n°o.4; Il Prato: Padua, Italy, 2007.

Science and Technology for the Conservation of Cultural Heritage, Edited by Miguel Angel Rogerio-Candelera, Massimo Lazzari, Emilio Cano, CRC Press, 2013

Semi-interpenetrating p(HEMA)/PVP hydrogels for the cleaning of water-sensitive painted artifacts: assessment on release and retention properties

R. Giorgi, J.A.L. Domingues, N. Bonelli & P. Baglioni
Department of Chemistry and CSGI, University of Florence, Florence, Italy

Nowadays, aqueous cleaning systems are preferred for the cleaning of painted artifacts because they are environmental friendly and offer several advantages in terms of selectivity and gentle removal of undesired materials. However, materials interaction with water can lead to mechanical stress between the substrate and the paint layers. The confinement of water cleaning systems in a hydrogel with high retention capability can limit this disadvantage. Hence, the aim of this work was to develop novel chemical hydrogels, specifically designed for the cleaning of water-sensitive painted artifacts. These are based on highly hydrophilic semi-interpenetrating p(HEMA)/PVP networks with suitable mechanical strength to avoid gel residues after cleaning treatment. To assess on the potential of these novel hydrogels their release and retention properties were compared with the widely used agar-agar hydrogel.

1 INTRODUCTION

The usage of neat or blended organic solvents for painting cleaning presents several drawbacks due to the poor selectivity and environmental impact. The uncontrolled penetration of solvents into the painted layers may cause swelling or leaching of binders and varnishes (Phenix, A. & Sutherland, K. 2001, The cleaning of paintings: effects of organic solvents on oil paint films. *Reviews in Conservation*. 2: 47–60). To overcome these issues, water-based cleaning systems, such as microemulsions, have recently received much attention (Giorgi, R., Baglioni, M., Berti, D., Baglioni, P., 2010, New Methodologies for the Conservation of Cultural Heritage: Micellar Solutions, Microemulsions, and Hydroxide Nanoparticles. *Accounts of Chemical Research*. 43(6): 695-704 (references therein)), because the amount of organic solvents is very low and it is confined in a stable way. This ensures a bigger control of the cleaning process and a very low environmental impact. Obviously, this approach can be followed on artifacts that are not water-sensitive, i.e. wall paintings and stones. In fact, easel paintings in contact with water are prone to swelling of the hydrophilic layers, which often leads to painting detachment (Pizzorusso, G., Fratini, E., Eiblmeier, J., Giorgi, R., Chelazzi, D., Chevalier, A., Baglioni, P., 2012, Physicochemical characterization of acrylamide/bisacrylamide hydrogels and their application for the conservation of easel paintings. *Langmuir*. 28(8): 3952−3961).

In the last decades, conservators devised several methods to limit solvents action through the use of thickeners (e.g. cellulose ethers; polyacrylic acids, etc.).

More recently, a new class of gels, known as “rigid gels”, has been applied for restoration purposes. Namely, polysaccharide-based gels (e.g. agar-agar and gellan gum) have been used as a container for the controlled release of water solution (Campani, E., Casoli, A., Cremonesi, P., Saccani, I., Signorini, E., 2007. L’uso di Agarosio e Agar per la preparazione di “Gel Rigidi”. *Quaderni del Cesmar7 n.4*. Padova: Il Prato.). These gels can be described as ‘physical gel’, because the gelled state depends on the intermolecular and intramolecular interactions of polymer chains, which are weak (Van der Waals forces and hydrogen bonds) in terms of bond energy. In water-swollen physical gels the competition of water-polymer and polymer-polymer hydrogen bonds may reflect in the decrease of hydrogel mechanical stability. Thus, a small mechanical stress is enough for hydrogel deformation. Hence, from a practical point of view, these characteristics make the hydrogel hard to be handled, when the water content is high, and usually these gels leave residues on the painted surface because the interactions with the support are competitive with the gel cohesion forces.

Studies have been carried out in order to reduce the risk of gel residues and to enhance the hydrogel retention characteristics, as well as their exchange capability with the surface to be treated. As a result, some innovative confining systems have been developed, as described in literature (Baglioni, P., Dei, L., Carretti, E., Giorgi, R. 2009, Gels for the Conservation of Cultural Heritage. *Langmuir*. 25(15): 8373–8374; Carretti, E., Bonini, M., Dei, L., Berrie, B.H., Angelova, L.V., Baglioni, P., Weiss, R.G., 2010, New Frontiers in Materials Science for Art Conservation: Responsive Gels and Beyond. *Accounts of Chemical Research*. 43(6): 751-760 (references therein); Pizzorusso, G., Fratini, E., Eiblmeier, J., Giorgi, R., Chelazzi, D., Chevalier, A., Baglioni, P., 2012, Physicochemical characterization of acrylamide/bisacrylamide hydrogels and their application for the conservation of easel paintings. *Langmuir*. 28(8): 3952−3961).

The current study was focused on designing a new class of chemical hydrogels (i.e. able to load aqueous systems) that fulfill the right equilibrium between retention and release properties in order to ensure an efficient and controlled cleaning. Gelled state depends on the building of a polymer network that is characterized by the presence of covalent bonds, which are stronger than the weak intermolecular forces involved in physical gels. Chemical gels exhibit improved mechanical properties that avoid any left residues and can swell in a liquid medium without gel solubilization.

2 SEMI-IPN P(HEMA)/PVP HYDROGELS

The ideal hydrogel properties for application in cleaning of paintings are achieved if two important features are combined: mechanical strength and hydrophilicity. These two characteristics allow, on one hand, simple manipulation of gel and absence of gel residues after cleaning treatment and, on the other hand, an efficient exchange process between the cleaning system and the artifacts surface. In this contribution, the combination of these two properties is obtained through the synthesis of semi-interpenetrating polymer networks (semi-IPN).

Semi-IPNs are polymer blends in which linear or branched polymers are embedded into one or more polymer networks during polymerization. To obtain the semi-IPN hydrogels, the linear polymer polyvinylpyrrolidone – PVP – was embedded into the forming network of poly(2-hydroxyethyl methacrylate) – p(HEMA). P(HEMA) and p(VP) are extensively used and studied polymers. P(HEMA) forms very resistant hydrogels, however, their hydrophilicity is not sufficient for loading water-based cleaning systems. P(VP), on the other hand, is an high hydrophilic polymer. The semi-IPN hydrogels can be designed by varying their component ratios (water, PVP, HEMA and cross-linker quantities) in order to tune their characteristics in terms of mechanical behavior (softness, elasticity, and resistance to tensile strength) and affinity to water (Domingues, J.A.L., Bonelli, N., Giorgi, R., Fratini, E., Gorel, F., Baglioni, P., Innovative hydrogels based on semi-interpenetrating p(HEMA)/PVP networks for the cleaning of water-sensitive cultural heritage artifacts. *Langmuir* - paper submitted).

Hydrogel synthesis was carried out by free radical polymerization of 2-hydroxyethyl methacrylate (HEMA) monomer and a cross-linker, N,N'-methylene-bisacrylamide (MBA), in a water solution with linear PVP (~1300 KDa). A series of different hydrogels was designed by varying the proportions of monomer/cross-linker ratio with PVP and water percentages. Physico-chemical characterization was carried out by thermal analysis that allowed to calculate the free/bound water ratios and by a Field Emission Gun - Scanning Electron Microscopy (FEG-SEM) Sigma, from Carl Zeiss (Germany), for the study of micro-structure and porosity.

3 HYDROGEL CHARACTERIZATION

All the semi-IPN hydrogels formulations were found to have interesting macroscopic characteristics and satisfactory mechanical properties. Specifically, these hydrogels exhibit a wide range of features: from semi-rigid and completely transparent to pliable and translucent. In fact, they are to some extent softer than ordinary chemical gels, which is an important feature to obtain better adhesion to rougher surfaces. Moreover, the achieved mechanical strength permits to synthesize hydrogels that are film-shaped, with a thickness of ca. 2mm.

These gels are able to load big amount of water solutions or aqueous detergent systems; the equilibrium water content (EWC) value provides an estimation of the amount of cleaning systems can be kept in contact with the artworks surfaces. EWC is calculated as follows:

$$EWC = 100(W_w - W_d)/W_w \quad (1)$$

where W_w and W_d are respectively the weights of fully water swollen and dry hydrogels.

The EWC values for the studied formulations vary from ca. 70% to 90% without any loss of transparency. High EWCs are strictly dependent on hydrogel porosity and hydrophilicity of the network. The obtained results highlight that the addition of linear chains of PVP into the reaction mixture permits to increase water affinity, porosity and, consequently, the EWC of the hydrogels.

Water inside swollen hydrogels can be classified into three different states, depending on the interactions with the polar part of the polymer chains: unfreezable, bound-freezable and free water (Li et al. 2008) Free Water Index (FWI) parameter can be determined by thermal analysis (differential scanning calorimetry – DSC). The FWI can be obtained by the given formula:

$$FWI = \Delta H_{exp}/WC\Delta H_{theo} \quad (2)$$

where the ΔH_{exp} [J/g] represents the melting enthalpy variation for free water, *WC* is the water weight fraction in the hydrogel and ΔH_{theo} is the theoretical value of the specific enthalpy of fusion for bulk water. The FWI values obtained highlight that the free water amount inside the swollen hydrogels is much higher than bound water. Therefore, aqueous system loaded into the hydrogels will behave mostly as free water. The free water content varies from ca. 70% to 80% in respect of the total water quantity in swollen hydrogels.

In order to obtain some information about the structure and porosity of the lyophilized hydrogel (xerogel), FEG-SEM images were acquired. FEG-SEM image of one of the formulations is shown in figure 1. In general, sponge-like network morphology is observed and pore dimensions are approximately in the range of 5 to 40 μm. The difference of porosities between different hydrogel formulations is due to three main factors: the first is the water content in the initial polymerization mixture, which is the main responsible for the final gel porosity and the pore dimension; the second is due to the PVP loss during first washing steps after polymerization; and the third, the cross-linker amount, which contributes, at constant PVP/HEMA/H_2O ratios, to a more compact network structure. Although a compact network is present these hydrogels are highly flexible (see figure 1 right). It should be noted that SEM images refer to xerogels, so hydrogels are expected to have much larger pores in the swollen state.

4 ASSESSMENT ON RELEASE AND RETENTION PROPERTIES

In order to evaluate the effectiveness and versatility of the investigated hydrogel systems, some assessment tests were carried out. The hydrogels dehydration kinetics (recorded at 55% RH and 20ºC) was evaluated to verify if during the time required for the cleaning process the amount of detergent solution is enough. This assessment confirmed that for the first hour the amount of water inside hydrogels is still above 95% of the initial water content. Additionally, water release tests were performed to quantify the water amount flowing into a high hydrophilic support during cleaning process. For this purpose, water-loaded hydrogels were gently dried on the surface, then put on 4 sheets of Whatman® filter paper and covered with a lid to avoid water evaporation. The filter paper sheets were weighted before and after 30 minutes of application. All hydrogels performed a homogenous release of water restricted to the paper contact area. After 30 minutes of contact, released water ranges from 16±1 mg/cm^2 to 33±3 mg/cm^2, depending on the hydrophilicity of the formulation, while the same test performed using an agar-agar hydrogel released 166±8 mg/cm^2. It was important to compare semi-IPN hydrogel action with the widely used agar-agar hydrogel system. Agar-agar hydrogels were chosen because, like semi-IPN p(HEMA)/PVP hydrogels, they are used in conservation treatments in film shaped form and with water based solvent systems. In order to highlight the effective confinement of the cleaning process, some release tests on paper painted with a water-soluble colorant were performed. Few minutes of application are enough to evidence the difference between the two systems. In fact, while the area treated with agar-agar gel (figure 2) shows color leaching, semi-IPN p(HEMA)/PVP hydrogels presents any alterations also after 5 minutes of contact. Furthermore, abundant color absorption is shown by agar-agar gel, while few color traces were observed on the semi-IPN hydrogel surface.

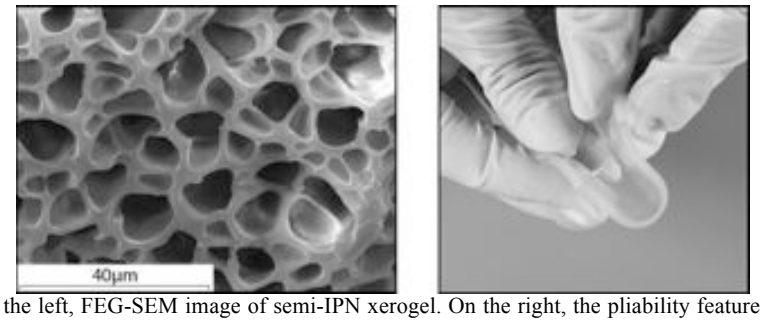

Figure 1. On the left, FEG-SEM image of semi-IPN xerogel. On the right, the pliability feature of the hydrogel is highlighted.

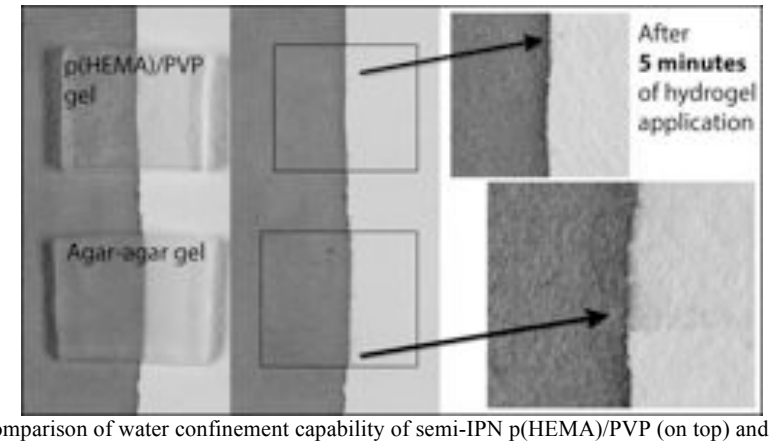

Figure 2. Comparison of water confinement capability of semi-IPN p(HEMA)/PVP (on top) and agar-agar (on bottom) hydrogels.

5 CONCLUSIONS

The assessment carried out on semi-IPN hydrogels has shown that these polymeric networks have most of the desired properties to achieve a high-controlled cleaning action, i.e. the appropriate equilibrium between release and retention properties. These features allow to obtain a real confinement of the cleaning system on the hydrogel-artifacts interface, and thus permit to use water based systems also on water–sensitive substrates, e.g. canvas paintings.

The direct comparison with the agar-agar hydrogel has highlighted that using semi-IPN hydrogels it is possible to obtain an enhanced control of the fluids penetration and to limit the interaction volume between cleaning system and treated surface.

REFERENCES

Baglioni, P., Dei, L., Carretti, E., Giorgi, R. 2009. Gels for the Conservation of Cultural Heritage. *Langmuir*. 25(15): 8373–8374.

Campani, E., Casoli, A., Cremonesi, P., Saccani, I., Signorini, E., 2007. L'uso di Agarosio e Agar per la preparazione di "Gel Rigidi". *Quaderni del Cesmar7 n.4*. Padova: Il Prato.

Carretti, E., Bonini, M., Dei, L., Berrie, B.H., Angelova, L.V., Baglioni, P., Weiss, R.G., 2010. New Frontiers in Materials Science for Art Conservation: Responsive Gels and Beyond. *Accounts of Chemical Research*. 43(6): 751-760 (references therein).

Domingues, J.A.L., Bonelli, N., Giorgi, R., Fratini, E., Gorel, F., Baglioni, P., (in preparation). Innovative hydrogels based on semi-interpenetrating p(HEMA)/PVP networks for the cleaning of water-sensitive cultural heritage artifacts. *Langmuir*.

Giorgi, R., Baglioni, M., Berti, D., Baglioni, P., 2010. New Methodologies for the Conservation of Cultural Heritage: Micellar Solutions, Microemulsions, and Hydroxide Nanoparticles. *Accounts of Chemical Research*. 43(6): 695-704 (references therein).

Pizzorusso, G., Fratini, E., Eiblmeier, J., Giorgi, R., Chelazzi, D., Chevalier, A., Baglioni, P., 2012. Physicochemical characterization of acrylamide/bisacrylamide hydrogels and their application for the conservation of easel paintings. *Langmuir*. 28(8): 3952−3961.

Phenix, A. & Sutherland, K. 2001. The cleaning of paintings: effects of organic solvents on oil paint films. *Reviews in Conservation*. 2: 47–60.

INTERNATIONAL JOURNAL OF CONSERVATION SCIENCE

ISSN: 2067-533X Volume 4, Special Issue, 2013: 715-722 www.ijcs.uaic.ro

INNOVATIVE METHOD FOR THE CLEANING OF WATER-SENSITIVE ARTIFACTS: SYNTHESIS AND APPLICATION OF HIGHLY RETENTIVE CHEMICAL HYDROGELS

Joana DOMINGUES, Nicole BONELLI,
Rodorico GIORGI, Emiliano FRATINI, Piero BAGLIONI*

Department of Chemistry "Ugo Schiff" and CSGI (Center for Colloid and Surface Science),
University of Florence, Via della Lastruccia 3, 50019 Sesto Fiorentino (FI), Italy.

Abstract

Cleaning is one of the most important processes for the conservation of cultural heritage artifacts, but also one of the most delicate and potentially damaging to the original materials. Nowadays, aqueous cleaning is usually preferred to cleaning with organic solvents, because it is environmental friendly and less aggressive to artifact's materials. However, in some circumstances, such as cleaning paper documents, easel paintings and textiles, water-based systems can be invasive. The interaction of water with the hydrophilic support favors mechanical stresses between substrate and paint layers, which can eventually lead to paint detachment or paint leaching. Water-based detergent systems (such as micellar solutions and oil-in-water microemulsions) offer several advantages in terms of selectivity and gentle removal of hydrosoluble (e.g. grime) and hydrophobic (e.g. aged adhesive) materials. The confinement and controlled release of these water-based systems is achieved through the synthesis and application of chemical hydrogels specifically designed for cleaning water-sensitive cultural heritage artifacts. These gels are based on semi-interpenetrating p(HEMA)/PVP networks. Semi-IPN hydrogels are prepared by embedding linear polyvinylpyrrolidone physically into a network of poly(2-hydroxyethyl methacrylate). Water retention and release properties were investigated. The micro-porosity was studied by Scanning Electron Microscopy. To demonstrate both efficiency and versatility of the selected hydrogels in confining the most appropriate water-based cleaning system a representative case study is presented.

Keywords: *Semi-IPN hydrogels; Cleaning; Nanocontainers; Gel structure.*

Introduction

In general, most of the materials and methods used for conservation treatments are initially designed for application in other fields and then adapted by restorers for their specific purposes. This implies that the common procedure may not have the most suitable features demanded by each particular case study. In the last decades our research group is being concerned in providing

* Corresponding author: baglioni@csgi.unifi.it

conservators new tools based on nanotechnology that are specifically designed to answer different issues in conservation of cultural heritage [1-3].

Usually, a cleaning process is carried out to remove superficial layers that may induce further degradation to the artifact. These layers can be hydrophilic (e.g. superficial grime) or hydrophobic (e.g. aged varnishes and adhesives). While the removal of hydrophilic layers is easily performed with aqueous methods, the removal of hydrophobic layers is commonly carried out through the use of pure organic solvents. Most organic solvents are toxic and do not allow a controlled cleaning since they can quickly diffuse into inner layers [4, 5].

Dissolving hydrophobic materials, such as polymers, through non-confined pure solvents can cause their penetration within artifacts' porous matrix. After solvent evaporation polymer residues may remain within the substrate porosity.

Nanostructured fluids (e.g. oil-in-water microemulsions, micellar solutions) have been developed by the CSGI (Center for Colloid and Surface Science) to address this problem [6-8]. A microemulsion is a high-performing cleaning tool since it can remove hydrophobic layers using a small amount of organic solvents. The microemulsion droplets contain the appropriate solvent able to swell or solubilize the polymeric layers, while the water in the dispersing phase can penetrate within the porous substrate of the artifact, avoiding the risk of redeposition of the dissolved polymers, because of its affinity with the hydrophilic pores of the surface.

The use of confining tools that are able to retain capillary penetration of water-based systems is particularly important in the specific case of water-sensitive substrates (e.g. paper manuscripts, canvas paintings).

Nowadays the most used confining methods in conventional conservation practice include the use of cellulose pulp poultices and some physical gels [9, 10] (cellulose derivatives, polyacrylic acids, polysaccharide-based gels, and others), which do not have the suitable retentive features for the cleaning of water-sensitive artifacts. For this reason, highly retentive chemical "sponges" that allow a controlled release of the cleaning system, limiting its action only to the first few layers of the painted surface, were developed. For this, efforts were focused on the polymer gel technology.

Gels can be divided into two major categories, depending on the nature of their bonds: physical and chemical gels. Physical gels are formed by electrostatic interactions between polymeric chains, so they are usually viscous systems that can respond to heat or be disrupted by mechanical forces. Polysaccharide based gels (e.g. agar-agar or gellan gum) are an example of physical gels and are, at present, one of the most promising tools used by conservators with the intent of retaining the cleaning agent [11]. These gels, however, are fragile and do not have the suitable retention features.

Chemical gels are, on the other hand, characterized by the presence of covalent bonds. They have a specific shape given during synthesis and have strong gel cohesion, so no gel residues are expected after treatment using chemical gels. Chemical gels are more versatile because depending on the components (monomer, cross-linker, liquid medium, etc.) and the quantitative proportions it is possible to obtain gels with different chemical-mechanical properties [12-14]. In the specific case of cleaning water-sensitive artifacts, the ideal container would be a highly retentive soft hydrogel. In this paper we present the potential application of highly retentive hydrogels based on semi-interpenetrating polymer networks (semi-IPN) composed by a cross-linked polymer network of polyhydroxyethylmethacrylate (p(HEMA)) and an interpenetrating linear polymer of polyvinylpyrrolidone (PVP) that does not form covalent bonds with HEMA. These two polymers are biocompatible materials, largely used in the biomedical and pharmaceutical areas. The amount of PVP modulates the hydrophilicity and softness of the final product, while p(HEMA), constituting the

three-dimensional network, largely determines the mechanical properties. A high equilibrium water content (EWC) of hydrogels, which is correlated to pore dimensions, and hydrophilicity of the polymer network, is consistent with high hydrogel softness. Moreover, polymer network hydrophilicity is related to hydrogels' retention capacity, because the interaction forces of aqueous system/polymer network may prevail over the ones of aqueous system/artifacts surface.

Materials and Methods

Synthesis of p(HEMA)/PVP hydrogels

HEMA monomer and the cross-linker N,N'methylenebisacrylamide (MBA) were mixed together in a water solution with linear PVP (average Mw~1300 kDa). The reaction mixture was bubbled with nitrogen for 5 minutes to remove oxygen and then radical initiator 2,2'-Azobis(2-methylpropionitrile) was added in a 1:0.01 monomer/initiator molar ratio. The reaction mixture was gently sonicated for 30 minutes in pulsed mode to eliminate possible gas bubbles. The polymerization reaction, started by thermal homolysis of the initiator, was performed for 4h at 60ºC. After polymerization, hydrogels were placed in containers with distilled water.

Table 1. Composition (w/w) of three representative semi-IPN p(HEMA)/PVP hydrogels already applied for cleaning of cultural heritage artifacts.

Hydrogel	HEMA	PVP	MBA	H_2O	Monomer/cross-linker ratio	HEMA/PVP ratio
H50	25.0%	24.9%	0.2%	49.9%	1:1 x 10^{-2}	1:1
H58	16.8%	25.1%	0.2%	57.9%	1:1.5 x 10^{-2}	1:1.5
H65	10.5%	24.5%	0.2%	64.9%	1:2 x 10^{-2}	1:2.3

Hydration cycle

To investigate how much water a semi-IPN hydrogel can load after synthesis until equilibrium is reached, hydrogel weight was registered at different times, as follows:

$$\text{Water uptake (\%)} = \frac{W_i - W_{0*}}{W_{0*}} \times 100 \quad (1)$$

where W_i is the hydrogel weight obtained at time *i*, W_{0*} is the hydrogel weight immediately after synthesis.

Fourier Transform Infrared Spectroscopy (FTIR)

A FTIR spectrometer (Thermo Nicolet Nexus 870) in attenuated total reflectance mode (ATR-FTIR), equipped with a Golden Gate diamond cell was used to verify the absence of gel residues after direct contact with canvas. Data were collected with a MCT detector with a sampling area of 150 μm^2. The spectra were obtained from 128 scans with 4 cm^{-1} of optical resolution.

Scanning Electron Microscopy (SEM)

A FEG-SEM ∑IGMA (Carl Zeiss, Germany) was used to acquire images from xerogels (freeze-dried hydrogels) using an acceleration potential of 1 kV and a working distance of 1.9 mm.

Results and Discussion

The investigated semi-IPN hydrogels were designed to address the problem of cleaning water-sensitive surfaces. Accordingly, the most important gel features are transparency, softness, high-retention and gel cohesion to avoid any gel residues on the surface after cleaning treatment. Each of these hydrogels' features is discussed in more detail further in this work.

Hydrogels' transparency and softness

Semi-IPN p(HEMA)/PVP hydrogels are transparent and soft, as highlighted in figure 1. The material's transparency is very important in restoration treatments because it allows the restorer a visual control of the cleaning process. These hydrogels can load as well other aqueous systems and pure solvents without losing their transparency. Their softness permits an acceptable adhesion to most surfaces, as illustrated in figure 1 (left). Furthermore, these hydrogels can remain attached to surfaces both in vertical position and upside down, allowing treatments on wall paintings or painted ceilings.

Fig. 1. Semi-IPN hydrogel (H65) on a travertine stone. On the left, the hydrogel applied in vertical position; on the right, the hydrogel removal is shown. It is worth noting that the stone surface is wet only in correspondence with the contact area.

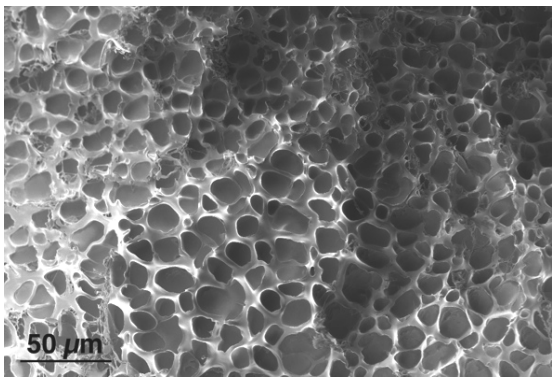

Fig. 2. SEM image of semi-IPN H65 hydrogel in xerogel form (lyophilized hydrogel).

Semi-IPN hydrogels present a mesoporosity that was investigated using a Scanning Electron Microscope (SEM). The SEM image of H65 xerogel's porosity is presented in figure 2. A sponge-like structure is noted, with pore dimensions varying from 5 to 40 μm. Hydrogels' porosity is mainly given by the presence of water during synthesis. Formulations with higher initial water amount in the reaction mixture show higher porosity.

Hydrogels' hydrophilicity and retention capacity

Three formulations were devised for addressing the specific demands of different case studies (see table 1). The main differences between gel formulations are the softness and retention capacity. The softer hydrogels are also the most hydrophilic. Hydrophilicity is correlated with the water content inside hydrogels, so less hydrophilic hydrogels have less water content. The water amount in the reaction mixture is 50% (w/w) in H50 and 65% (w/w) in H65. After the synthesis, the newly formed semi-IPN sponge can still load a high quantity of water until equilibrium water content (EWC) is reached. Curves in figure 3 show the difference in water loading capacity (i.e. hydrophilicity) of two hydrogel formulations (H50 and H65). H65 hydrogel, the most hydrophilic one, displays a water uptake of ~134%, while H50 have a water uptake of ~64%.

The hydration cycle permits to investigate the time required to reach the EWC after synthesis; all the investigated gel formulations need about 6 days. Only when the EWC is reached, can the hydrogels be used for cleaning procedures. Furthermore, if needed, it is possible to exchange the already water-loaded hydrogels with another water-based system, such as oil-in-water microemulsions, or pure organic solvents, by putting them in a filled container with the liquid to be loaded inside hydrogels. This exchange takes approximately 12h.

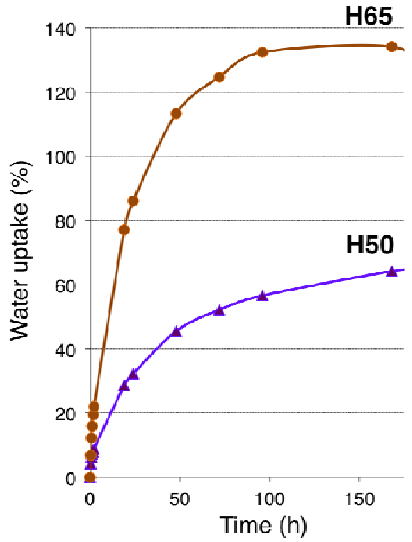

Fig. 3. Hydration cycle for two semi-IPN hydrogel formulations.

After 4h exposure to the air in a controlled environment (55% relative humidity and 20ºC), water-loaded hydrogels (shaped as a 1 cm square, with 2 mm thickness) still maintain a water content of around 90% with respect to EWC. This means that these hydrogels limit the

liquid evaporation rate and, thus, allow a longer contact between cleaning system and artifact's surface.

Hydrogels' cohesion

The cross-linked polymer network of semi-IPN hydrogels implies very high gel cohesion, which prevents gel residues on the surface after cleaning treatments.

To confirm this statement, ATR-FTIR spectra, shown in figure 4, were collected from a cotton canvas, which is a very hydrophilic surface, after direct contact with semi-IPN hydrogels. For instance, the characteristic intense bands assigned to the carbonyl stretching vibration of both HEMA and PVP (respectively 1724 and 1654cm^{-1}) are not visible in the spectra of cleaned canvas; this confirmed that no detectable gel residues are left on canvas due to gel contact.

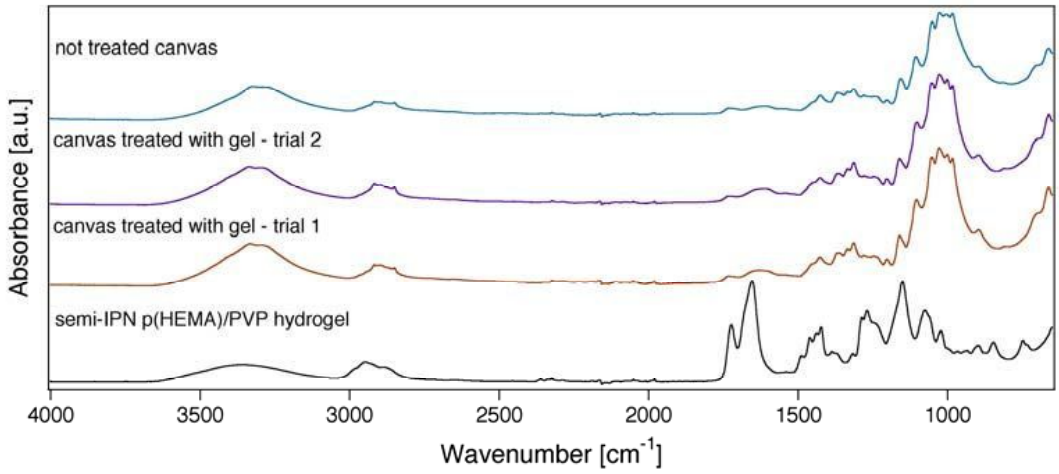

Fig. 4. ATR-FTIR spectra to verify the absence of gel residues on canvas after direct contact with semi-IPN hydrogels.

Cleaning tests

These semi-IPN hydrogels permit a highly controlled cleaning and could replace the common methods used in conservation, such as the use of a wetted cotton-swab (largely used for the application of water or other solvents directly over the painted surface). In order to make a comparison between these two techniques a mock-up sample of a water-sensitive material (canvas) was prepared. Acrylic and vinyl tempera were used to paint the canvas. On the top of the paint layer, a thin deposit of the hydrophilic artificial grime mixture developed by Wolbers [15] was applied. It is well known that acrylic and vinyl color applied on canvas tend to lose adhesion with the support when in contact with water. For that reason, this mock-up sample was a good reference material to check the efficiency of this new gel-based technique. Cleaning tests were carried out using different hydrogel formulations, and compared with a classic wetted cotton-swab cleaning. Results are summarized in figure 5. None of the hydrogel formulation led to color removal. The best cleaning result was achieved with formulation H65. On the other hand, evident color traces were noted on cotton-swab after its use (Fig. 5 right), due to the swelling and loss of adhesion of the paint layer favored by water.

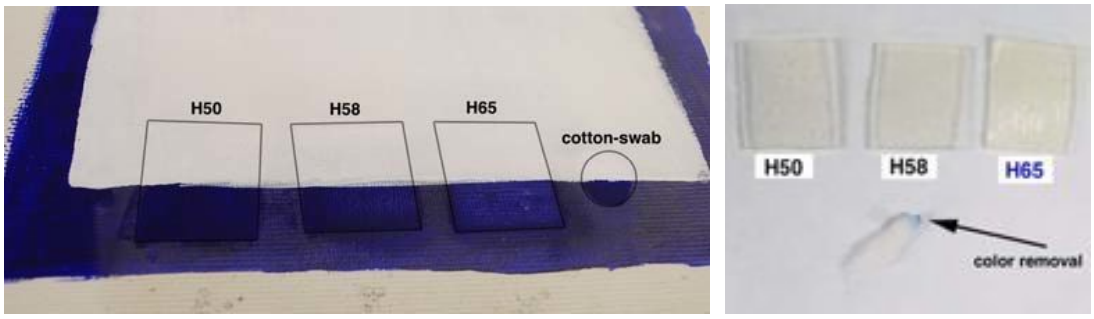

Fig. 5. Cleaning tests on a canvas painted with modern tempera (acrylic/vinyl resins) and coated with artificial grime. Cleaning was performed with water-loaded semi-IPN hydrogels applied for 5 minutes. Cotton-swab wetted with water was used for comparison purpose.

Conclusions

Chemical semi IPN hydrogels are a suitable tool to achieve a controlled cleaning action on water-sensitive cultural heritage artifacts. They are transparent and easy to manipulate, can load high quantities of water-based cleaning systems and keep them in contact with surfaces for the time required for the cleaning. Several advantages in respect to traditional cleaning methods (physical gels and cotton swab) were observed: due to the strong gel cohesion no residues are left on the surface after cleaning and no pigments removal was observed after contact with water-sensitive paint layers.

Funding Body

J. D. acknowledges financial support provided by Fundação para a Ciência e a Tecnologia (FCT) through a Ph.D. research grant (SFRH/BD/73817/2010). This work was partly supported by the CSGI, the European Union, Project NANOFORART (FP7-ENV-NMP-2011/282816) and the Ministry for Education and Research (MIUR, PRIN-2009P2WEAT).

References

[1] P. Baglioni, D. Chelazzi, R. Giorgi, G. Poggi, *Colloid and Materials Science for the Conservation of Cultural Heritage: Cleaning, Consolidation, and Deacidi cation*, **Langmuir**, **29**, 2013, pp. 5110−5122.

[2] P. Baglioni, D. Chelazzi (eds), **Nanoscience for the Conservation of Works of Art**, Royal Society of Chemistry, Oxfordshire, 2013.

[3] P. Baglioni, D. Berti, M. Bonini, E. Carretti, L. Dei, E. Fratini, R. Giorgi, *Micelle, Microemulsions, and Gels for the Conservation of Cultural Heritage*, **Advances in Colloid and Interface Science**, 2013, DOI 10.1016/j.cis.2013.09.008.

[4] N. Stolow, *Application of Science to Cleaning Methods: Solvent Action Studies on Pigmented and Unpigmented Linseed Oil Films*, **Recent Advances in Conservation, Proceedings of the IIC Rome Conference, Rome, Italy, 1961**, Butterworths, London, 1963, pp. 84−88.

[5] A. Phenix, K. Sutherland, *The Cleaning of Paintings: Effects of Organic Solvents on Oil Paint Films*, **Reviews in Conservation**, **2**, 2001, pp. 47−60.

[6] M. Baglioni, D. Berti, J. Teixeira, R. Giorgi, P. Baglioni, *Nanostructured Surfactant-Based Systems for the Removal of Polymers from Wall Paintings: A Small-Angle Neutron Scattering Study*, **Langmuir**, **28**, 2012, pp. 15193-15202.
[7] M. Baglioni, R. Giorgi, D. Berti, P. Baglioni, *Smart Cleaning of Cultural Heritage: a New Challenge for Soft Nanoscience*, **Nanoscale**, **4**, 2012, pp. 42-53.
[8] R. Giorgi, M. Baglioni, D. Berti, P. Baglioni, *New Methodologies for the Conservation of Cultural Heritage: Micellar Solutions, Microemulsions, and Hydroxide Nanoparticles*, **Accounts of Chemical Research, 43**, 2010, pp. 695-704.
[9] R. Wolbers, **Cleaning Painted Surfaces: Aqueous Methods**, Archetype, London, 2000.
[10] P. Cremonesi, **L'Uso di Tensioattivi e Chelanti nella Pulitura di Opere Policrome**, Il Prato, Padua, 2004.
[11] E. Campani, A. Casoli, P. Cremonesi, I. Saccani, E. Signorini, *Use of Agarose and Agar for preparing "Rigid Gels"*, **Quaderni del Cesmar 7**(4), Ed. Il Prato, Padova, 2007.
[12] M. Bonini, S. Lenz, E. Falletta, F. Ridi, E. Carretti, E. Fratini, A. Wiedenmann, P. Baglioni, *Acrylamide-Based Magnetic Nanosponges: A New Smart Nanocomposite Material*, **Langmuir**, **24**, 2008, pp.12644-12650.
[13] G. Pizzorusso, E. Fratini, J. Eiblmeier, R. Giorgi, D. Chelazzi, A. Chevalier, P. Baglioni, *Physicochemical Characterization of Acrylamide/Bisacrylamide Hydrogels and Their Application for the Conservation of Easel Paintings***, Langmuir**, **28**, 2012, pp. 3952-3961.
[14] J. Domingues, N. Bonelli, R. Giorgi, E. Fratini, F. Gorel, P. Baglioni, *Innovative Hydrogels Based on Semi-Interpenetrating p(HEMA)/PVP Networks for the Cleaning of Water-Sensitive Cultural Heritage Artifacts*, **Langmuir**, **29**, 2013, pp. 2746-2755.
[15] R. Wolbers, *The Use of a Synthetic Soiling Mixture as a Means for Evaluating the Efficacity of a Aqueous Cleaning Materials on Painted Surfaces*, **Conservation-Restauration Biens Culturels**, **4**, 1992, pp. 22-29.

Received: October, 11, 2013
Accepted: December, 07, 2013

Appl. Phys. A (2014) 114:705–710
DOI 10.1007/s00339-013-8150-0

Applied Physics A
Materials Science & Processing

Chemical semi-IPN hydrogels for the removal of adhesives from canvas paintings

Joana Domingues · Nicole Bonelli · Rodorico Giorgi · Piero Baglioni

Received: 9 July 2013 / Accepted: 8 November 2013 / Published online: 29 November 2013

Abstract Semi-interpenetrating (IPN) poly (2-hydroxyethyl methacrylate)/polyvinylpyrrolidone hydrogels were synthesized and used for the removal of adhesives from the back of canvas paintings. The high water retention capability and the specific mechanical properties of these gels allow the safe cleaning of water-sensitive artifacts using water-based detergent systems. The cleaning action is limited to the contact area and layer-by-layer removal is achieved while avoiding water spreading and absorption within water-sensitive substrates, which could lead, for example, to paint detachment. The use of these chemical gels also avoids leaving residues over the treated surface because the gel network is formed by covalent bonds that provide high mechanical strength. In this contribution, the physicochemical characterization of semi-IPN chemical hydrogels is reported. The successful application of an o/w microemulsion confined in the hydrogel for the removal of adhesives from linen canvas is also illustrated.

1 Introduction

Several conservation issues are continuously demanding innovative materials and techniques capable of providing efficient long-term preservation of cultural heritage artifacts. Cleaning is very challenging because of the difficulty in removing soiling materials with efficiency and with a high selective and controlled action. Wet cleaning provides several tools for gentle removal of unwanted materials, but the use of neat solvents has limitations due to the porosity of the artifact that favors the capillary absorption of the liquid phase, with the consequent spreading of the solubilized materials within the original artwork's materials [1]. Moreover, in the case of easel paintings, the low control of solvents penetration may cause swelling or leaching of the artifacts' organic materials [2].

Recently, several nanostructured fluids have been formulated with enhanced properties in terms of cleaning capability. Most of them are water-based systems efficient in the swelling, solubilization and removal of hydrophobic coatings, e.g. microemulsions, micellar solutions. Moreover, oil-in-water microemulsions guarantee the confinement of the specific solvent for the material to be removed within oil microemulsion droplets preventing the spreading into the artifact [3, 4]. These systems are very versatile and optimal for several applications, yet, in some cases, limitations could still persist. In fact, in the case of water-sensitive artifacts (e.g. paper manuscripts or canvas paintings), the strong interaction between the aqueous continuous phase of the microemulsion/micellar solution and the hydrophilic substrates can lead to deformations, halos and detachment of material. For this reason, in order to benefit from these nanofluids, it is of paramount importance to use highly retentive containers capable of efficiently confining these detergent systems, with the aim of limiting their cleaning action merely at the interface.

Solvent gels, i.e, solvents in their thickened state, are one of the present methods used by conservators to minimize solvent penetration into the artifact [5]. However, the use of solvent gels entails a considerable risk related to the residues that remain on the surface after cleaning. In fact, after the cleaning procedure it is always necessary to

J. Domingues · N. Bonelli · R. Giorgi · P. Baglioni (✉)
Department of Chemistry Ugo Schiff and CSGI,
University of Florence, Via della Lastruccia 3, Sesto Fiorentino,
50019 Florence, Italy
e-mail: baglioni@csgi.unifi.it

J. Domingues
e-mail: domingues@csgi.unifi.it

perform an appropriate removal of the residues through the use of organic solvent blends. To overcome this limitation, conservators and scientists have recently devised new confining methods, one of which is the use of polysaccharide-based physical gels (e.g. agar-agar, gellan gum) for the cleaning of various types of materials [6]. However, these physical gels do not exhibit the appropriate features for cleaning water-sensitive artifacts, since the weak bond interactions of the gel structure can lead to excessive water release. Chemical hydrogels, on the other hand, have a polymeric network constituted by covalent bonds and, therefore, exhibit improved mechanical features. Moreover, in latter studies chemical gels have shown to have high retention capability and controlled water release without leaving any gel residues on the artifact [7, 8]. Chemical gels can be shaped in the desired form during the synthesis and can load high amounts of liquid phase, without undergoing gel solubilization.

In this paper we report the innovative use of hydrogels based on semi-interpenetrating polymer networks (semi-IPN) loaded with an o/w microemulsion for the removal of aged adhesives from a backside of a canvas painting. In relation to previous acrylamide/bisacrylamide hydrogels [7], semi-IPN hydrogels have similar hydrophilic features, but are more resistant, transparent and are highly retentive and, therefore, appropriate for cleaning water-sensitive artifacts. In a previous work (see reference [8]) hydrophilic layers of grime were removed from a Thang-Ka (water-sensitive substrate based on tempera magra technique) using water-loaded semi-IPN hydrogels. In this paper we used p(HEMA)/PVP hydrogels to remove hydrophobic layers, such as aged polymers, using the appropriate detergent system (a microemulsion) confined into the gel network. We showed that these gels are very versatile and can be used to remove different kinds of materials from various types of water-sensitive substrates.

The semi-IPN hydrogels described here are constituted by a network of poly(2-hydroxyethyl methacrylate) [p(HEMA)], which contributes to the hydrogel mechanical strength, and the interpenetrated linear polymer polyvinylpyrrolidone (PVP), that contributes to the hydrogel hydrophilicity. Some of the most important characteristics of these hydrogels are the softness [9] and their capability to confine the cleaning action exclusively to the contact area, where only the first few layers of the artwork's surface are in contact with the solvent system [8] allowing a controlled layer-by-layer cleaning treatment. The hydrogels' capability to load different cleaning systems (e.g. pure and mixed solvent systems, micellar solutions, microemulsions) is shown here for the first time.

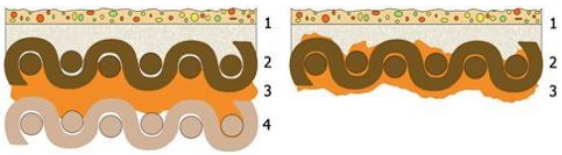

Fig. 1 Schematic cross-section of a painting with a lining (*left*) and after its removal using solvent technology (*right*). *1* Preparation and painted layers; *2* original canvas; *3* adhesive; *4* canvas used for lining

The case study reported is a lining removal. A lining consists of a structural treatment where a new canvas is attached to the backside of the canvas support (see Fig. 1, left). Aging of linings leads to an accelerated degradation of the painting caused by acid formation due to molecular decay of the used adhesives, so lining removal is often necessary. Adhesives removal is very stressful for the painting because, on one hand the use of pure solvents can transport the dissolved polymer into the canvas fibers and, in the worst cases, into the preparation layers (see Fig. 1, right) and, on the other, canvas can easily absorb water-based systems, leading to the swelling of the hydrophilic layers of the painted artifact, which may lead to paint detachment.

2 Experimental

2.1 Synthesis of hydrogels

The semi-IPN hydrogels were prepared by embedding PVP (average Mw $\approx$1,300 kDa) physically into the forming hydrogel network of HEMA. For this purpose HEMA monomer and the cross-linker *N*,*N*′-methylenebisacrylamide (MBA) were mixed together in a water solution with linear PVP. The reaction mixure was bubbled with nitrogen for 5 min to remove the oxygen and then the radical initiator α, α′-azoisobutyronitrile was added in a 1:0.01 monomer/initiator molar ratio. The reaction mixture was gently sonicated for 30 min in pulsed mode to eliminate the possible gas bubbles. Different formulations of hydrogels were prepared by varying the proportions of monomer/

Table 1 Compositions (w/w) of the selected semi-IPN hydrogels; HEMA/MBA and HEMA/PVP ratios

	H50	H58	H65
HEMA (%)	25.0	16.8	10.5
MBA (%)	0.2	0.2	0.2
PVP (%)	24.9	25.1	24.4
Water (%)	49.9	57.9	64.9
HEMA/MBA ratio	$1:1 \times 10^{-2}$	$1:1.5 \times 10^{-2}$	$1:2 \times 10^{-2}$
HEMA/PVP ratio	50/50	40/60	30/70

The acronym HXX refers to the XX percentage of water in the reaction mixture

cross-linker ratio with PVP and water percentages. The composition of the three investigated systems is reported in Table 1. The polymerization reaction by thermal homolysis of the initiator was performed for 4 h at 60 °C. After polymerization, the hydrogels were washed and placed in containers with distilled water.

Polysaccharide-based physical gels (agar–agar and gellan gum) were also prepared by dispersion of dry powders in water with 3 % (w/w). Powders were supplied by C.T.S. Italy (trademarks AgarArt and Kelcogel).

2.2 Physicochemical characterization

The gel content (G) gives the fraction between the mass of the final semi-IPN p(HEMA)/PVP hydrogel and the mass of the two components in the initial mixture, which can be calculated as follows [10]:

$$G\,(\%) = (W_d/W_0) \times 100 \quad (1)$$

where W_d is the dry weight of the hydrogel and W_0 is the weight of HEMA and PVP in the initial reaction mixture. The equilibrium water content (EWC) of hydrogels gives information on the polymer network hydrophilicity and can be calculated as follows:

$$\mathrm{EWC} = [(W_w - W_d)/W_w] \times 100 \quad (2)$$

where W_w is the weight of the water swollen hydrogel in equilibrium obtained at least 7 days after polymerization reaction.

Water release feature provides a better understanding of the retention capability of each gel system. The surfaces of fully swollen hydrogels were gently dried and the gel was put on three sheets of Whatman® filter paper inside a plastic Petri dish with lid to avoid water evaporation. The sheets of filter paper were weighed before and after 30 min of gel application.

The loading gel capacity toward different cleaning systems was calculated by immersing the lyophilized H58 hydrogel into the selected solvents. Squared hydrogel films of about 1 cm^2 and 2 mm of thickness were used. Both hydrogel weights and size were registered before and after immersion in the solvent to estimate the quantity of loaded solvent by each gel. The solvents were chosen from those commonly used by conservators [11].

A FTIR spectrometer (Thermo Nicolet Nexus 870) in attenuated total reflectance FT-infrared mode (ATR-FTIR), equipped with a Golden Gate diamond cell was used to investigate on possible gel residues after a cleaning treatment. Data were collected with an MCT detector with a sampling area of 150 μm^2. The spectra were obtained from 128 scans with 4 cm^{-1} of optical resolution.

A FEG-SEM ΣIGMA (Carl Zeiss, Germany) was used to acquire images from xerogels (freeze-dried hydrogels) using an acceleration potential of 1 kV and a working distance of 1.4 mm.

2.3 Removal of aged polymer adhesives

To evaluate the effectiveness of the prepared hydrogel systems, cleaning tests on model samples were performed. Linen canvas samples were previously treated with two different polymers widely used in lining procedure, Mowilith® DM5 (vinyl acetate/*n*-butyl acrylate copolymer) and Plextol® B500 (ethyl acrylate/methyl methacrylate copolymer). To simulate the natural aging process samples were submitted to an artificial aging as described in the literature [12].

The hydrogels were loaded with EAPC o/w microemulsion [1] through immersion for at least 12 h before application on canvas. This microemulsion is composed of water (73.3 wt%), sodium dodecyl sulfate (3.7 wt%), 1-pentanol (7.0 wt%), propylene carbonate (8.0 wt%) and ethyl acetate (8.0 wt%). The hydrogel loaded with the microemulsion EAPC was kept in contact with the canvas surface for 4 h. To avoid evaporation of the microemulsion, the hydrogel was covered with a plastic foil. A Whatman® filter paper was placed on the backside of the canvas to verify the absence of dissolved polymer or solvent diffusing through the canvas. After the gel application, the aged polymeric adhesive was swollen and softened and could be easily removed with gentle mechanical action.

3 Results and discussion

The three p(HEMA)/PVP hydrogels formulations here presented were designed to address different needs in conservation concerning cleaning. The gel content (G) in this type of hydrogels is usually low because there are no chemical bonds between polymer network and interpenetrated linear polymer, so any excess of the latter can be washed out. H50 hydrogel presents a G value of 90 % (Table 2), which is comparable with the G of acrylamide

Table 2 Some physicochemical properties of the selected p(HEMA)/PVP, acrylamide [7] and polysaccharide hydrogels

	G (%)	EWC (%)	Water release (mg/cm^2)
H50	90	72	8
H58	78	80	15
H65	74	87	16
Acrylamide "Hard"	95	95	27
Acrylamide "Soft"	88	97	56
AgarArt	-	97	30
Kelcogel	-	97	33

chemical gels. This is a considerable fact since there is a 50/50 p(HEMA)/PVP ratio. This sustains the presence of hydrogen bonds between HEMA and PVP [13]. However, increasing linear PVP amount with respect to HEMA leads to a substantial drop in *G* at a specific p/(HEMA)/PVP ratio, meaning that the available area of HEMA network is not enough to encompass more PVP.

In general, all the synthesized semi-IPN hydrogels are transparent and soft. The systems differ mainly in hydrophilicity, i.e., water loading and water release features. These properties can be tuned before synthesis by variation of their component ratios (HEMA/PVP, HEMA/cross-linker, water/reaction mixture). In particular, from H50 to H65 the hydrophilicity character increases as demonstrated by the EWC values reported in Table 2. The physical gels (AgarArt and Kelcogel) have an EWC of 97 %, which correlates with an excessive water release for cleaning water-sensitive substrates, as illustrated in a previous work [8]. In fact, water release test shows that physical gels release water at least twice as much as semi-IPN hydrogels. Acrylamide gels have a high EWC and show an higher water release with respect to semi-IPN hydrogels, which are for that reason more suitable for the cleaning of water-sensitive substrates.

Table 3 Amount of loaded solvents in hydrogel H58 and loading percentage with respect to the water loaded gel

	Solvent/xerogel (w/w)	%
Acetic acid	11.17	270
Benzyl alcohol	10.70	254
2-Methoxyethanol	4.02	33
Ethylene glycol	3.98	32
Ethanolamine	3.81	26
Water	3.02	0
Ethyl alcohol	2.97	−2
Propylene glycol	2.72	−10
Methyl alcohol	2.47	−18
2-Butanol	1.74	−42
Cyclohexane	n.l.	n.l.
Heptane	n.l.	n.l.
p-Xylene	n.l.	n.l.
Triethanolamine	n.l.	n.l.
Toluene	n.l.	n.l.
Acetone	n.l.	n.l.
Butyl acetate	n.l.	n.l.
2-Butoxyethanol	n.l.	n.l.
Methyl ethyl ketone	n.l.	n.l.
Propylene carbonate	n.l.	n.l.

n.l. not loaded

Semi-IPN p(HEMA)/PVP hydrogels are capable to load pure solvents as well. The loading capacity for some pure solvents is presented in Table 3. As expected, only the more polar solvents are loaded in semi-IPN hydrogels.

Mesoporosity was investigated through FEG-SEM images obtained from freeze-dried hydrogels (xerogels). It is known that some structure collapse may occur when ice forms. To verify this, EWC was calculated before and after freeze-drying process. A difference was noticed especially for H65 hydrogel that showed an EWC decrease of ca. 8 % that has to be considered when analyzing FEG-SEM images. FEG-SEM images of H50 and H65 hydrogels (Fig. 2) show the presence of a sponge-like structure. The difference between H50 and H65 hydrogels' porosity is mainly due to the quantity of water in the reaction mixture (50 and 65 % w/w, respectively), but also to PVP loss after polymerization, noted from *G* value, which contributes to larger pores due to the volume fraction of the macromolecule.

To confirm that these chemical gels do not leave residues on the surface after a cleaning treatment ATR-FTIR spectra were performed on canvas previously in contact with water-loaded semi-IPN gels. ATR-FTIR spectra reported in Fig. 3 show two reference spectra (a cotton canvas and a H50 hydrogel) and spectra from two canvas samples treated with H50 and H65. The characteristic carbonyl stretching vibration bands of HEMA and PVP are not present in the spectra of the treated canvases, proving that no detectable gel residues are left after the cleaning procedure.

The removal of aged adhesives from the back of canvas paintings can be done using oil-in-water microemulsions. However, in order to ensure a controlled cleaning process, the confinement of this cleaning tool inside hydrogels is

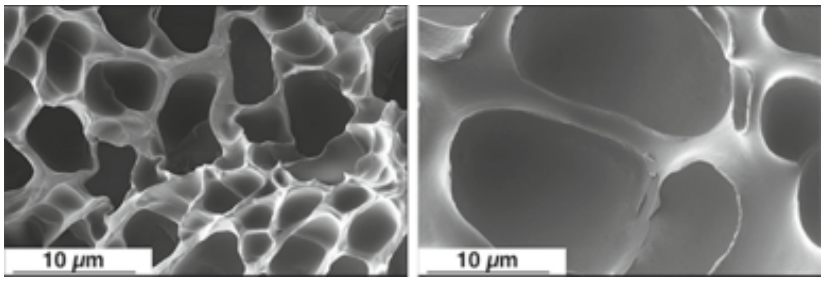

Fig. 2 FEG-SEM images of H50 (*left*) and H65 (*right*) xerogels

important to minimize fibers swelling due to contact with the water phase. It has been recently shown that an ethyl acetate/propylene carbonate based microemulsion (μEAPC) can be effectively loaded inside acrylamide hydrogels and provide an efficient removing of lining adhesives [7]. The use of p(HEMA)/PVP hydrogels loaded with this microemulsion was considered mainly because of the high water retention capability. The application of μEAPC loaded hydrogels H50 and H65 for the removal of aged adhesives is illustrated in Fig. 4.

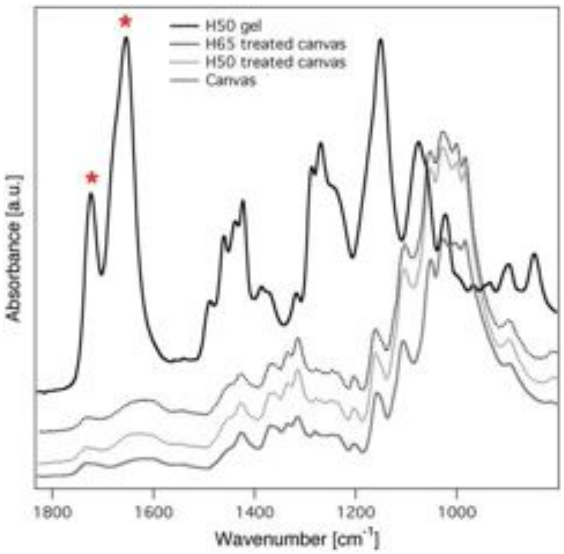

Fig. 3 ATR-FTIR fingerprint region spectra of a canvas, of H50 hydrogel and of canvases previously in contact with p(HEMA)/PVP hydrogels H65 and H50. Marked bands (*asterisk*) correspond to characteristic C=O stretching vibration of HEMA (1,724 cm^{-1}) and PVP (1,654 cm^{-1})

The artificially aged polymer adhesives, swollen after application of p(HEMA)/PVP hydrogels loaded with EAPC, are easily removed by gentle mechanical action. In Fig. 4 (centre and right), the enhanced swelling of these adhesives, after contact with the microemulsion confined inside hydrogels, is clearly detectable. In addition, the Whatman® filter paper placed on the backside of the canvas samples did not show traces of polymer transported by the microemulsion on the backside of the canvas. This confirms the hydrogel's effectiveness in confining the cleaning action only at the interface. The H65 hydrogel showed better efficacy in swelling both polymers making it the most appropriate confining tool for this kind of cleaning procedure under these circumstances. The required application time of 4 h allows the swelling and the partial solubilization of the polymer by the microemulsion. We have observed that a shorter application time results in a non complete swelling of the polymer leading to an inhomogeneous removal. The cleaning results are highlighted by optical microscopy images given in Fig. 5. The adhesive removal obtained through the application of H50 shows an incomplete cleaning action (Fig. 5, right) since the amount of microemulsion confined into the gel available for the cleaning is lower than in the H65 hydrogel. As a result, the

Fig. 4 Application of H50 hydrogel on the canvas glued with Plextol® adhesive, which, after swelling, could be removed by gentle mechanical action (*left* and *center*); removal of Mowilith® adhesive after application of H65 hydrogel (*right*)

Fig. 5 Optical microscopy images (×100 magnification) of the canvas with Plextol® before (*left*) and after removal of the aged adhesive using EAPC microemulsion confined in H65 (*center*) and H50 (*right*) hydrogels

canvas cleaned with H65 hydrogel presents a better cleaning, without visible damage of canvas fibers (Fig. 5, center).

4 Conclusions

Water-sensitive artifacts, i.e. artifacts that are constituted by hydrophilic materials, are always a concern for conservators that must apply gentle and controlled methods for efficient and safe removal of soiling materials, adhesives or aged varnishes. Chemical hydrogels based on semi-IPNs of p(HEMA)/PVP have demonstrated to be highly retentive and with good cleaning efficiency for the removal of hydrophobic layers, such as aged polymers, through the confinement of high-performing nanostructured fluids. This efficient combination of hydrogels and cleaning systems confined into the chemical gel network is a step forward in the conservation of cultural heritage and could be potentially applicable to different case studies.

Acknowledgements The authors acknowledge Dr. Chelazzi for providing the aged canvas samples. J. D. acknowledges financial support provided by *Fundação para a Ciência e a Tecnologia* (FCT) through a Ph.D. research grant (SFRH/BD/73817/2010). This work was partly supported by the CSGI, the European Union, Project NANOFORART (FP7-ENV-NMP-2011/282816) and the Ministry for Education and Research (MIUR, PRIN-2009-P2WEAT).

References

1. P. Baglioni, D. Chelazzi, R. Giorgi, G. Poggi, Langmuir **29**, 5110–5122 (2013)
2. A. Phenix, K. Sutherland, Rev. Conserv. **2**, 47–60 (2001)
3. M. Baglioni, R. Giorgi, D. Berti, P. Baglioni, Nanoscale **4**, 42–53 (2012)
4. M. Baglioni, D. Berti, J. Teixeira, R. Giorgi, P. Baglioni, Langmuir **28**, 15193–15202 (2012)
5. R. Wolbers, Cleaning painted surfaces: aqueous methods (Archetype, London, 2000).
6. E. Campani, A. Casoli, P. Cremonesi, I. Saccani, E. Signorini, Quaderni del Cesmar. **7**, 4 (2007)
7. G. Pizzorusso, E. Fratini, J. Eiblmeier, R. Giorgi, D. Chelazzi, A. Chevalier, P. Baglioni, Langmuir **28**, 3952–3961 (2012)
8. J.A.L. Domingues, N. Bonelli, R. Giorgi, E. Fratini, F. Gorel, P. Baglioni, Langmuir **29**, 2746–2755 (2013)
9. F. Yanez, A. Concheiro, C. Alvarez-Lorenzo, Eur. J. Pharm. Biopharm. **69**, 1094–1103 (2008)
10. S. Ming Kuo, S. Jen Chang, Y. Jiin Wang, J. Polym. Res. **6**, 191–196 (1999)
11. G.D. Smith, R. Johnson, WAAC Newsl. **30**, 11–19 (2008)
12. A. Chevalier, D. Chelazzi, P. Baglioni, R. Giorgi, E. Carretti, M. Stuke, M. Menu, R. Duchamp, in Proceedings of the ICOM-CC 15th Triennial Meeting, 22–26 September 2008, New Delhi, (Allied Publishers Pvt Ltd, New Delhi, 2008), p. 581
13. Y. Huang, J. Yang, Novel colloidal forming of ceramics (Springer, Berlin Heidelberg, 2011), p. 124